

NITROGEN-PLANT-SOIL INTERACTIONS AT THE ROOT-
RHIZOSPHERE, CROPPING SYSTEM, AND NATIONAL
SCALES

By

ISAAC JAMES MADSEN

A dissertation submitted in partial fulfillment of
the requirements for the degree of

DOCTORATE OF PHILOSOPHY

WASHINGTON STATE UNIVERSITY
Department of Crop and Soil Sciences

MAY 2017

© Copyright by ISAAC JAMES MADSEN, 2017
All Rights Reserved

© Copyright by ISAAC JAMES MADSEN, 2017
All Rights Reserved

To the Faculty of Washington State University:

The members of the Committee appointed to examine the dissertation of ISAAC JAMES MADSEN find it satisfactory and recommend that it be accepted.

William L. Pan, Ph.D., Chair

Steven D. Stehr, Ph.D.

Harold P. Collins, Ph.D.

Richard A. Rupp, Ph.D.

ACKNOWLEDGEMENT

I would like to acknowledge my major advisor Bill Pan for showing me that no matter how bleak the circumstances of life maybe, it is never so bleak that you should stop pursuing your knowledge of the world. I would like to acknowledge Richard Rupp for first introducing me to geographic information systems and changing my perspective on the world which we live in. I would like to acknowledge Steven Stehr for his instruction of my interdisciplinary policy work and assisting me in my journey through the tangles of political science. I would like to acknowledge Hal Collins for mentoring me while I was working at the Prosser research station and providing me with the necessary infrastructure for conducting the Potato -Winter Wheat -Sweet Corn work.

NITROGEN-PLANT-SOIL INTERACTIONS AT THE ROOT- RHIZOSPHERE, CROPPING SYSTEM, AND NATIONAL SCALES

Abstract

by Isaac James Madsen, Ph.D.
Washington State University
May 2017

Chair: William L. Pan

The transport and transformation of N at all scales is of paramount importance to humans. Not only is N crucial for our survival, being a central building block in protein, but N can also be toxic when found in high concentrations in the wrong locations. This work focuses on the importance of the place of N at three distinct scales. 1.) At the seedling root system scale we examined the effects of the concentration of N on causing symptoms of root toxicity, and found increasing ammoniacal-N to increase the symptoms of toxicity to roots. 2.) At the field scale, cover cropping and reduced tillage were assessed for their potential to decrease soil NO_3^- leaching and increase of N exportation efficiency. 3.) At the national scale a research project database was used to assess the amount of research that has gone into the development of best management practices.

TABLE OF CONTENTS

	Page
Abstract.....	iv
TABLE OF CONTENTS	v
LIST OF TABLES	ix
LIST OF FIGURES	x
CHAPTER 1: INTRODUCTION.....	1
CHAPTER 2: ROOT SYSTEM ARCHITECTURE (RSA) ALTERACTIONS DUE TO VARIABLE RATE AND SOURCES OF AMMONIACAL-N BASED FERTILIZER.....	4
Introduction	4
Ammoniacal-N Fertilizer Induced Toxicity in Field Crops	4
NH₃: The Dominant Toxic N Species	5
Root Symptoms in Response to NH₃/NH₄⁺ Toxicity	5
Spatiotemporal Nature of RSA Development	6
Objectives and hypothesis	6
Methods	7
Rhizotron Design	7
Image Acquisition and Measurements	7
Experimental Design	8
Results & Discussion	9
Apical Halt as a Response to increasing Urea Rates:	9
Timing and Depth of Lateral Root Initiation in Response to Urea Rates	13
Summary of RSA Changes due to Increasing Urea Rates:	16
Depth of Tap Root Apexes in Urea vs. AS Treatments:	17
Lateral Branching Initiation Points in AS vs. Urea Treatments:	20
Conclusions:	23
CHAPTER 3: SEMI-AUTOMATED SPATIAL ANALYSIS OF ROOT TOXICITY SYMPTOMS IN RELATION TO SOIL CHARACTERISTICS OF FERTILIZER REACTION ZONES	24
Introduction:	24

Automated Image Analysis of Roots	24
The Fertilizer Reaction Zone	24
Model applications	25
Methods	26
Experimental Setup	26
Data Analysis	27
Results & Discussion	30
Qualitative Analysis of Root Images	30
Root Classification and Validation	36
Interpolated Concentration	37
Model Profile and Validation	38
Relationships Between Root color and modeled Ammonium	44
Soil Moisture and Root Color	50
Conclusion	53
CHAPTER 4: COVER CROPPING AND REDUCED TILLAGE EFFECTS ON SEQUENTIAL NITROGEN USE EFFICIENCY IN AN IRRIGATED POTATO- WINTER WHEAT-SWEET CORN CROPPING SEQUENCE IN THE PACIFIC NORTHWEST	55
Introduction	55
Nitrate Leaching The Columbia Basin	55
Potatoes Susceptible to Leaching	55
Cover Cropping Effects on Nitrogen Leaching and NUE	56
Reduced Tillage Effects on Nitrogen Leaching and NUE	56
Cover Crops in Cropping Sequence Including Potatoes	57
NUE Assessments of Crop Sequences	57
Materials and Methods	59
Experimental Site and Design	59
Plant and Soil Sampling and Analysis	60
Statistical Analysis	61
Results and Discussion:	62

Field and Year Effect	62
Cover Cropping Effects on NO ₃ ⁻ Leaching	69
Cover Cropping and Reduced Tillage Effects on Single Year NEE	73
Cover Crop and Reduced Tillage Effects on sNEE in the CP Sequence	75
Cover Crop and Reduced Tillage Effects on sNEE in the PW Sequence.....	76
Cover Crop and Reduced Tillage Effects on sNEE in the WC Sequence	77
Summary:.....	80
Conclusion:	80
CHAPTER 5: THE UTILITY OF A FEDERAL RESEARCH DATABASE IN DETERMINING FUTURE RESEARCH NEEDS RELATED TO BEST MANAGEMENT PRACTICES FOR CONTROLLING THE LOSS OF REACTIVE NITROGEN FROM AGRICULTURE TO THE ENVIRONMENT	81
Introduction	81
Nr Loss from Agricultural Systems	81
Nr Loss to the Environment is as a “Wicked Problem”	81
Potential Role of Scientific Knowledge in Reducing Nr Loss.....	82
The Policy Subsystem With in Which the Research of Nr Loss Exists	83
The REEIS Database.....	85
REEIS Question.....	86
Methods	86
Query Development.....	86
Results and Discussion:.....	88
Query Results:.....	88
BMP Evaluation Projects on a State By State Basis	89
Meta-Analysis and Literature Reviews of BMPs.....	91
BMPs in Policy Solutions.....	92
Recommendations to NIFA Regarding BMP Evaluation Research	92
Bibliography	94
APPENDIX A: ABBREVIATIONS.....	112

**APPENDIX B: SOIL COLOR-MOISTURE CALIBRATION AND APPLICATION
USING FLATBED SCANNERS..... 114**

LIST OF TABLES

Table 1: Statistics For Depth of Lateral Branching Points	21
Table 2: Statistics For DAP of Lateral Branching Initiation	22
Table 3: Hydrus-1D Model Parameters	30
Table 4: Error Matrix for Detecting Soil Pores, Soil Aggregates, and Roots.....	36
Table 5: All Crops Yield by Year and Treatment.....	65
Table 6: Cover Crop N Recovery	66
Table 7: Mineral N ($\text{NH}_4^+ + \text{NO}_3^-$) in the Soil Profile.....	67
Table 8: Annual NEE Calculated by Crop.....	74
Table 9: sNUE, sNEE, and N Balance Analyzed by Treatment.....	79
Table 10: Synonyms Used in Query	87
Table 11: Rhizosphere Features and the Corresponding Resolution at which each Figure will become a Pixel	116
Table 12: Soils Used for the Analysis of Texture effects on Heterogeneity of Slopes	127

LIST OF FIGURES

Figure 1: Acrylic root box fixed to the face of an Epson V37 scanner for root imaging.	7
Figure 2: Canola roots at 2 (A), 4 (B) and 6 (C) DAP. Canola seeds were placed approximately 50 mm above a urea band which increases from 0-74.1 mg urea cm ⁻¹	10
Figure 3: The distance of apical halt above the fertilizer band over increasing rates of urea at 4 DAP.....	11
Figure 4: Paired images taken 5 DAP (A) and 8 DAP (B) in the 18 kg N ha ⁻¹ zone the root grows between two macrospores previously occupied by urea pellets (C).	12
Figure 5: Canola roots growing below the fertilizer band between the urea rates of 0 and 74.1 mg cm ⁻¹ at 10 DAP.....	13
Figure 6: Average date of lateral root emergence before day 10 as influenced by the urea rate..	14
Figure 7: Relationship between depth of lateral branching points and increasing urea rates on days 4, 5, 6 and 7.	15
Figure 8: Depth of lateral branching points as influenced by urea rate at 14 DAP. The red line represents the depth at which the fertilizer was placed, and each dot represents a single point of lateral branching.....	16
Figure 9: Canola roots exposed to urea (A), AS (B), and control (C). The red and white lines are the locations of the urea and AS bands respectively.....	18
Figure 10: Urea and AS applied at 28.0 kg N ha ⁻¹ depths 10 DAP.	19
Figure 11: Tap root apexes trips grown above urea (A), AS (B), and control (C).	20
Figure 12: Depth of lateral branching points in canola plants exposed to AS, urea the control. Each dot represents one lateral branching point.	23
Figure 13: Cross section showing seed and urea row orientation in relation to the scanner face.	27

Figure 14: Canola seedling root system exposed to urea band 12.8 mg N cm ⁻¹ on 3, 6, 8 DAP...	32
Figure 15 : Canola seedling root system exposed to urea band 12.8 mg N cm ⁻¹ on 3, 6, 8 DAP..	32
Figure 16: Canola seedling root system exposed to urea band 12.8 mg N cm ⁻¹ on 3, 6, 8 DAP...	33
Figure 17: Canola seedling root system exposed to urea band 6.4 mg N cm ⁻¹ on 3, 6, 8 DAP.....	33
Figure 18: Canola seedling root system exposed to urea band 6.4 mg N cm ⁻¹ on 3, 6, 8 DAP.....	34
Figure 19: Canola seedling root system exposed to urea band 6.4 mg N cm ⁻¹ on 3, 6, 8 DAP....	34
Figure 20: Canola seedling root system exposed to no urea band 3, 6, 8 DAP.....	35
Figure 21: Canola seedling root system exposed to no urea band on 3, 6, 8 DAP.....	35
Figure 22: Inverse distance weighted interpolation of Ammoniacal-N from sampling points taken on DAP 15.....	37
Figure 23: Comparison of measured and modeled ammonium distributions.	39
Figure 24: Model sensitivity to NH ₃ gas diffusion rate.	39
Figure 25: Model sensitivity to changes in the rate of urea to NH ₃ reaction.	40
Figure 26: Model sensitivity to changes in rate of NH ₃ to NH ₄ ⁺ reaction.	41
Figure 27: Model sensitivity to changes in the rate of NH ₄ ⁺ to NO ₂ reaction.	42
Figure 28: NH ₄ ⁺ and NH ₃ concentrations by depth at 72 h (3 DAP), 144 h (6 DAP), and 240 h (8 DAP).	43
Figure 29: Modeled NH ₄ ⁺ concentrations and root skeleton overlay on 3, 6, and 8 DAP.	43
Figure 30: Modeled NH ₃ concentrations and root skeleton overlay on 3, 6, and 8 DAP.	44
Figure 31: Root health as determined by color in relations to modeled NH ₄ ⁺ concentrations on 3,6, and DAP.....	45
Figure 32: Root health as determined by color in relations to modeled NH ₃ concentrations on 3,6, and 8 DAP.....	46

Figure 33: Correlations between root color and modeled NH_4^+ concentrations on 3, 6, and 8 DAP.....	47
Figure 34: Correlation between root color and modeled NH_4^+ concentrations on 3 DAP.	48
Figure 35: Correlation between root color and modeled NH_4^+ concentrations on 6 DAP.	49
Figure 36: Correlation between root color and modeled NH_4^+ concentrations on 8 DAP.	50
Figure 37: Gravimetric moisture and root skeleton overlay.	51
Figure 38: Correlations between moisture and root color on DAP 3, 6, and 8.....	52
Figure 39: Correlations between moisture and root color on DAP 3.	53
Figure 40: The normalized harvested and residue fractions of all crops overall	64
Figure 41: Initial soil NO_3^- in the fall of 2011.....	70
Figure 42: Over winter NO_3^- changes in the CPW sequence in the winters of 2012-2013 and 2013-2014.	71
Figure 43: Over winter NO_3^- changes in the PWC sequence in the winters of 2012-2013 and 2013-2014.	72
Figure 44: Over winter NO_3^- changes in the PWC sequence in the winters of 2012-2013 and 2013-2014.	73
Figure 45: Model of the policy subsystem in which Nr loss to the environment research is directed and funded.....	84
Figure 46: (right) Break down of BMP assessment research by agency.(right) Number of BMP assessment projects over time.....	89
Figure 47: Number BMP evaluation projects by state.....	91
Figure 48: In-situ image of color change (A) surrounding the site of urea dissolution (B).	118

Figure 49: Illustration of a cross section of the scanner face-soil matrix continuum demonstrating the different micro-topographical features of the soil..... 120

Figure 50: Demonstrates the manual classification of soil micro-topography using GIS. 121

Figure 51: Histograms of the 'light' and 'dark' areas surrounding the site of urea dissolution. .. 123

Figure 52: Histogram of the red value of the 'light' zone near the site of urea dissolution. 123

Figure 53: Reclassification of original image (A), using the five categories of 'large aggregates' (B), 'intermediate space' (C), 'light pore space' (D), 'dark pore space' (E), and 'aggregates' (F).
..... 124

Figure 54: The relationship between the field capacity and the slope of the color-moisture calibration curve..... 128

Dedication

I would like to dedicate this to my parents Mitch and Nancy Madsen for their seemingly unending love and boundless curiosities which have inspired me in every step of this journey.

CHAPTER 1: INTRODUCTION

Nitrogen (N) is necessary for all life. It is the back bone of protein chains, DNA, and RNA. However, N is not always beneficial to living organisms. High concentrations of ammoniacal-N in the root zone have been shown to have toxic effects on roots of many species of crop plants. NO_3^- has been shown to be a human health hazard. In addition to these direct effects NO_3^- can cause algal blooms which lead to anoxic environments killing aquatic organisms. Understanding the conditions and locations in which N is beneficial or harmful is critical for making decisions from the single plant scale to the international policy scale. The scope of this paper is to look at decisions which reduce the negative impacts and increase the positive impacts of N at the single plant, the field, and the national research policy scale.

At the single plant scale we examine the effects of banding ammonium based fertilizer beneath a canola seed row at varying rate and form (Creamer and Fox 1973). Canola has been grown with increasing frequency in the Pacific North West over the last several years. The management practices have had to adapt from a wheat centric system to include canola. Specifically in terms of fertilizer placement beneath the seeding row. Wheat has a fibrous root system which allows the root system architecture to adapt to the localized toxicity of urea bands. Canola on the other hand, with a single tap root, is presumably more susceptible to ammoniacal-N toxicity. Agricultural producers have the opportunity to control the rate and the source of N when applying fertilizers in the field. The rate of the fertilizer must be considered not only on a per hectare basis, but in terms of what concentration ammoniacal-N the root is exposed to.

At the field scale a major concern of N loss to the environment is NO_3^- leaching through the soil profile (Galloway et. al 2003). A method of preventing leaching loss is through using

cover crops (Tonitto et al. 2005). In irrigated agriculture in the Pacific North West potatoes, wheat, and corn are often grown in sequence. This sequence is particularly susceptible to leaching loss due to the shallow rooted potatoes which allow NO_3^- leaching deep into the soil profile. We suggest that the addition of cover crops into this sequence will reduce the leaching of NO_3^- deeper into the profile there by increasing the efficiency of the system as a whole.

Finally, at the national scale research policy plays an important role in determining actual environmental policy. A precursor to constructing effective environmental policy is an accurate understanding of the environmental policy, and a scientific understanding of potential technical solutions. Consequently, it is critical to have an effective research policy to increase the body of scientific knowledge surrounding the problem and potential solutions. The case of reactive nitrogen leaching from agriculture and into the environment is an environmental policy which requires a well-rounded understanding of where, when, and how NO_3^- is leaching. In addition to this there must be a well-rounded understanding of technical solution which can reduce the NO_3^- loss. Therefore, agencies with mandated with research related to agricultural and environmental problems require a method for directing research into new avenues and assessing the completeness of current avenues of research. In order to assess the completeness of research pertaining to technical solutions an assessment of best management practices of nitrogen in agriculture was completed.

The rate, place, and source of the nitrogen emerged as common themes in at all three scales. The rate at which N is applied is an important aspect of controlling the distance to which N moves and the effective damage which N can cause when in the wrong place. Place is of special importance when considering the movement of N at all three of these scales and should

be considered in all decisions regarding N management. The source is also important as the level of damage can be greatly mitigated depending on the source of N.

CHAPTER 2: ROOT SYSTEM ARCHITECTURE (RSA) ALTERATIONS DUE TO VARIABLE RATE AND SOURCES OF AMMONIACAL-N BASED FERTILIZER

Introduction

Ammoniacal-N Fertilizer Induced Toxicity in Field Crops

Depression of yield and plant health due to toxicity from N fertilizer banding is well documented (Britto and Kronzucker 2002). Toxicity symptoms have been detected both on the roots and shoots of many crop species (Dowling 1998). Controlling the rate and the formulation of the fertilizer being applied has been shown to mitigate the effects of the toxicity. The placement of fertilizer involves a variety of techniques including incorporation, banding with the seed, below the seed, and to the side. Each fertilizer placement has advantages. However, placing fertilizer directly below the seed is a common placement technique in minimum tillage dryland systems today. Nitrogen source as well as the placement is a critical factor in considering N fertilizer induced toxicity. A number of different N sources have been used in toxicity experiments including anhydrous ammonia, urea ammonium nitrate (UAN), urea, di-ammonium phosphate (DAP), mono-ammonium phosphate (MAP), and ammonium sulfate (AS) (Abbes et al. 1995, Angus et al. 2014, Coskun et al. 2013, Creamer and Fox 1980, Dowling 1998, Kosegarten et al. 1997, Passioura and Wetselaar 1972). These sources have been shown to have different effects on roots and the formation of the fertilizer reaction zone (FRZ). The FRZ is that region around the placement of the fertilizer that is radically influenced by the chemistry of the soil (Heaney 2001, Singh 1971). Field studies have demonstrated that the banding of fertilizer at planting can have effect on stand establishment (Angus et al. 2014, Grant et al. 2010, Mason 1971) and crop yield (Angus 2014).

NH₃: The Dominant Toxic N Species

The evolution of NH₃ or NH₄⁺ from a fertilizer band is determined by the soil master variables of pH, CEC, and moisture (Heaney 2001). Equally important is the chemical composition of the N source. Urea is a commonly used N source in many toxicity studies (Heaney 2001). As urea dissolves in the soil the pH of the solution surrounding the urea pellets increases resulting the conversion of NH₄⁺ to NH₃ (Pang et al 1973, Heaney 2001). NH₃ has been shown to be the most toxic species of ammoniacal-N to roots (Bennett and Adams 1970). AS, unlike urea, results in a lower solution pH and a higher concentration of NH₄⁺ than NH₃. The resulting concentration of NH₄⁺ from AS should have two consequences of one reducing the transport of ammoniacal-N away from the FRZ and two decreasing the concentrations of highly toxic NH₃. These effects have been observed to increase wheat (*Triticum aestivum*) root proliferation in the FRZ (Passioura and Wetselaar 1972).

Root Symptoms in Response to NH₃/NH₄⁺ Toxicity

The current literature describes two major classes of root symptoms resulting from roots encountering N fertilizer band. The first are those related to changes in root system architecture (RSA) and second those indicating localized physiological stress or cell death. RSA refers to the overall spatial distribution of roots within the soil (Gregory 2006). Common metrics of RSA modification are changes in root mass, root stunting, lateral root emergence, and zones of non-proliferation. A decrease in overall root mass has been observed in many field crops (Bennet and Adams 1970, Zhang and Rengel 2002, Su et al. 2015). Root stunting is defined as an overall reduction in root length. Quantitatively this can be described by a reduction of seminal axis length in fibrous rooted crops and a reduction in tap root length in tap rooted crops (Bennet and Adams 1970, Britto and Kronzucker 2002, Dowling 1998). Another change in RSA due to toxicity from a urea band found in tap rooted crops is premature lateral branching (Su et al. 2015). RSA may also change by roots not growing into the FRZ, creating a zone described as a non-proliferation zone because of the absence of roots in comparison to natural growth of the root system (Creamer and Fox 1980). In addition to modifications of RSA signs of physiological stress have also been

detected in some studies. The signs of physiological damage which have been detected are a discoloration or browning of the root and shrinkage of the root width (Passioura and Wetselaar 1972, Su et al. 2015).

Spatiotemporal Nature of RSA Development

Previous studies on toxicity induced changes to RSA have primarily relied on destructive sampling techniques. However, RSA is dynamic in both time and space; changing by mm and by day (Carminati et al. 2010, Esser et al. 2010, Giles et al. 2012, Logsdon et. al 2013). This level of spatial and temporal dynamism lends itself to being studied through visual observations and repeated measures as made possible through modern digital technology such as flatbed scanners. The utility of document scanners in imaging extracted and in-situ roots to track the growth and development of roots and their interactions with the soil is well documented (Pan and Bolton, 1991; Pan et al. 1998, Pan et al., 2001; Hammac et al. 2012). Recently, document scanners were used to quantify ammoniacal-N toxicity symptoms in terms of canola RSA and root morphological responses to banded urea rates of 34 kg N ha⁻¹ and 67 kg N ha⁻¹ (Pan et al. 2017). While rate affected the distance of apical halt, no effects on lateral emergence and root shrinkage were detected due to increasing fertilizer rate.

Objectives and hypothesis

The objective of this study was to document and model the effects of increasing rate and varied fertilizer type on root system architecture in canola seedlings over time. Specifically, examined whether increasing fertilizer rates increased the distance at which apical halt occurred from the fertilizer band and whether increasing N rate had a major effect on the premature initiation of lateral branching. Additionally hypothesized that urea will stimulate greater changes in RSA than AS with respect to premature lateral emergence and apical halt.

Methods

Rhizotron Design

The rhizotrons in this study were composed of wooden boxes attached to Epson V37 scanners (Epson Perfection V37, Epson America, Long Beach, CA). An acrylic glass box was fixed to the face of the scanner (Figure 1) . The dimensions of the boxes were 18.5 h by 21.5 w by 7.5 d cm (width by height by thickness). All experiments used a Palouse Silt Loam (fine-silty, mixed, superactive, mesic Pachic Ultic Haploxeroll) collected near Pullman, WA.

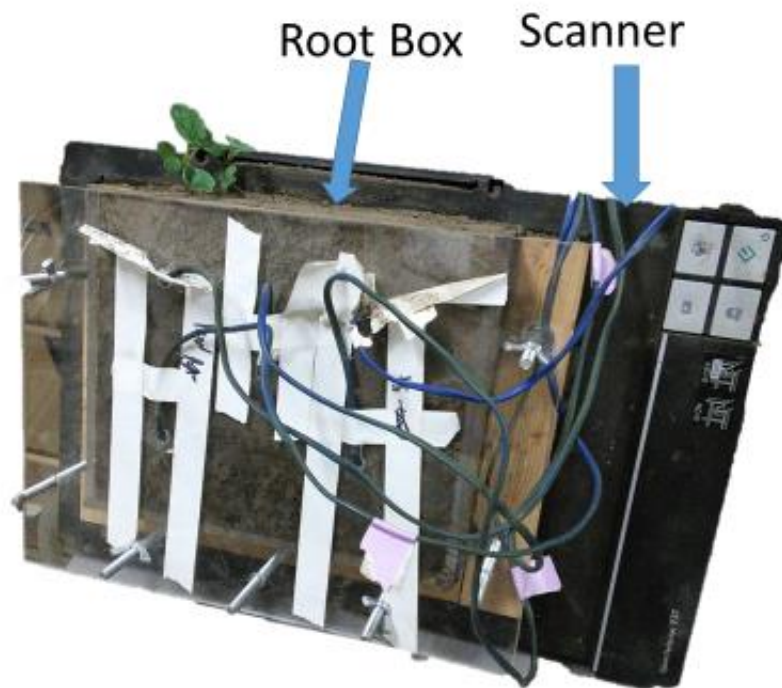


Figure 1: Acrylic root box fixed to the face of an Epson V37 scanner for root imaging.

Image Acquisition and Measurements

Images were captured every 24 hours at 1890 pixel cm^{-1} with VueScan scanning software (Vue Scan, Hamrick Software). The images were then spatially referenced using ArcMap (ESRI ArcMap, Redlands, CA). Root tip points and lateral branching points were visually detected and point markers

were placed at each event with a time stamp. Depths were calculated using the “Calculate Geometry” tool in ArcMap. Distances between root branching and root apical points relative to fertilizer band locations were calculated using ArcMap’s “Near” tool. Analysis of data was conducted in R stats software (R Foundation for Statistical Computing, R, Vienna, Austria).

Experimental Design

Urea rate trial

In the first experiment, canola (*Brassica napus cv. Amanda*) seeds and urea pellet fertilizer were placed parallel to the scanner face. Seeds were placed approximately 25 mm below the soil surface and urea pellets were placed approximately 75 mm below the soil surface. The rate of fertilizer was increased from 0 mg urea cm⁻¹ to 74.1 mg cm⁻¹ by increments of 4.6 mg urea cm⁻¹ per 1.5 cm along the scanner until the rate reached 55.6 mg urea cm⁻¹, at which point it was increased by increments of 9.3 mg urea cm⁻¹ to 74.1 mg urea cm⁻¹. Based on a 19.05 cm row spacing the minimum rate would be 8.9 kg N ha⁻¹ and the maximum would be 142.6 kg N ha⁻¹. The direction of the gradient of increase (left to right or right to left) was randomly selected in order to remove any unaccounted for environmental bias. Linear regressions relating the N rate to changes in RSA were conducted using the ‘base’ package of R statistical software and R studio (R Core Team 2016, Vienna, Austria, Rstudio Team 2016, Boston, MA).

Ammonium Source Trials

In the second experiment the 4 scanners were divided into 3 sections: a) control, b) 14.6 mg N cm⁻¹, and c) 14.6 mg N cm⁻¹ as AS. Fertilizer and seed were oriented parallel to the scanner face and depths of 25 mm and 75 mm respectively. ANOVA between the AS, urea, and control was conducted using the ‘base’ package of R statistical software and R studio (R Core Team 2016, Vienna, Austria, Rstudio Team 2016, Boston, MA).

Results & Discussion

Apical Halt as a Response to increasing Urea Rates:

Canola roots exposed to a continuously increasing rate of urea from 0–74.1 mg urea cm⁻¹ showed a variation in the timing and depth of symptoms occurrence dependent on the rate of the urea applied. The image series showed apical halt, lateral branching, and apparent necrosis increasing with urea rate (Figure 2). The distance between the stopping point of the root apex and the urea band increased as fertilizer rate increased (Figure 2). The relationship between the apical location and the rate of the urea on day 4 was fitted with an exponential line with an r^2 of 0.83. At a rate of 9.3 mg urea cm⁻¹ the exponential curve predicts the distance of the root tip from the fertilizer line is 7.24 mm from the fertilizer point. That distance more than doubles to 15.16 mm at 27.8 mg urea cm⁻¹. From 32.4 to 74.1 mg urea cm⁻¹ the distance between the root tips and the fertilizer line only changes by 2.84 mm. No tap roots are seen to pass through the fertilizer reaction zone in rates greater than 9.3 mg urea cm⁻¹. In one instance a tap root was observed passing through the fertilizer band, but this occurred 8 days after planting (DAP) and 3 days after the corresponding roots grown in the control passed the same depth (Figure 3). Roots were not observed growing through the fertilizer band at rates higher than 13.9 mg urea cm⁻¹. Multiple roots were seen to appear beneath the fertilizer band, but because these roots could not be traced back to the seed and therefore could not be confirmed to be either tap roots or laterals with functioning gravitropism (Figure 5).

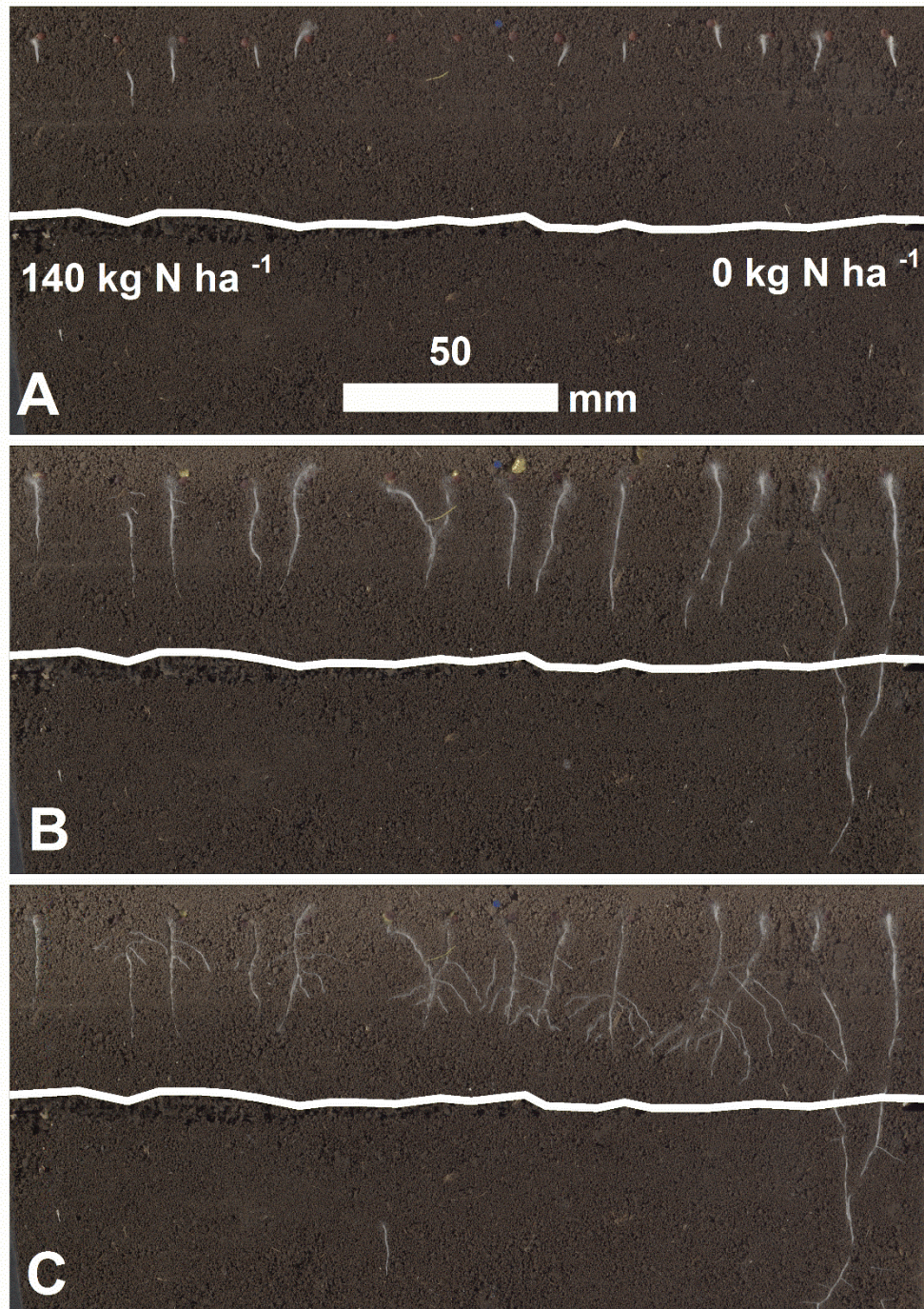


Figure 2: Canola roots at 2 (A), 4 (B) and 6 (C) DAP. Canola seeds were placed approximately 50 mm above a urea band which increases from 0-74.1 mg urea cm⁻¹.

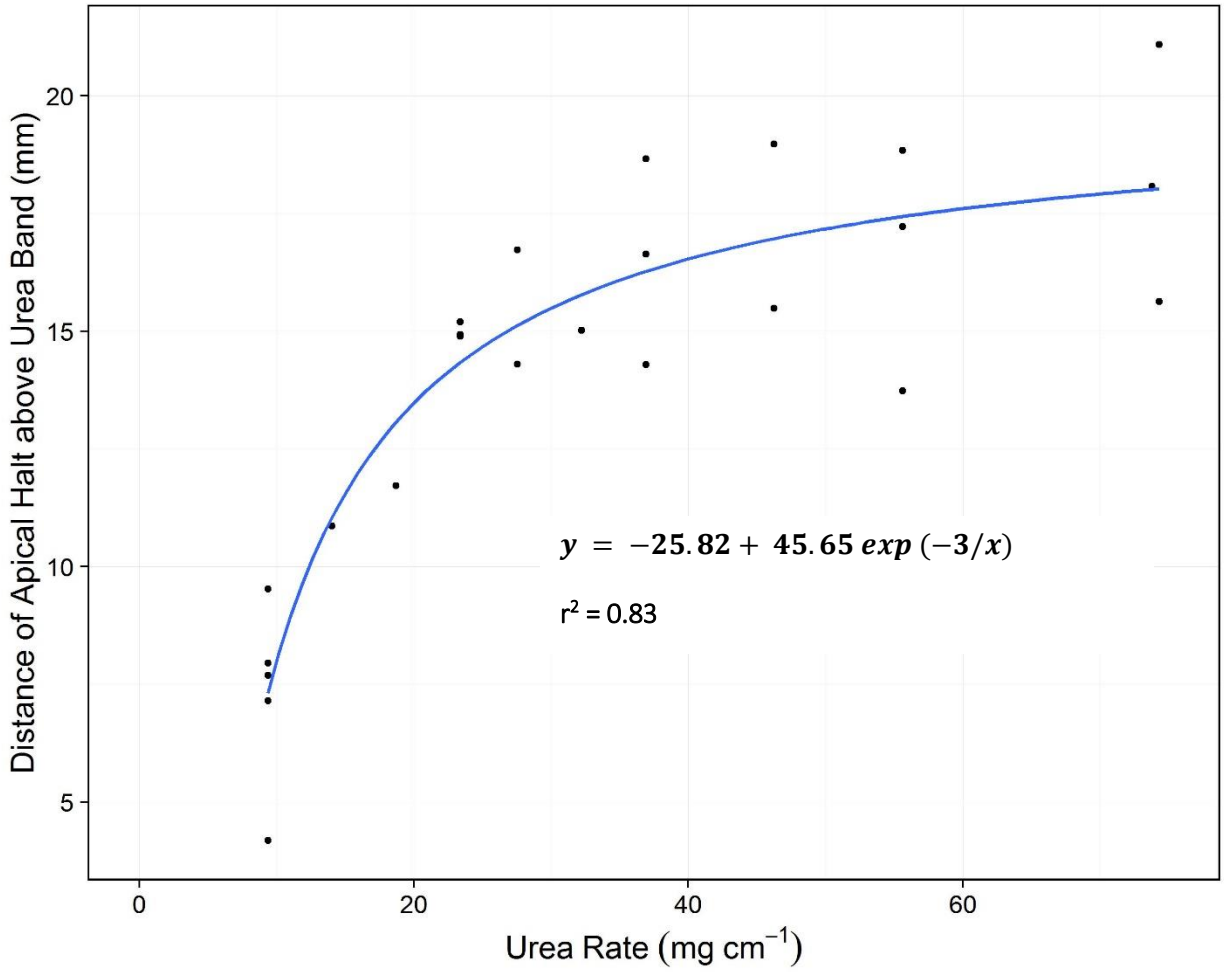


Figure 3: The distance of apical halt above the fertilizer band over increasing rates of urea at 4 DAP.

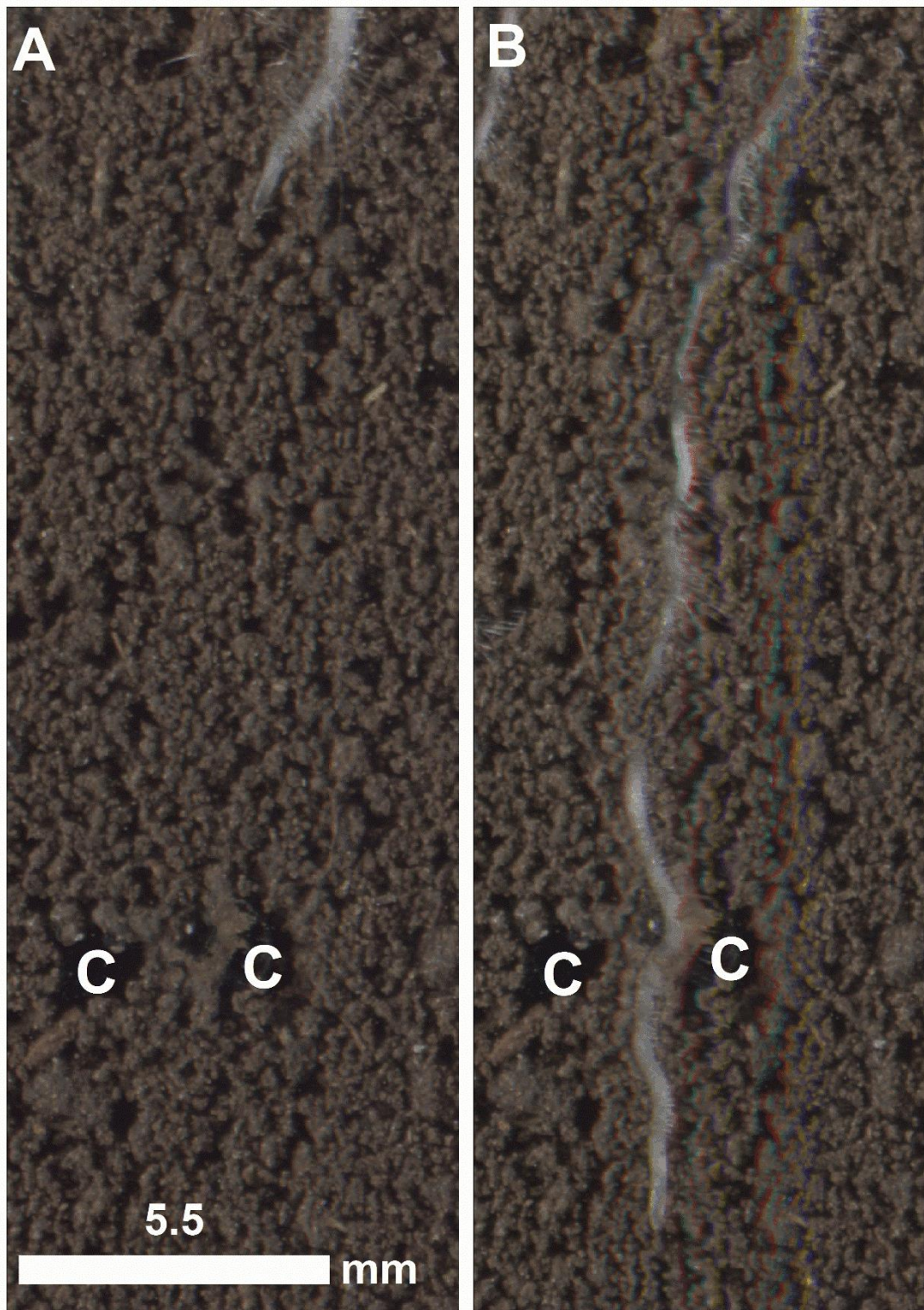


Figure 4: Paired images taken 5 DAP (A) and 8 DAP (B) in the 18 kg N ha⁻¹ zone the root grows between two macrospores previously occupied by urea pellets (C).

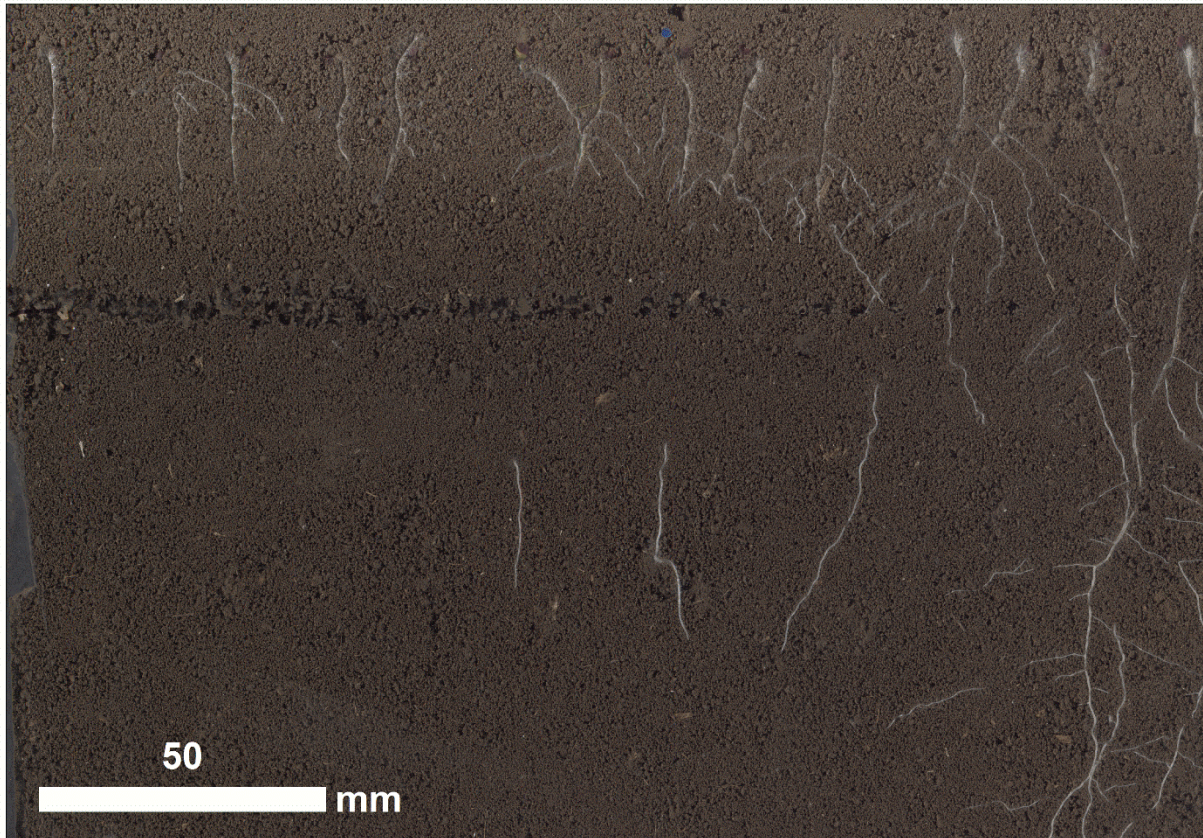


Figure 5: Canola roots growing below the fertilizer band between the urea rates of 0 and 74.1 mg cm⁻¹ at 10 DAP.

Timing and Depth of Lateral Root Initiation in Response to Urea Rates

The average day of lateral emergence was exponentially ($r^2 = 0.66$) decreased with increasing urea fertilizer rates (Figure 6). However, the premature emergence in lateral roots is tightly tied to the depth at which laterals were seen to emerge. The average depth of lateral emergence was found to be significantly increase by day. The average depths of day 4, 5, and 6 being significantly different from each other. At 4 DAP lateral branching was first observed at urea application rates between 13.9 and 64.8 mg urea cm⁻¹. At 5 DAP lateral emergence was observed in all treatments. By 6 DAP roots exposed to urea rates of greater than 55.6 mg urea cm⁻¹ had ceased producing lateral roots. At day 7 only roots below 23.2 mg urea cm⁻¹ were initiating lateral roots (Figure 7). This demonstrates that both timing and depth of lateral emergence were changed due to increasing fertilizer rates.

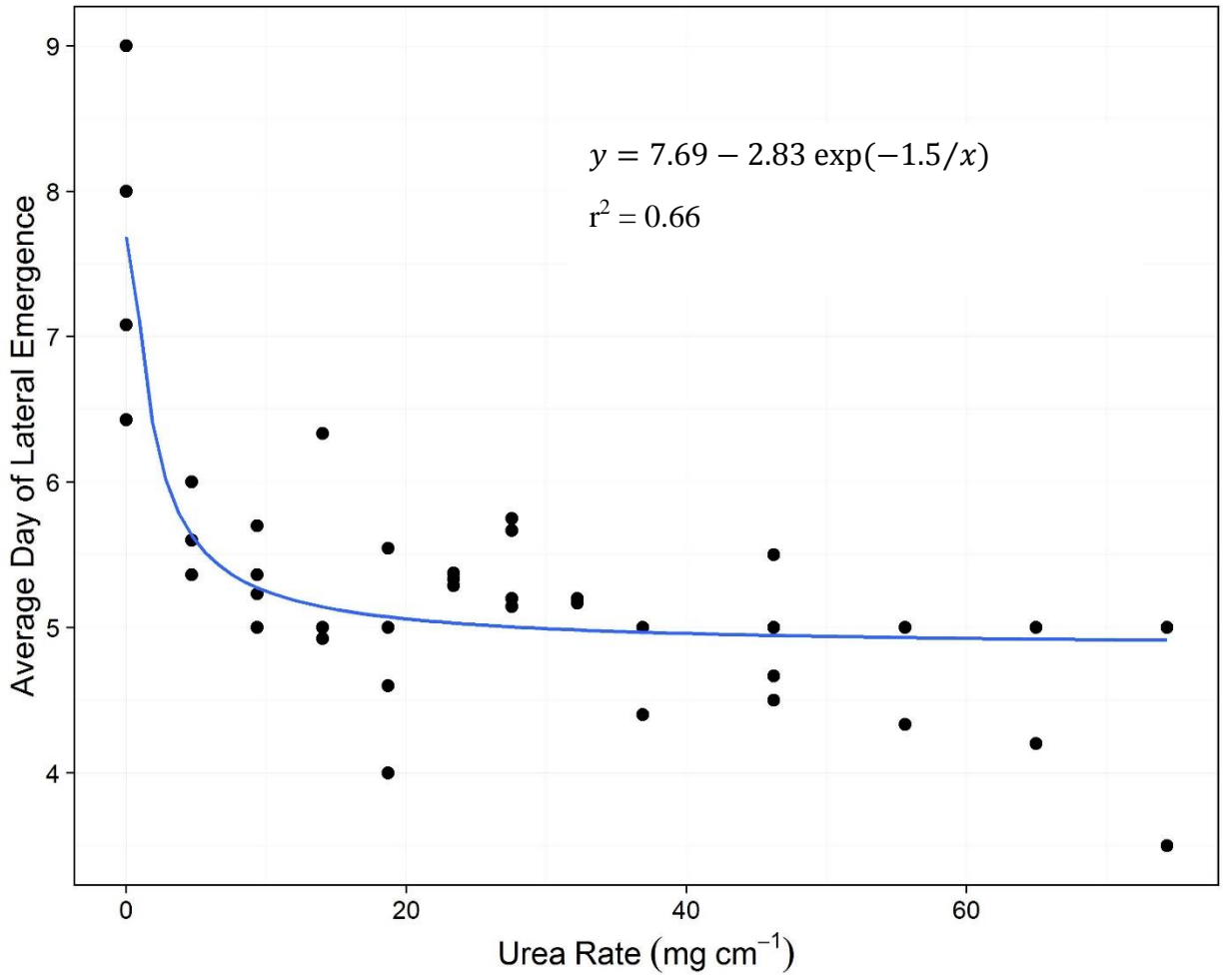


Figure 6: Average date of lateral root emergence before day 10 as influenced by the urea rate.

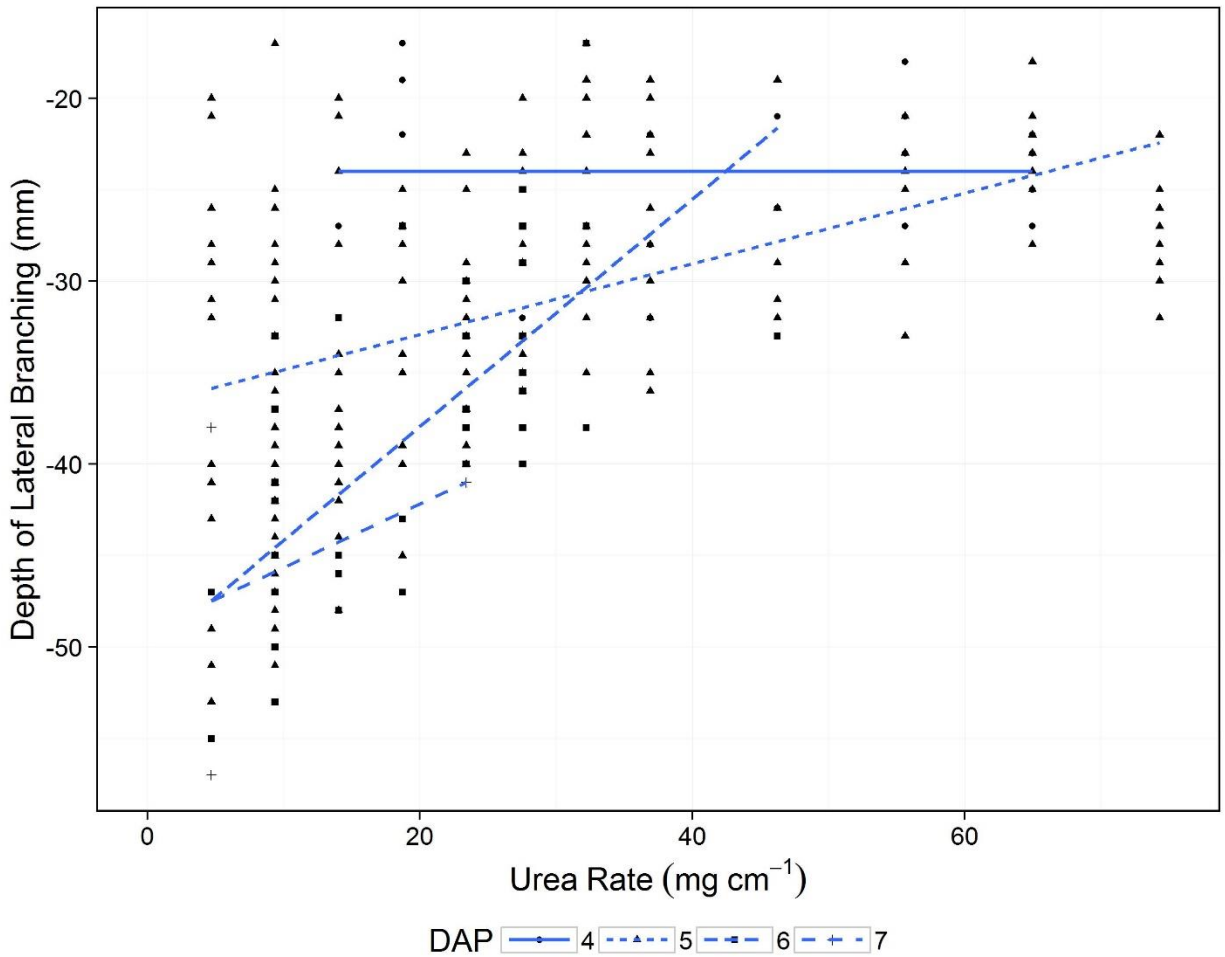


Figure 7: Relationship between depth of lateral branching points and increasing urea rates on days 4, 5, 6 and 7.

The discussion on lateral branching to this point has focused on lateral branching which occurs above the fertilizer band and is thus strongly influenced by apical death. However, at to day 14 of the study lateral branching occurred below the fertilizer band at urea rates as high as 23.2 mg urea cm⁻¹ (Figure 2). Importantly there is no lateral emergence directly above the fertilizer band in all urea treatments. These results suggest that at urea rates up to 23.2 mg urea cm⁻¹ canola roots may survive ammoniacal-N toxicity and reestablish a growing root system below the fertilizer band. Previous field experiments using canola have shown an increase in lateral root biomass in the 0-5 cm depths of the soil profile when 180 kg N ha⁻¹ was banded 5 cm below the surface (Su et al. 2015).

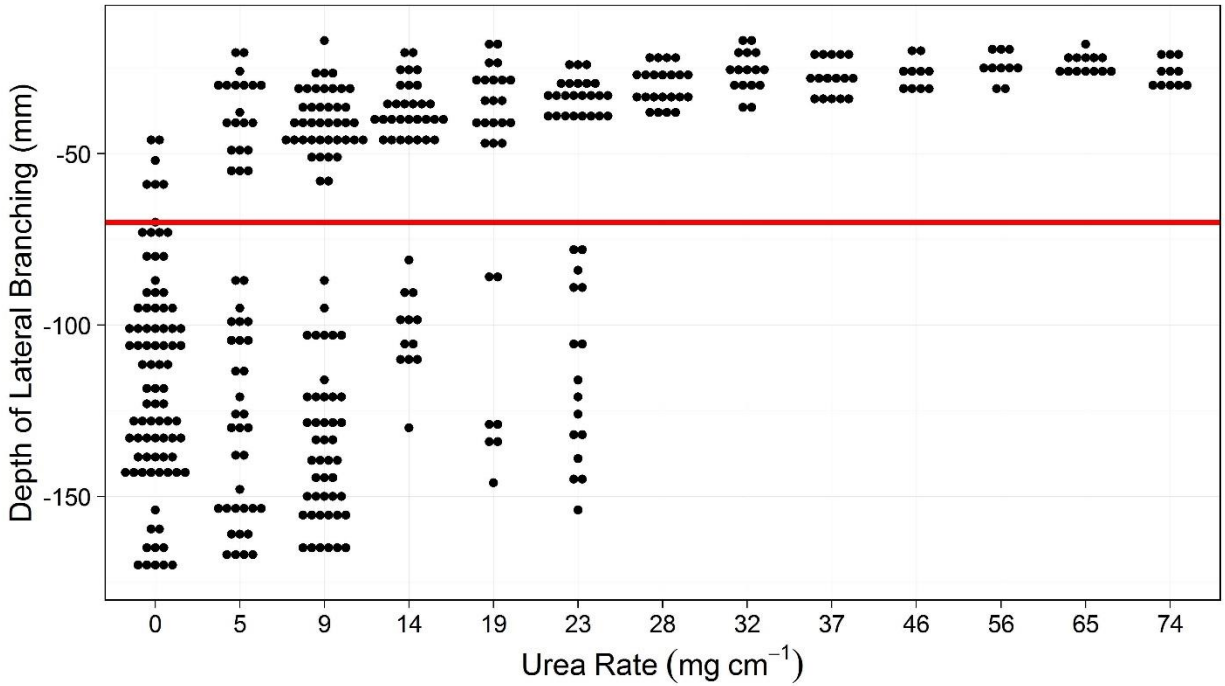


Figure 8: Depth of lateral branching points as influenced by urea rate at 14 DAP. The red line represents the depth at which the fertilizer was placed, and each dot represents a single point of lateral branching.

Summary of RSA Changes due to Increasing Urea Rates:

The RSA responses of Canola to $\text{NH}_3/\text{NH}_4^+$ toxicity surrounding the fertilizer band can be explained primarily by examining the apical movement through the soil profile. The tap roots of canola in the control grew through the soil column without impedance. Roots which grew through the urea band were either halted or delayed at varying distances from the urea band. The distance at which the root apexes halted from the band was determined by the rate of the urea applied which in turn controlled the initiation of lateral emergence from the tap root (Figure 3). From this observation the severity of symptoms can be broken down into two categories dependent on the rate of urea application: from 4.6-27.8 and > 27.8 mg urea cm^{-1} . Between 4.6-27.8 mg urea cm^{-1} the roots appear to be responding to increases in rate with increasingly affected RSA. However, at 27.8 mg urea cm^{-1} and above the

relationship between increasing modifications to RSA and increasing rates of urea appears to level off as survival any root survival becomes increasingly rare.

Depth of Tap Root Apexes in Urea vs. AS Treatments:

A visual inspection of the images contrasting the effect of urea and AS on canola root growth showed that all but one tap root stopped prior to reaching the fertilizer band in the urea treatments while multiple tap roots were able to penetrate the fertilizer band in the AS treatment (Figure 9). The average apical depth at day 10 of the experiment was -64, -97, and -126 mm for the urea, AS, and control treatments respectively (Figure 10). As previously noted in the increasing rate experiment with urea only a few root apexes can be found below the fertilizer band in the urea treatments. Although the tap roots in the AS treatment were able to grow through the fertilizer zone, they were significantly retarded by the AS compared to the control. Close up images of the root tips above the fertilizer band showed the roots exposed to urea exhibited more signs of necrosis and shrinkage than root tips exposed to the AS treatment (Figure 11).

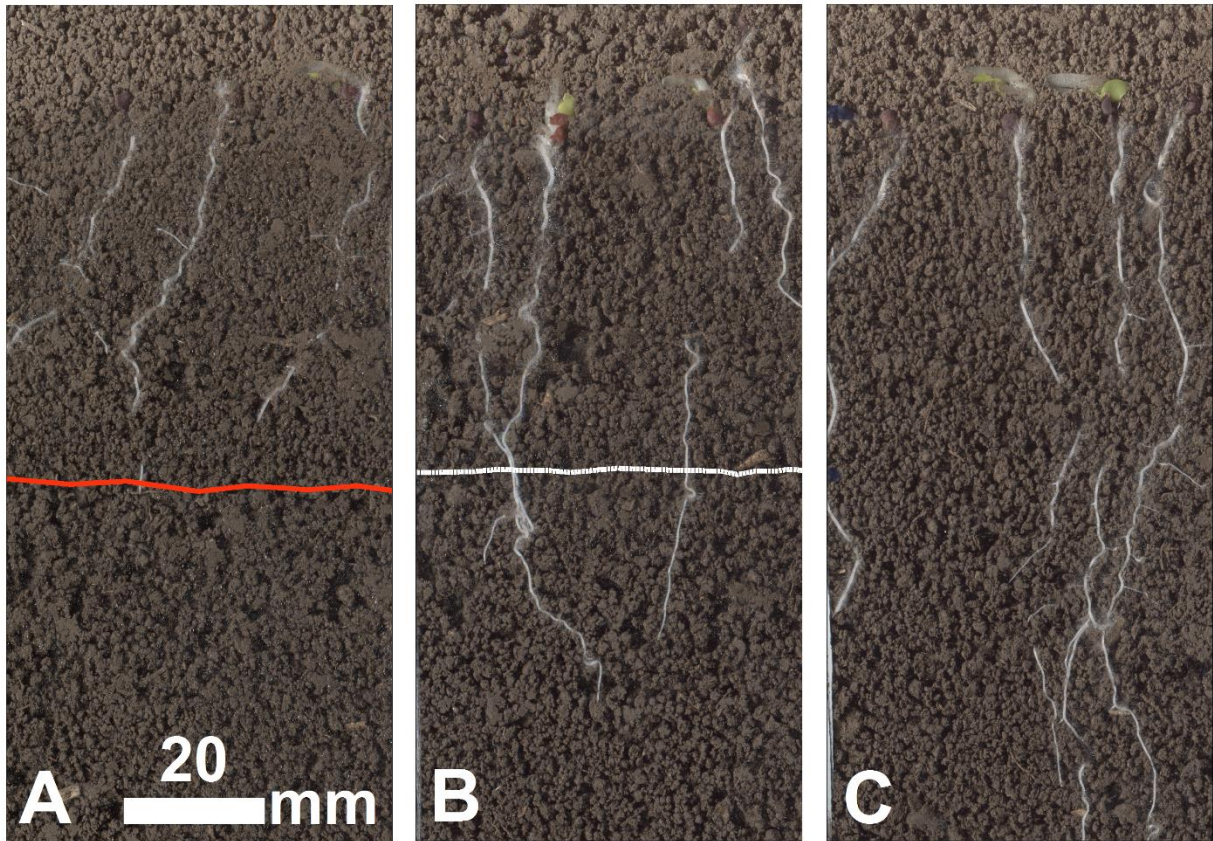


Figure 9: Canola roots exposed to urea (A), AS (B), and control (C). The red and white lines are the locations of the urea and AS bands respectively.

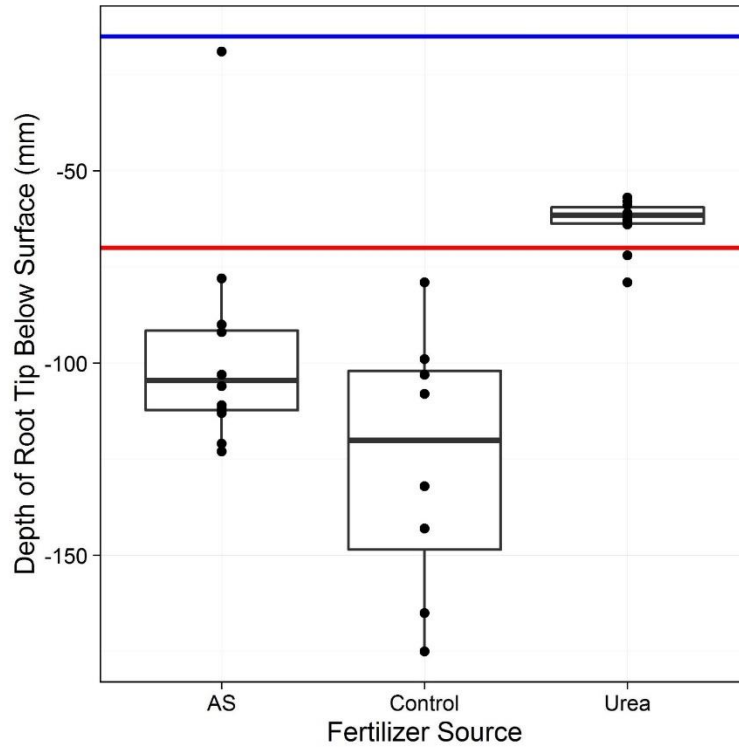


Figure 10: Urea and AS applied at 28.0 kg N ha⁻¹ depths 10 DAP.

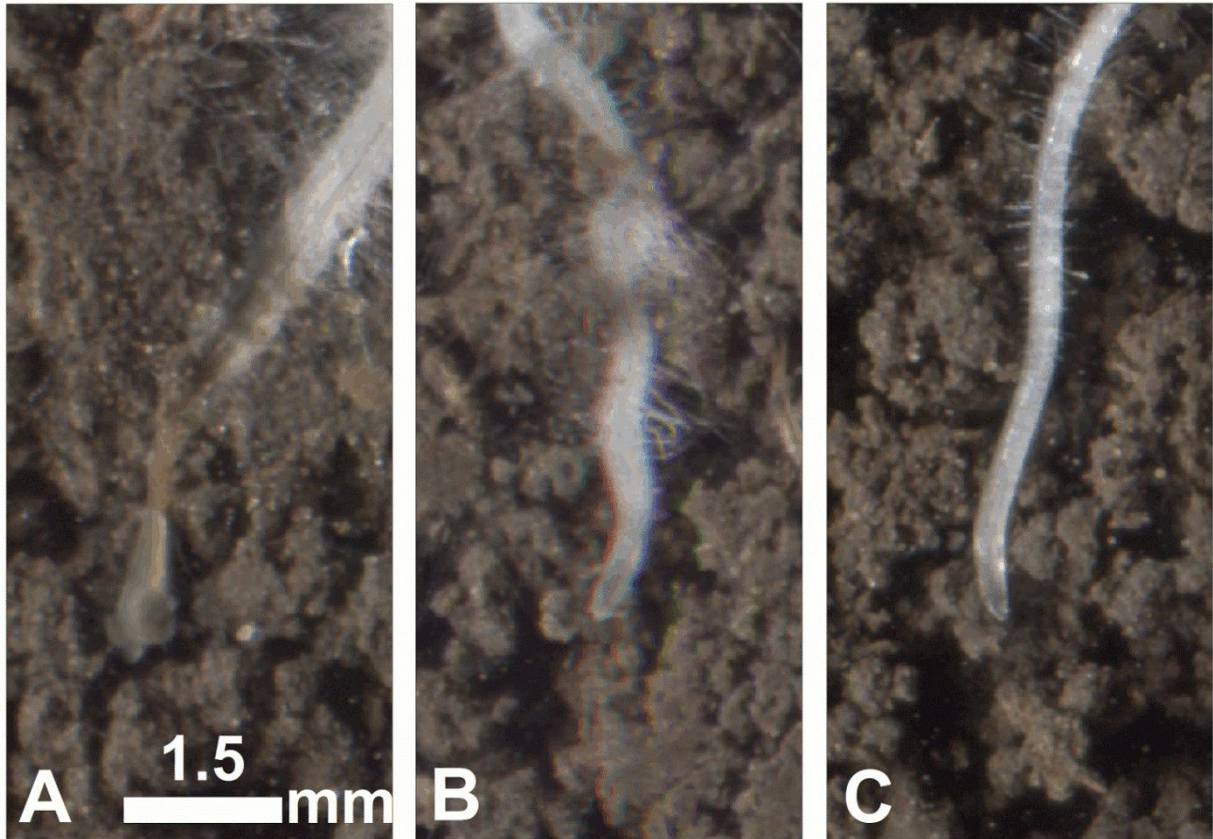


Figure 11: Tap root apices trips grown above urea (A), AS (B), and control (C).

Lateral Branching Initiation Points in AS vs. Urea Treatments:

Both the urea and AS had significant effects on the lateral branching point depth (Figure 12). The average depth of lateral branching points was 74.8, 32.3 and 39.1 mm below the soil surface in the control, AS, and urea (Table 1). The urea and the AS did not have significantly different lateral branching depths from each other, but both were significantly different from the control. In the urea treatments this was attributed to apical death. However, in the AS treatments the majority of tap root apices did not die prior to reaching the fertilizer band, and simply stalled near the AS band. Which indicates that while the AS did not stop the root apex from growing it temporarily suppressed apical dominance allowing for premature lateral emergence.

Table 1

Statistics For Depth of Lateral Branching Points						
	n	Mean		Median	SD	Variance
AS	4	-32.4	a	-32.5	4.8	23.4
Urea	4	-39.1	a	-39.4	1.6	2.5
Control	4	-74.8	b	-76.4	6.9	48.2

LSD = 7.95

All treatments initiated lateral branching on day 5 (Figure 11). The average lateral initiation date for the AS treatment was (5.7 DAP) significantly earlier than the average initiation of the control (7.8 DAP)(Table 2). Urea on the other hand was not significantly different from either the control or AS lateral initiation at 6.6 DAP. Urea had a later average lateral initiation date than AS because the AS treatment stopped lateral initiation at 8 DAP (Figure 11). The halt of lateral initiation in the AS treatments was likely due to the recovery of apical dominance by roots exposed to AS. Lateral root initiation is controlled by the ratio of cytokinin to auxins (Aloni et al. 2005, Werner and Schmulling 2009, Su et al. 2011). Auxin is produced in the shoots and promotes lateral emergence while cytokinin is produced in the root tips and transported longitudinally within the root inhibiting lateral initiation (Aloni et al. 2005). Damage or death of the root tip reduces the amount of cytokinin being produced in the root tip leading to the initiation and growth of lateral roots. The early initiation of lateral root emergence in both urea and AS treatments indicate a halt in cytokinin production. However, the halt of lateral emergence after day 7 indicate that cytokinin production had again begun, and lateral root initiation was suppressed. This suggests that the earlier average lateral initiation date in the AS treatments was a sign of decreased toxicity when compared with urea. This theory also supports the observation of increased apical death in urea treatments (Figure 9 and 10).

Table 2

Statistics For DAP of Lateral Branching Initiation						
	n	Mean	Median	SD	Variance	
AS	4	5.7 a		5.6	0.4	0.1
Urea	4	6.6 b		5.9	1.6	2.5
Control	4	7.8 ab		7.9	0.5	0.3

LSD = 1.59

Previously AS has been shown to have less severe effects on wheat roots than urea (Passioura and Wetselaar 1972). A primary difference between AS and urea is the pH of the two materials. The reactions immediately surrounding a urea fertilizer are considerably more basic than those of AS (Pang et al. 1973). The elevated pH results from the increase in the ratio of $\text{NH}_3:\text{NH}_4^+$ (Kissel et al. 2008). The distance at which the root tip halted in the urea treatments indicated that the toxic form of ammoniacal-N had moved further in the urea treatments than the AS suggesting the transport of NH_3 in its gas phase (Figure 10). Additionally it has been shown in the previous studies NH_3 is more toxic to plant roots than NH_4^+ (Bennet and Adams 1970). Indicating increased levels of NH_3 are responsible for both the more severe symptoms and increased distance of symptoms on roots from the source when comparing urea to AS.

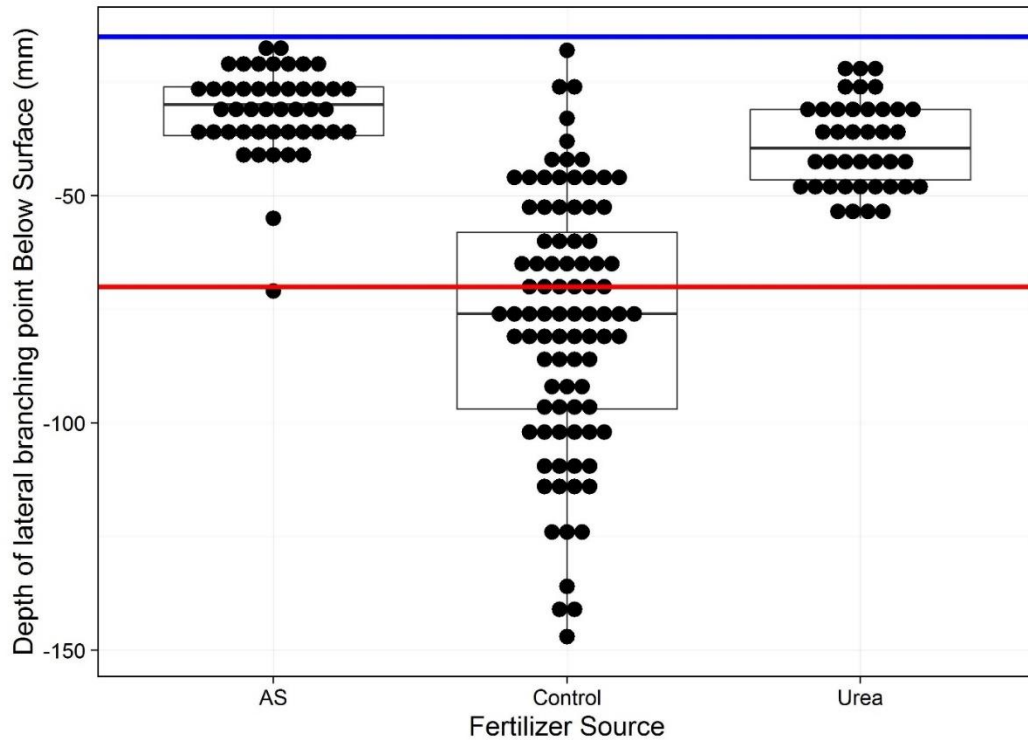


Figure 12: Depth of lateral branching points in canola plants exposed to AS, urea the control. Each dot represents one lateral branching point.

Conclusions:

- RSA was seen to change with both the rate and the source of the fertilizer.
- While, any amount of urea placed below a Canola seed will modify RSA, urea rates above 27.2 mg cm⁻¹ leave no chance for survival.
- Urea causes greater damage to occur at greater distances than the AS treatment indicating that ammonia plays a large role in urea toxicity.

CHAPTER 3: SEMI-AUTOMATED SPATIAL ANALYSIS OF ROOT TOXICITY SYMPTOMS IN RELATION TO SOIL CHARACTERISTICS OF FERTILIZER REACTION ZONES

Introduction:

Automated Image Analysis of Roots

There have been significant advancements in recent years in imaging and quantifying plant root mass in both 2D and 3D spaces (Neumann 2009). Much of the automation work has focused on linking genetics to phenotypic root system architecture (Pierret et al. 2003). These systems typically do not evaluate germplasm interactions with soil stressors. These interactions have largely been ignored based on their dynamic spatial heterogeneity. Some notable exceptions are studies focused on soil moisture, pH, and O₂ (Garrigues et al. 2006, Blossfeld et al. 2009). The central thesis of the present research is to tie localized soil chemical data with root health in order to better understand the impacts of highly variable environments on root health. An ideal test subject is the symptomology and timing of plant root response to a fertilizer reaction zone (FRZ) (Pan et al., 2016).

The Fertilizer Reaction Zone

The fertilizer reaction zone is a well-documented soil zone surrounding a fertilizer band. The localized disturbance of soil chemical processes due to banding of fertilizers below the surface is well documented (Heaney 2001, Pang et al. 1973). The FRZ is the volume of soil which is in immediate contact with and under the influence of chemical reactions dominated by the dissolution and secondary reactions of a concentrated fertilizer source. Soil variables in a FRZ, including pH, moisture, and oxidation reduction are radically altered and controlled by the chemistry of the fertilizer. (Heaney 2001, Pang et al. 1973, Kissel et al. 2008). Nevertheless, the initial conditions of the bulk soil also play a large role in determining the chemical reactions following fertilizer banding (Pang et al. 1973). In addition, the

chemical speciation of mineral nutrients in the surrounding soil is dominated by fertilizer chemistry, making it important to consider the fertilizer forms when predicting the resulting

FRZ chemistry. Different sources of N will have much different FRZs from each other. In this work we used urea. The FRZ of urea can be two pH units higher than the bulk soil (Pang et al 1973). The presence of ammoniacal-N has been correlated with the level of root toxicity symptoms (Bennet and Adams 1970). The distance at which symptoms occur from the band of N is thus inherently connected to the spread of ammoniacal-N through the soil. The spread of ammoniacal-N will be dominated by NH_3 gas, since its diffusion is roughly 1000 times greater than that of ammonium (Bell 2006).

While the formulation, of the fertilizer is the driving factor in determining the properties and development of a FRZ, the intrinsic bulk soil properties and environmental conditions at the time of application are also important in FRZ formation (Kissel et al. 2008). The texture of the soil greatly influences the rate at which anions will move through the soil specifically inhibiting NH_4^+ spread through the soil and quickly adsorbing it to soil cation exchange sites (Fenn and Kissel 1976). The moisture of the soil determines the rate of multiple reactions in the chain of reactions leading from urea to NO_3^- , and also affects rates of gas and soluble ions through soil (Ponnamperuma 2012; Patrick and Reddy 1976, Zhong et al. 2015). Accurate description of the FRZ is important for determining where the levels of ammoniacal-N are elevated and for predictions of fertilizer toxicity reactions.

Model applications

Modeling the dissolution and transformation of urea and subsequent reaction products is a means of describing the FRZ. Due to the difficulties of directly measuring the concentration of NH_3 in the soil, modeling can be used to better understand the spatial and temporal distribution of NH_3 in the soil. The purpose of the model in this study was to add a temporal dimension to the

measurements of soil ammoniacal-N to simulate elevated soil NH_3 relative to the locations of root symptoms at different time intervals.

The main goal of this research is to study root interactions with N fertilizer and water with high temporal and spatial resolution. Spatial information systems have been used to analyze root systems in the past (Gasch et al. 2011, Le Bot et. Al 2010, Lobet and Draye 2013, Ma Qingua 2013, and Vosllness 2013, Silva 2014). However, in the cases cited above only two used the highly developed data storage capabilities of GIS software (Gasch et al. 2011, Silva 2014). When dealing with large data sets, such as the ones presented here, GIS software can prove to be a useful tool for analyzing root-soil interactions. It was hypothesized that the symptoms of ammoniacal-N toxicity in the roots will correspond to localized gradations in modeled NH_4^+ , NH_3 and moisture over time.

Methods

Experimental Setup

An 18.5 h by 21.5 w by 7.5 d cm wide growth container was attached to the face of an Epson V37 document scanner (Epson Perfection V37, Epson America, Long Beach, CA). Four growth containers were used and each scanner was divided in half with a plastic divider allowing for a total of 8 seeding rows and their corresponding fertilizer bands. Seed rows and fertilizer bands were placed perpendicular to the scanner face allowing for the simulation of 8 separate scanner rows (Figure 13). The fertilizer band and seeding row were 7.52 cm long. The seed row was placed approximately 2.5 cm below the surface, and the urea band was placed 5.0 cm below the seed row. The two fertilizer treatments were replicated three times each and the control was replicated twice. The high and low urea treatments were 12.84 mg N cm^{-1} and 6.42 mg N cm^{-1} respectively. The control had 0 mg N cm^{-1} . Prior to planting, the soil was wetted to 0.2 g g^{-1} moisture and allowed to equilibrate in a sealed container for more than 24 h. Plants were grown on a lab bench and on a 16:8 h light/dark cycle. Scanner timing and resolution were controlled using VueScan automated scanning software (VueScan, Hamrick Software). Images were set to be

collected every 4 h at $1890 \text{ pixel cm}^{-1}$, occasionally a software or hardware error lead to missing images in the time sequence.

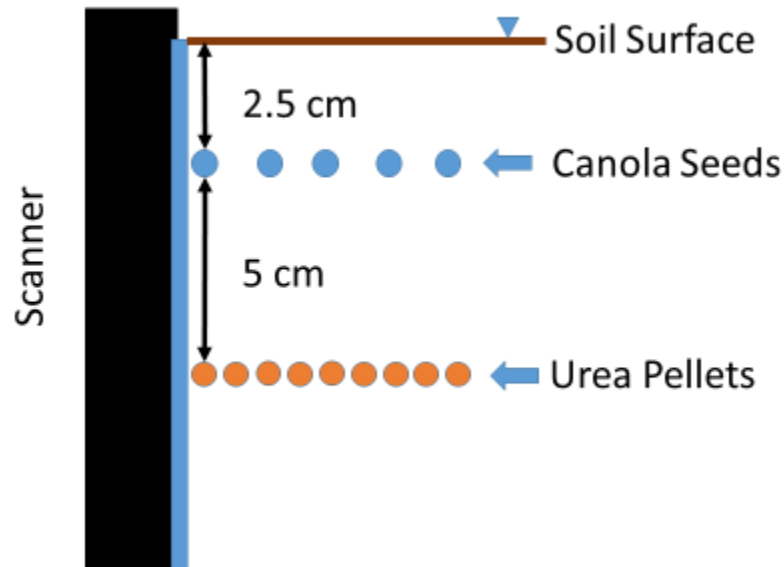


Figure 13: Cross section showing seed and urea row orientation in relation to the scanner face.

Data Analysis

Our data analytical approach centered on the integration of three measured and modeled soil and root data sources into a single spatial data frame to visualize and analyze the dynamics of toxicity surrounding a fertilizer toxicity zone.

Image classification and symptom identification. The image data was subset from the initial 4 h interval to a 24 h interval for improved analytical efficiency. A two phase process was used in order to accurately describe the location and the timing of symptoms and soil processes. In the first phase of classification, roots were separated from the soil based on color. In the second phase, root health was detected measuring the root color as a proxy for root health.

A pixel by pixel statistical approach was used to classify the roots and soil. The Maximum likelihood (ML), Majority Filter, Boundary Clean, Aggregate, and Reclassify Tools

from ArcMap's spatial analyst tool box were used in the classification process (ESRI ArcMap, Redlands, CA). A signature file with three classes (roots, soil aggregates, and soil pores) was developed through visual inspection. Each classification was defined using 30 scattered polygons from a single image from the time sequence. The ML tool was then run on all images in the time sequence and the classified rasters were passed on to the remaining Spatial Analyst tools for noise reduction. The generalized images were then submitted to a validation process. The validation process was conducted on a total of 16 images with 4 sets of 4 images coming from different DAP on different scanners. A total of 784 points (49 per image) were selected from the 16 images. All of the points representing soil pores and aggregates were randomly selected across the 16 images, but many of the root points were manually selected, as a random scattering of points selected an inadequate number of root points. Each point was visually assigned an "observed", value of "root", "soil aggregate", or "soil pore", and the corresponding "predicted" value was extracted from the generalized image. The predicted and observed values were then compared using a confusion matrix (Table 3). The confusion matrix was constructed using the Caret package in R (R Core Team 2016, Vienna, Austria, Rstudio Team 2016, Boston, MA).

Root health was quantified by determining the average red value of the root on a mm by mm basis. ArcMap was used to construct root centerlines which were common across all times for an individual root system. The first step in creating a centerline was converting the classified rasters into shapefiles having the three feature classes mentioned above. The root polygons for every time in the series were merged to make a single polygon which represented the maximum extent to which the roots reached. A centerline was then created for the maximum root extent polygon using a 'create skeleton' tool. The red values of the initial rasters were then summarized

along the centerline at increments of every 1mm using zonal statistics. The data was exported and root color was analyzed in R statistical software (R Core Team 2016, Vienna, Austria, Rstudio Team 2016, Boston, MA). Maps of root health were made by classifying the root as ‘healthy’ if the red value was equal to or greater than 120 or ‘unhealthy’ if the red value was less than 120.

Destructive sampling and interpolation of NH_4^+ . Destructive samples were taken on DAP 15. One set of samples per scanner was taken for a chemical analysis of NH_4^+ and NO_3^- . Six samples per seed row (twelve per scanner) were extracted using a 7mm wide corer for chemical analysis. The samples were taken in a manner to allow for a vertical transect of 4 samples passing directly through the simulated planter row, and 2 more samples to the left and the right of from the planter row. Three moisture samples were taken per scanner. The three moisture samples were taken from three apparently distinct color zones in the soil in order to include the widest range of moisture values. The zones of soil moisture included a 0 to 3 cm top depth, a 3 to 10 cm middle depth and a below 10 cm bottom depth. Samples were weighed, oven dried at 105 C for 24 hr, and reweighed to determine the gravimetric moisture. All samples were spatially referenced by taking a scan of each sampling location and manually referencing the sample point to the image.

Parameterization of N transformation and transport model. Hydrus-1D was used to model the conversion of urea to NH_3 , NH_4^+ , NO_2 , and NO_3^- and the subsequent transport of these N forms through the soil profile from the original fertilizer location (University of California Riverside, Riverside, CA). The approximate ranges for the diffusion rates of the solutes and the first order degradation rates were determined through literature review and relied heavily on

modeling work done in Wang et al. 1998 and Shah et al. 2004. Fine tuning of the parameters was done by comparing the NH_4^+ profile after 360 h (15 DAP) to the measured data collected at 15 DAP.

Table 3

Hydrus-1D Model Parameters			
N species	Aqueous Diffusion Coefficient ($\text{cm}^2 \text{h}^{-1}$)	Gaseous Diffusion Coefficient ($\text{cm}^2 \text{h}^{-1}$)	First Order Reaction Rates (h^{-1})
Urea	0.03	-	0.01350
NH_3	0.01	10	0.10000
NH_4^+	0.01	-	0.00735
NO_2	0.05	-	0.01000
NO_3^-	0.05	-	0.00000

Because the model calculations were only run in one dimension, the interpolation of the models into the two dimensional space of the scanner images was done by using three vertical vectors, one centered on the fertilizer point and the other two located 25 mm from the fertilizer in opposing directions. The side vectors were set to 0 mg cm^3 ammoniacal-N while the row centered on the fertilizer point was set to values exported from the model at 24 h time steps

Results & Discussion

Qualitative Analysis of Root Images

Urea modified the root architecture in both the high (6.4 mg N cm^{-1}) and the low ($12.8 \text{ mg N cm}^{-1}$) urea treatments when compared with the control. The most notable symptom was apical halt and premature lateral emergence as noted in chapter 3. Lateral branching occurred above the fertilizer band in all replicates of both the 6.4 mg N cm^{-1} and $12.8 \text{ mg N cm}^{-1}$ urea treatments by 3 DAP (Figure 14 – 19). In the control, two lateral roots on DAP 3 were initiated above the equivalent depth of the urea band, but there appeared to be much less lateral initiation

in the 0 mg N cm⁻¹ control plants than the treated plants (Figure 20 & 21). Tap root growth also markedly differed in the control plants where the tap roots passed immediately through the vicinity of the equivalent depth of the urea band by 3 DAP (Figures 20 & 21). In contrast, all visible tap roots stopped a minimum of 7 mm from the fertilizer band in the low treatment and 8 mm in the high treatment (Figure 14 & 19). The tap root remained traceable from the seed until coming within 15 mm of the urea band or the equivalent depth in reps 1 and 3 of the high treatment, in reps 2 and 3 of the low treatment, and in rep 1 of the control (Figures 14, 16, 18, 19, and 20). The other 3 replicates had severe gaps in the visibility of the root sections, especially in the case of rep 2 of the high treatment (Figures 15, 17, and 21). By 8 DAP, lateral roots proliferated within 5 mm of fertilizer band in two of the three reps (Figures 17 & 18). No roots lateral roots proliferated within 5 mm of the urea band in the high treatments.

In addition to the RSA symptoms, it is worth noting that there were also physiological morphological changes by DAP. The tap root in all of the scanned plants except one of the controls showed signs of shrinkage and browning (Figures 14-19 & 21). The roots exposed to the high N treatment shrank from the apex and progressed basipetally indicating that the fertilizer band was the source of these symptoms (Figures 14 & 16). This progression of shrinkage and browning has been formerly detected using similar scanning methods (Pan et al. 2016). Additionally, researchers using destructive sampling have found 'browning' of maize (*Zea mays*) roots surrounding a urea band of 76 mg N cm⁻³ (Creamer and Fox 1980). Conversely, browning and shrinkage also occurred in the control plant, but progressed in an acropetally direction moving from the base of the tap root toward the root apex.

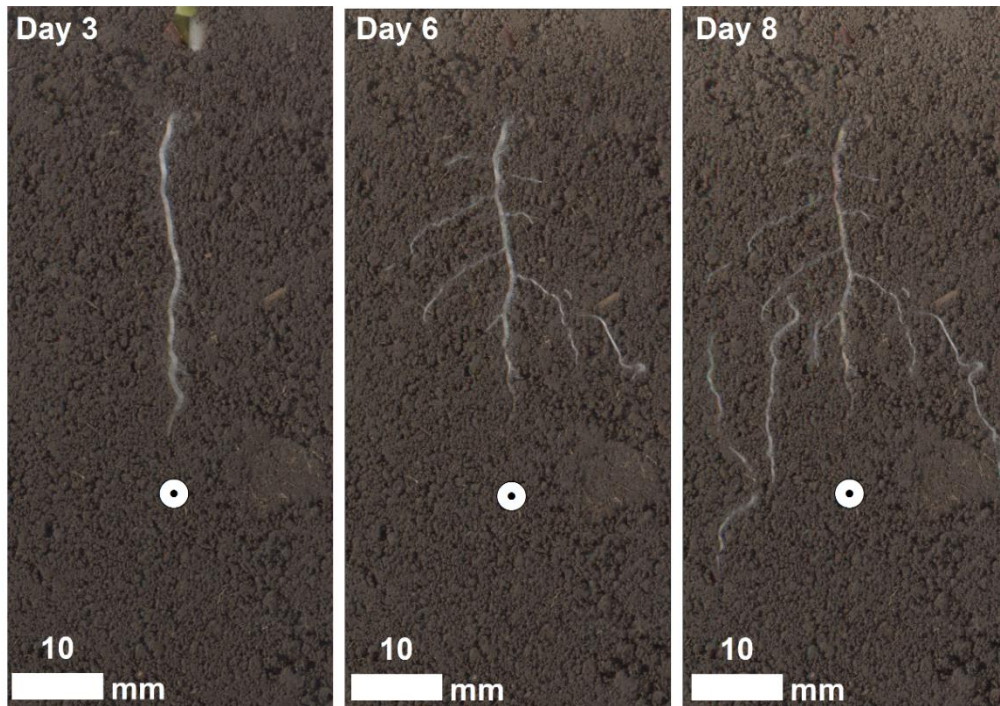


Figure 14: Canola seedling root system exposed to urea band $12.8 \text{ mg N cm}^{-1}$ on 3, 6, 8 DAP.

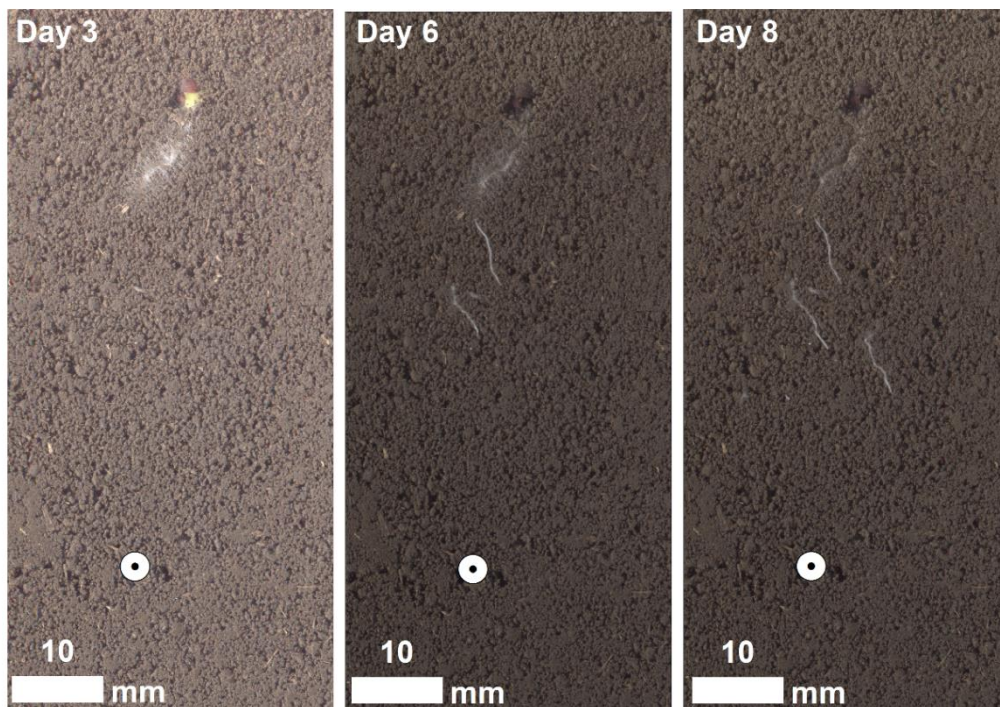


Figure 15 : Canola seedling root system exposed to urea band $12.8 \text{ mg N cm}^{-1}$ on 3, 6, 8 DAP.

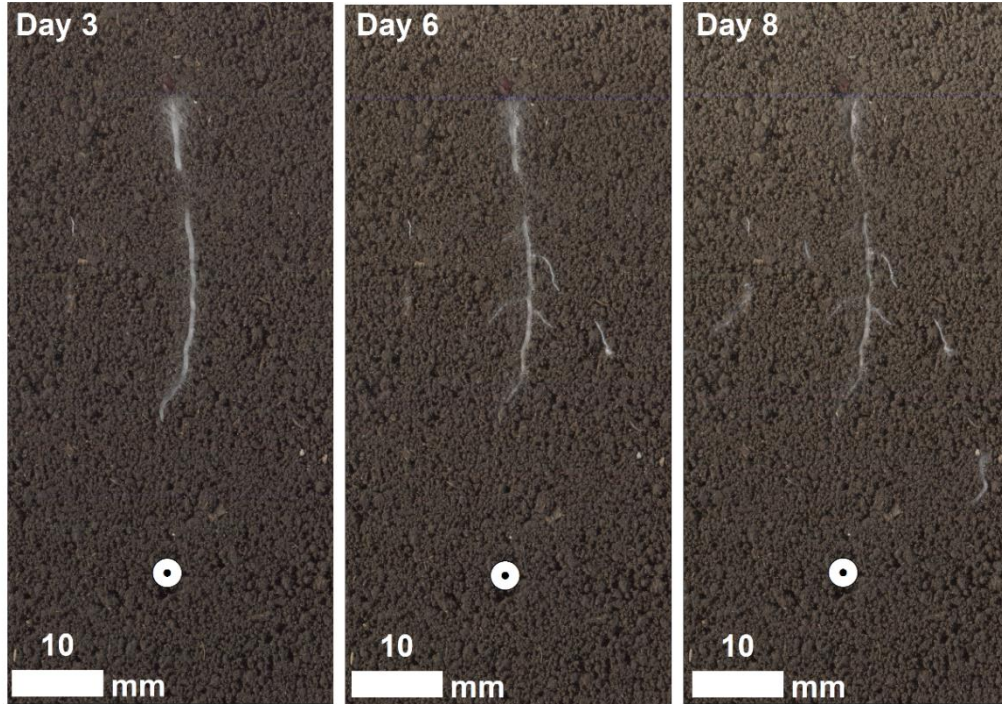


Figure 16: Canola seedling root system exposed to urea band $12.8 \text{ mg N cm}^{-1}$ on 3, 6, 8 DAP.

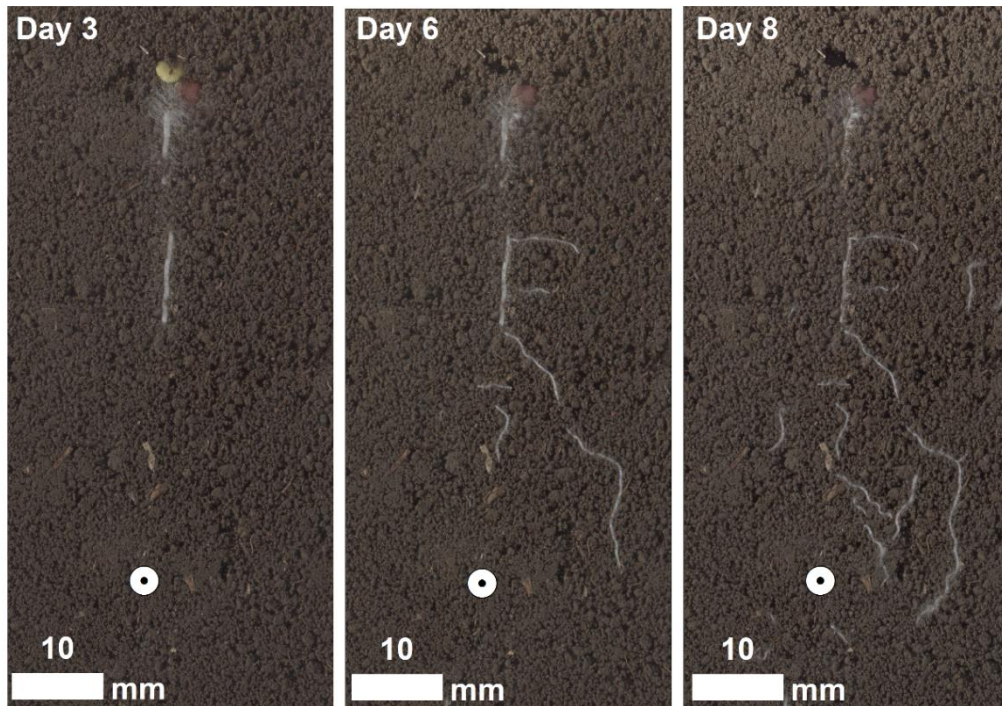


Figure 17: Canola seedling root system exposed to urea band 6.4 mg N cm^{-1} on 3, 6, 8 DAP.

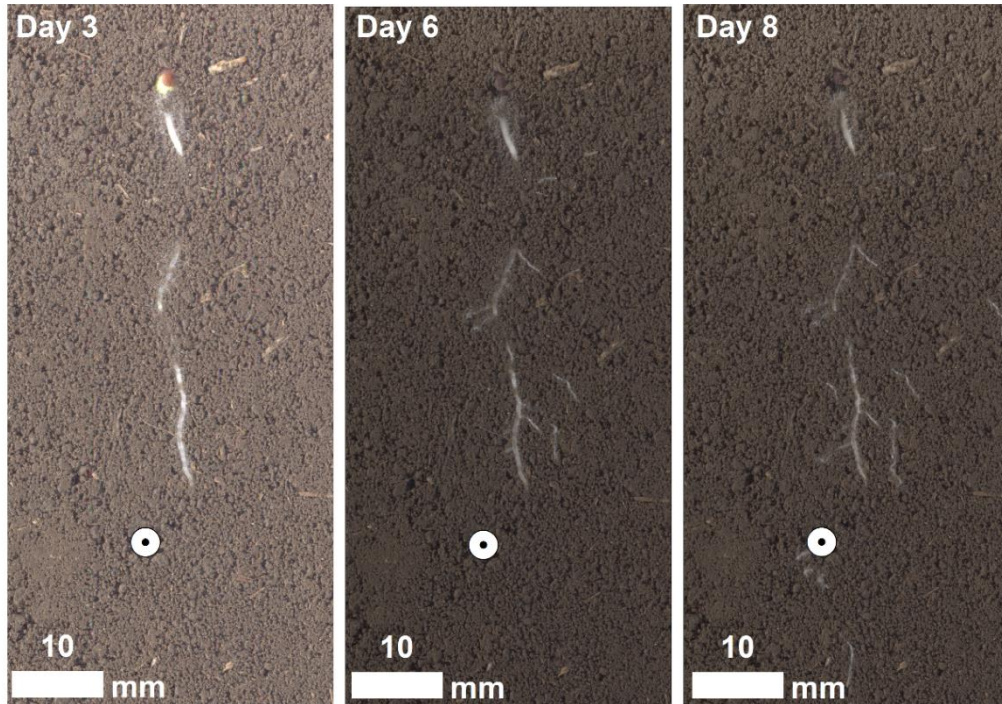


Figure 18: Canola seedling root system exposed to urea band 6.4 mg N cm^{-1} on 3, 6, 8 DAP.

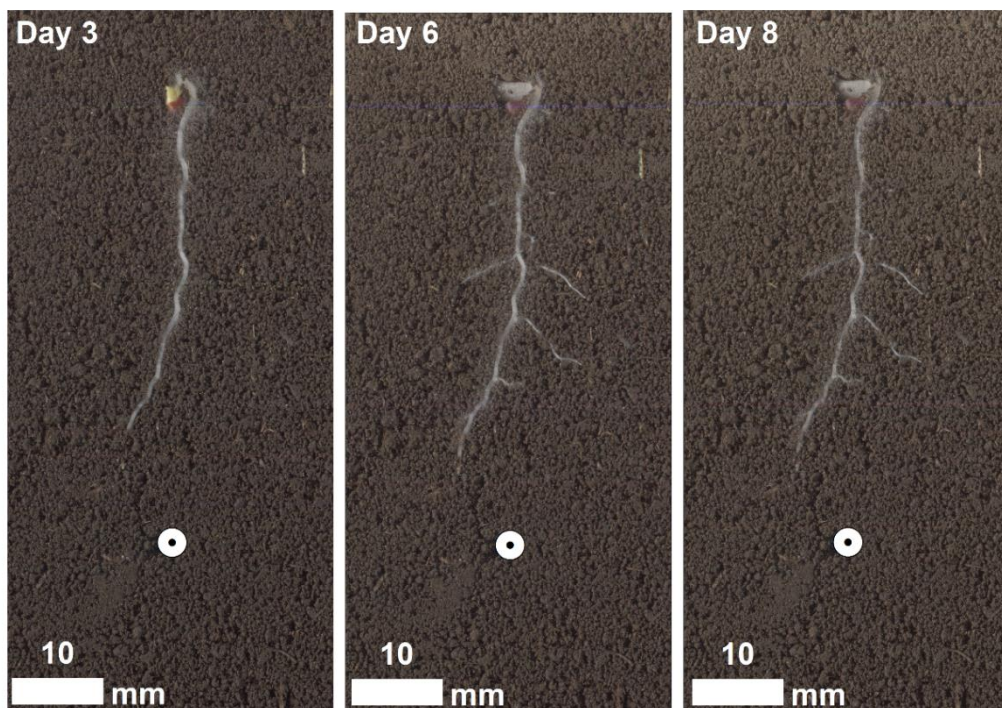


Figure 19: Canola seedling root system exposed to urea band 6.4 mg N cm^{-1} on 3, 6, 8 DAP.

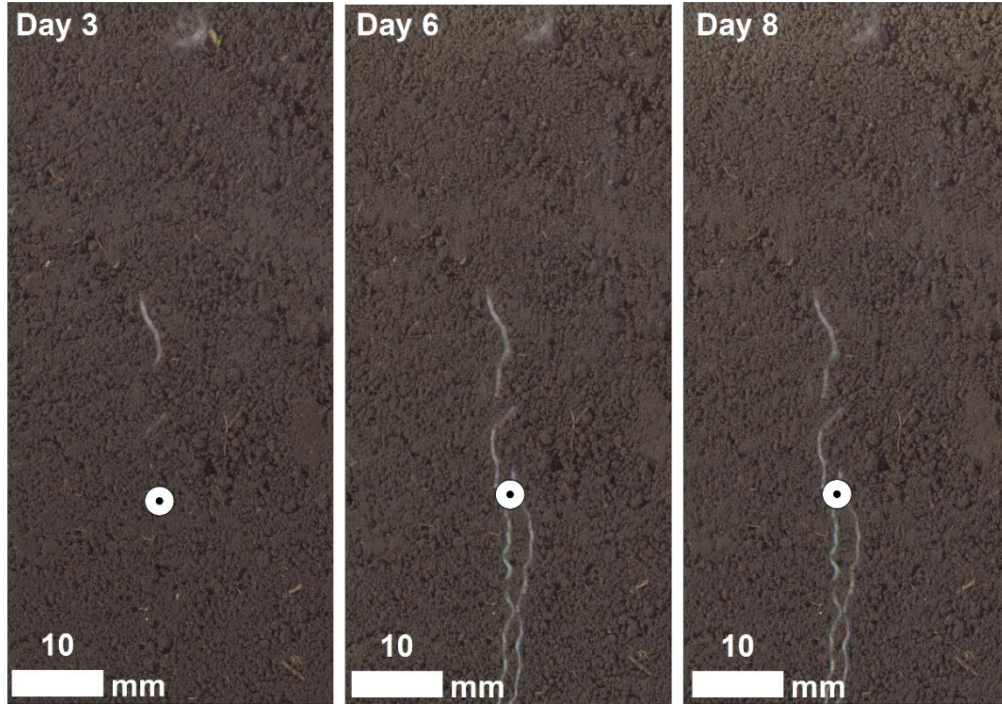


Figure 20: Canola seedling root system exposed to no urea band 3, 6, 8 DAP.

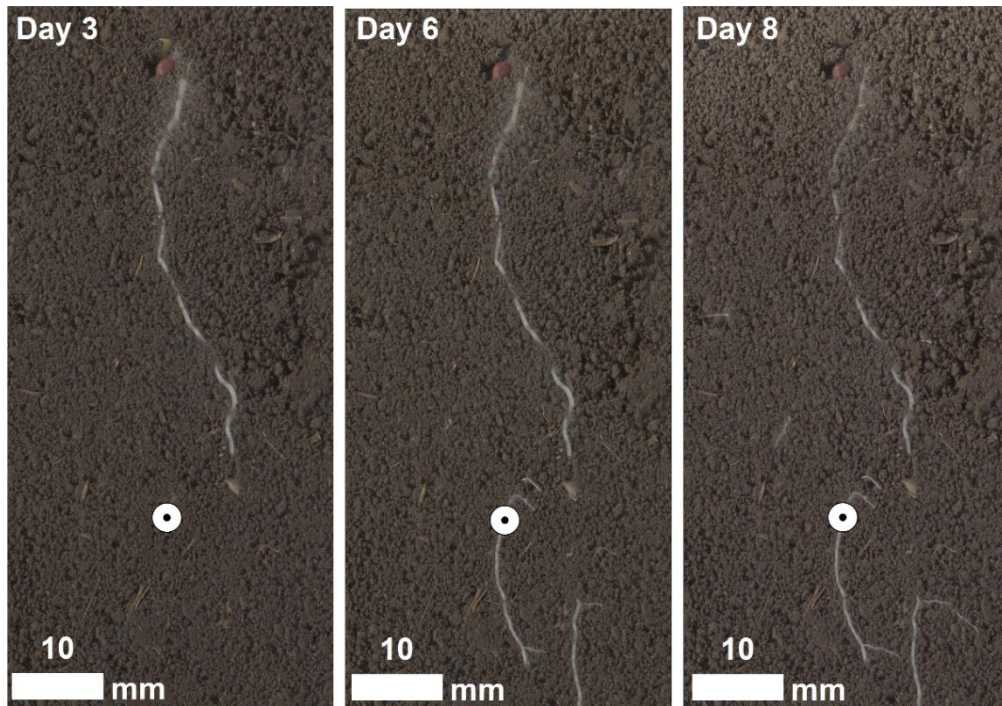


Figure 21: Canola seedling root system exposed to no urea band on 3, 6, 8 DAP.

Root Classification and Validation

Root and soil pixels were correctly classified with a high degree of certainty, with 92% of 185 visually identified root reference points being correct, and 98% of the 174 predicted root points were positively confirmed as roots (Table 4). From this we can see that our method strongly avoid predicting a root when there is not a root, making it a conservative classification method. A conservative classification method is more likely to miss detecting root points than miss classifying soil as roots. Much of the work on automated detection of roots has focused around RSA traits such as root length, branching rate, and branching angle. The majority of quality checks is done by comparing a manual measure of length with an automated measure of length (Ingram and Leers 2000). A pixel by pixel validation of root detection is more important to this study as the focus of the study was on the health of the roots at individual points rather than the overall root architecture. Some researchers have previously used root color to predict root health, but have done so with visual inspection and considered it a qualitative variable (Comas et al. 2000, Reid et al. 1993). Root color may change as a result of aging and suberization, not necessarily root death (Rewald and Ephrath 2012).

Table 4

Error Matrix for Detecting Soil Pores, Soil Aggregates, and Roots				
Reference				
Prediction	Root	Aggregate	Pore	
Root	171	3	0	98
Aggregate	13	310	4	95
Pore	1	24	259	90
	92	91	98	
Over all Accuracy = 0.94				

Interpolated Concentration

The interpolation of ammoniacal-N surrounding the urea placement for 6.4 mg N cm⁻¹ and 12.8 mg N cm⁻¹ showed elevated levels of ammoniacal-N surrounding the point of urea placement (Figure 22). The concentration ranged from 0.536 mg NH₄⁺ cm⁻³ at the center of the 12.8 mg N cm⁻¹ urea treatment down to a background concentration of 0.002 NH₄⁺mg cm⁻³ in the bulk soil. The highest concentrations of ammoniacal-N were found to be 10 mm above the depth of fertilizer placement. This suggests ammonia gas generated after urea hydrolysis may have tended to diffuse upwards from the fertilizer, since this gaseous form has a specific density of 0.717 kg m⁻³. This observation is consistent with previous research indicating that ammoniacal-N migrates as NH₃ gas up through the soil profile (Creamer and Fox 1980), due to NH₃ having a lower density than O₂.

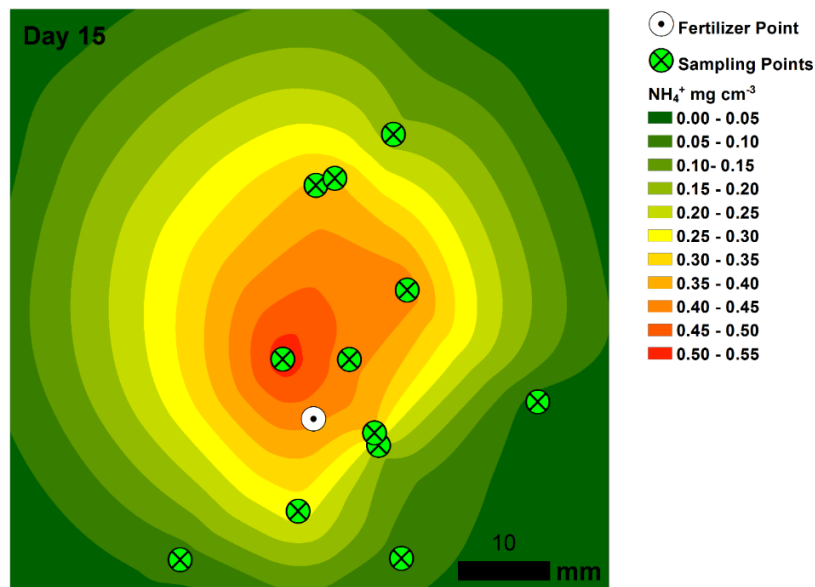


Figure 22: Inverse distance weighted interpolation of Ammoniacal-N from sampling points taken on DAP 15

Model Profile and Validation

The Hydrus-1D model was able to accurately predict the relative magnitude of the range and amplitude of ammonium concentrations at 15 DAP, but the depth of the peak ammonium concentration was offset. The observed values showed an upward shift in the elevated ammonium that peaked 10 mm above the band, while the model distributed the ammonium peaked only 4 mm from the original band location (Figure 23). The rate of NH_3 gas diffusion, the conversion of urea to NH_3 , the rate of NH_3 to NH_4^+ conversion, and the conversion of NH_4^+ to NO_2 were found to be the four most important factors when comparing the measured and modeled NH_4^+ depth distribution. Increasing the rate of gaseous diffusion from $10 \text{ cm}^2 \text{ hr}^{-1}$ to $100 \text{ cm}^2 \text{ hr}^{-1}$ flattened the shape of the profile distribution. Decreasing the rate of gaseous diffusion from $10 \text{ cm}^2 \text{ hr}^{-1}$ to $1 \text{ cm}^2 \text{ hr}^{-1}$ led to a narrower distribution which peaked above the concentration of the control (Figure 24). The decreasing NH_3 diffusion rate had a similar impact on NH_3 as NH_4^+ as diffusion rate increases the amount of NH_3 escaping both out the bottom and the top of the soil profile increases (Figure 24). Assuming the gaseous diffusion of NH_3 is 1000 times greater than the dissolution of NH_4^+ in solution $10 \text{ cm}^2 \text{ hr}^{-1}$ is at the lower end of the range used in previous modeling work (Shah et al. 2004, Wang et al. 1998). Because the field was wetted to near field capacity, some reduction in the rate NH_3 diffusion was probable (Moldrup et al. 2000).

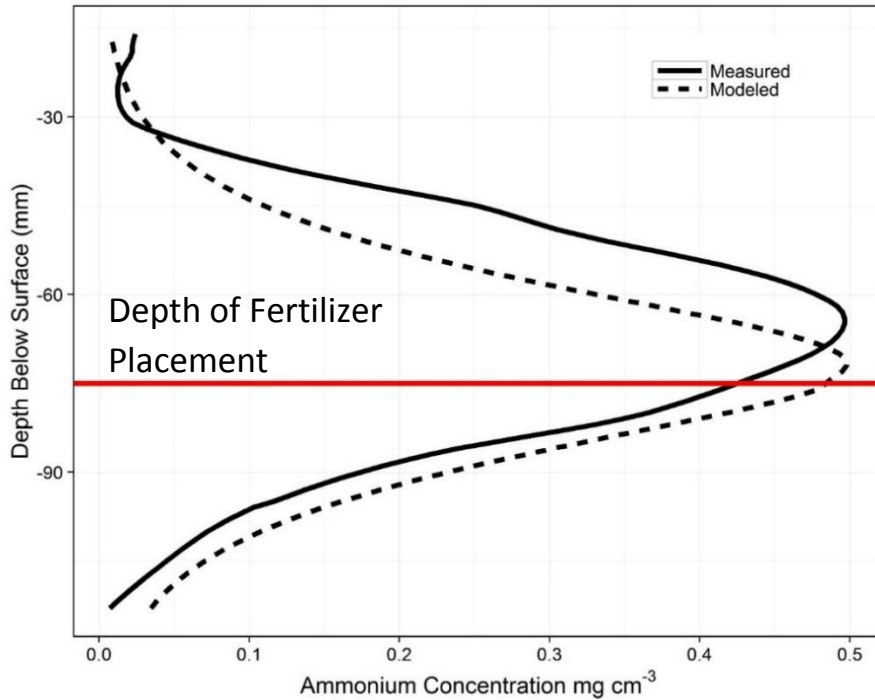


Figure 23: Comparison of measured and modeled ammonium distributions.

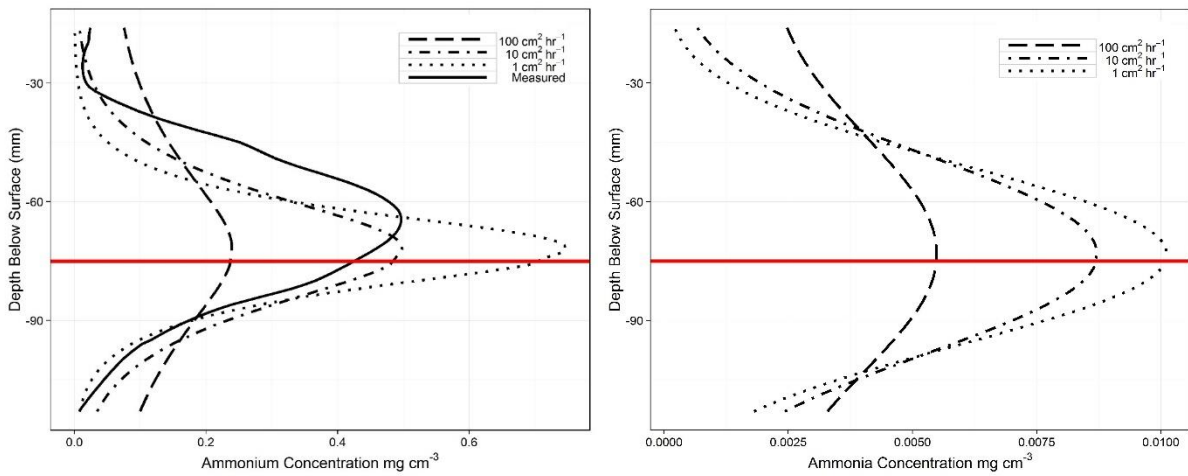


Figure 24: Model sensitivity to NH_3 gas diffusion rate.

The dissolution of the urea pellets and hydrolysis of urea, due urease activity, also had an interesting effect on final NH_4^+ concentrations. Increasing the first order rate constant of the urea to NH_3 from 0.0135 hr^{-1} to 0.135 hr^{-1} lead to a decrease in peak concentration to around 0.15 mg cm^{-3} lower the

measured 0.5 mg cm^{-3} . Interestingly, decreasing the constant also decreased the peak concentration from 0.5 mg cm^{-3} to 0.32 mg cm^{-3} . However, the shape of the distribution changed depending on whether the first order rate constant was increased or decreased (Figure 25). Ling and El-Kadi (1998) estimated that the first order rate constant for urea hydrolysis was between 0.015 and 0.023 hr^{-1} .

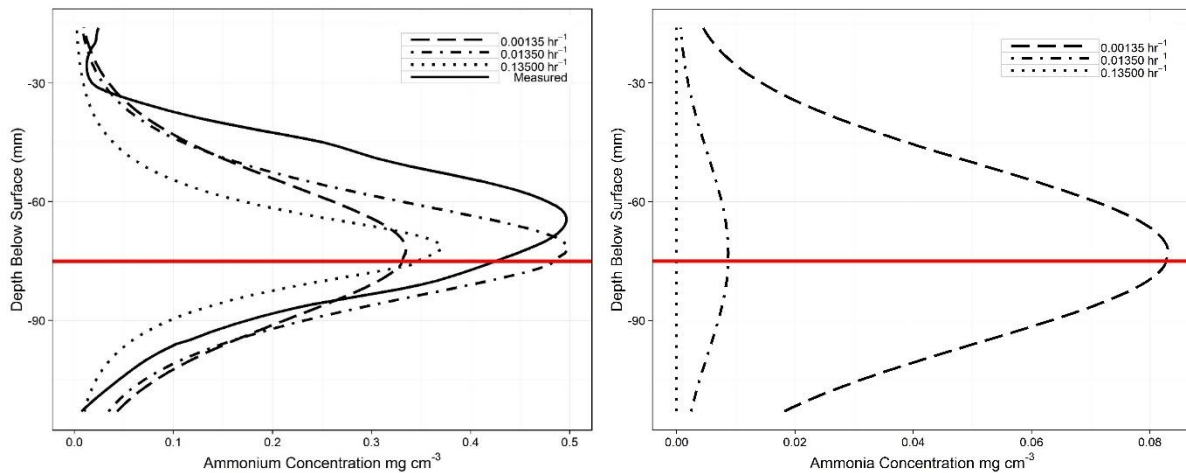


Figure 25: Model sensitivity to changes in the rate of urea to NH_3 reaction.

The conversion of NH_3 to NH_4^+ also plays an important role in the distribution of ammoniacal-N throughout the profile. A reduction in the rate of NH_3 to NH_4^+ conversion leads to an increase in the amount of time which NH_3 may migrate as a gas. The conversion process is dominated by the pH of the soil solution (Kissel et al. 2008, Shah et al. 2004). The dissolution of urea has been shown to increase the pH in the fertilizer microsite by up to two units across varying soils (Pang et al. 1973). The elevated pH surrounding a FRZ would lead to a greatly decreased conversion rate (Heaney 2001, Izaurralde et al. 1987, Yadvinder-Singh and Beachamp 1988.). If the conversion rate is decreased at the same time as the gas diffusion rate of NH_3 is increased, the NH_3 escapes from the profile, but if the diffusion rate is slowed while the conversion rate is slowed, there are no major changes to the shape of the ammoniacal-N distribution as the whole process has in effect been simply slowed (Figure 26).

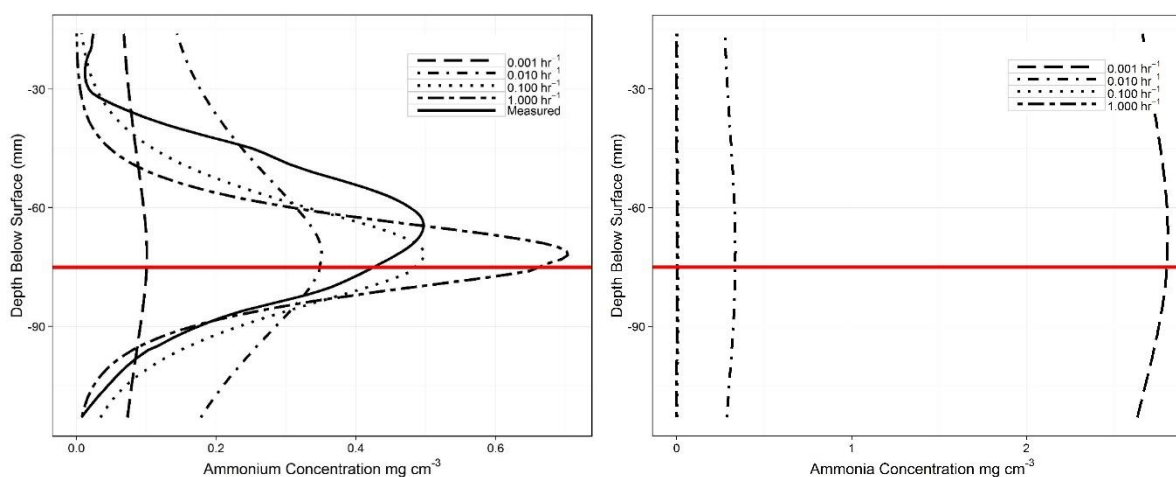


Figure 26: Model sensitivity to changes in rate of NH_3 to NH_4^+ reaction.

The third important factor affecting the final ammoniacal-N distribution was the rate of nitrification. Nitrification rates can also be greatly depressed in the FRZ leading to N remaining in ammoniacal forms in the FRZ (Yadvinder-Singh and Beachamp 1988). However, the value we chose for the first order reaction rate constant for nitrification ($0.00735 \text{ mg cm}^{-2}$) was not so much lower than those considered in previous modeling studies which ranged from 0.00783 - 0.03 mg cm^{-2} (Hanson et al. 2006). Any increase in the rate of nitrification led to a sudden decrease in NH_4^+ (Figure 27). Some attempt was made to model the movement of transformation of various nitrogen species through two different soil materials in order to represent the heterogeneity of the FRZ. The first material simulated the localized area surrounding the fertilizer band with elevated pH and decreased nitrifying bacteria and the second material simulated the bulk soil with near neutral pH and moderate levels of nitrifying bacteria. The results of the two material model fit well to the measured data at 360 h, but the time steps between 0 and 360 h showed highly non-normal results occurring at the seams between the two materials. A more accurate representation of the overall process would be two feedback loops which would connect the dissolution of urea to a localized increase in pH and the movement of NH_3 to a localized decrease in

nitrification. This process has been modeled to better include the biological and chemical feedbacks in custom software written in Fortran (Wang et al. 1998). However, modeling these particular feedback loops is not within the abilities of Hyrdus-1D. The results which were spatially referenced and interpolated as raster data in Arcmap were based on the best achievable model using Hyrus-1D (Figure 11).

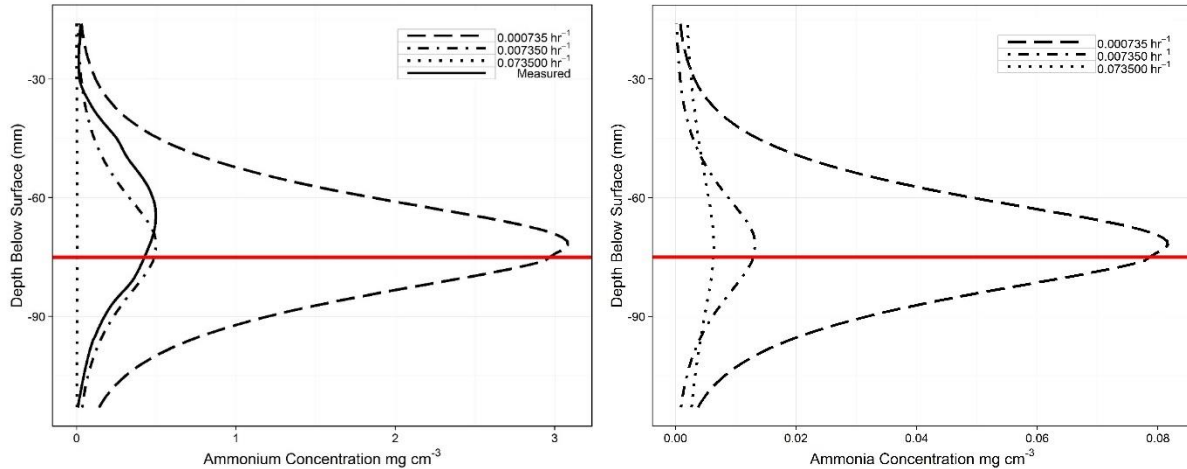


Figure 27: Model sensitivity to changes in the rate of NH_4^+ to NO_2 reaction.

The concentrations of both NH_4^+ and NH_3 changed over time decreasing from with peak solution concentration decreasing from above $0.9129 \text{ mg N cm}^{-3}$ at day 72 h to $0.0658 \text{ mg N cm}^{-3}$ 240 h (Figure 28). The modeled results show that by 240 h the ammonium had almost entirely dissipated from the soil profile while there were still substantial amounts of NH_4^+ . NH_3 to be toxicity in cotton (*Gossypium hirsutum*) has been detected at rates as low as $0.0031 \text{ mg N cm}^{-3}$ (Bennet and Adams 1970). Toxicity in Maize (*Zea mays*) was much higher at $0.1680 \text{ mg N cm}^{-3}$ (Blanchar 1967). Reductions in radicle length have been shown in Canola (*Brassica napus*) grown aeroponically over a solution of 102 mM of $\text{NH}_3(\text{OH})$ (Dowling 1998). Using the aeroponic method cotton was seen to have significantly less reductions in root length than canola (Dowling 1998). In the modeled data NH_3 concentrations at 3 DAP were shown to be two orders of magnitude greater than those required for incipient toxicity in cotton

(Bennet and Adams 1970). The model data was then interpolated using an IDW interpolation tool in ArcMap (Figure 28). The resulting rasters were used as background NH_3 and NH_4^+ concentrations throughout the imaged data (Figure 29 & 30).

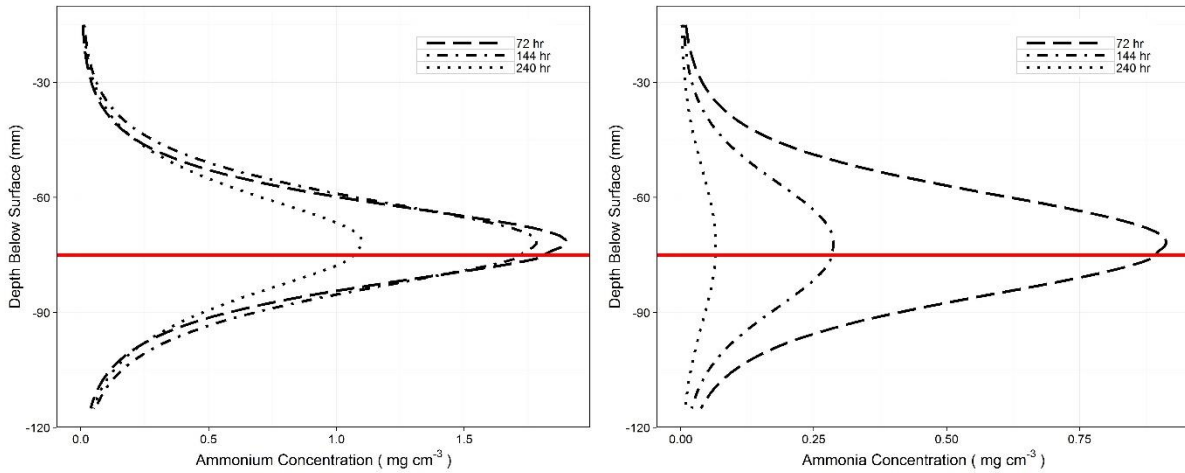


Figure 28: NH_4^+ and NH_3 concentrations by depth at 72 h (3 DAP), 144 h (6 DAP), and 240 h (8 DAP).

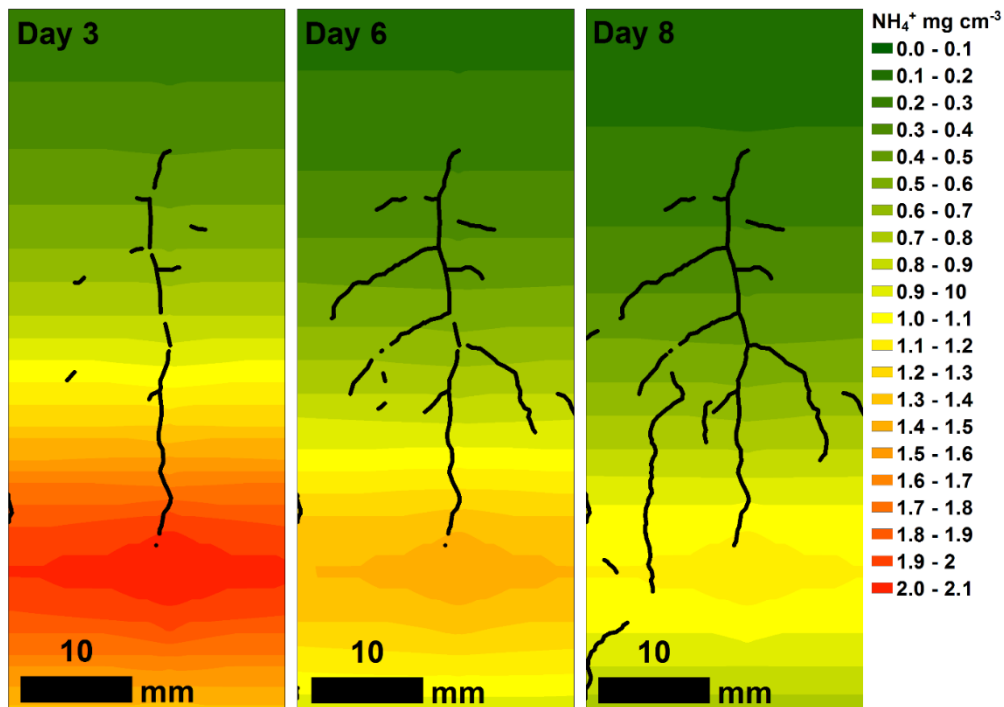


Figure 29: Modeled NH_4^+ concentrations and root skeleton overlay on 3, 6, and 8 DAP.

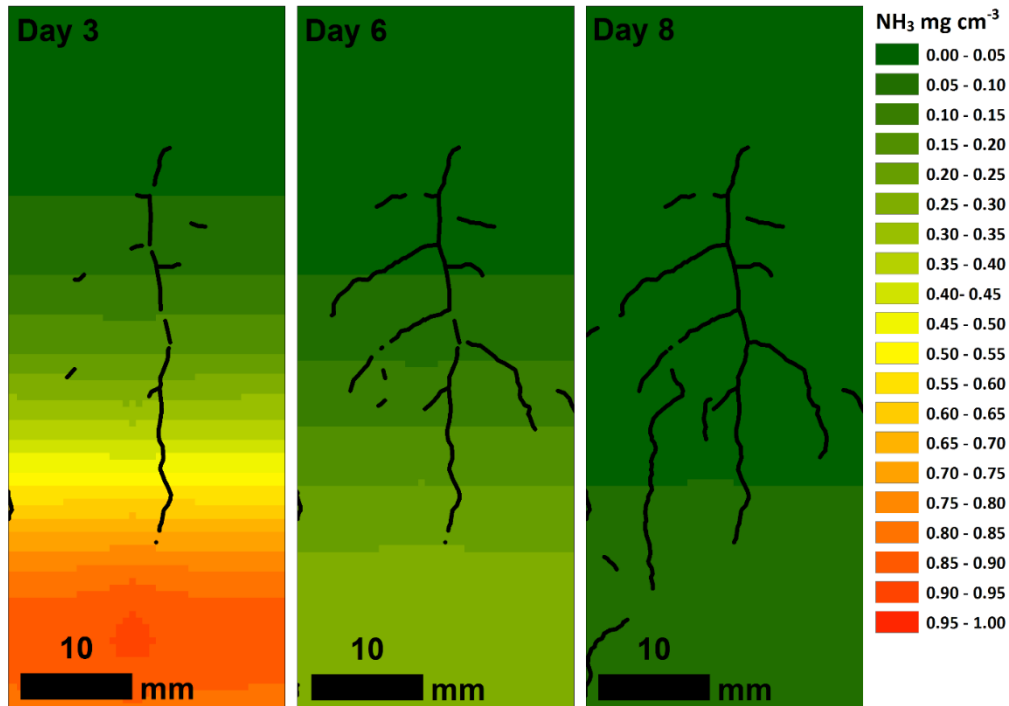


Figure 30: Modeled NH_3 concentrations and root skeleton overlay on 3, 6, and 8 DAP.

Relationships Between Root color and modeled Ammonium

In comparing the gradation in the modeled and NH_4^+ to the health of roots, determined by root health. It can be seen that in rep 1 of the high treatment roots defined as ‘unhealthy’ are concentrated in the high NH_4^+ near the tip of the tap root. However, by 8 DAP, a lateral which has achieved gravitropism, and is growing past the depth of the fertilizer band, appears to be healthy (Figure 31). Similarly the changes in NH_3 overtime indicate that the symptoms on at 3 DAP were an effect of the heightened concentrations of NH_3 , but that by 8 DAP there is little connection between the unhealthy roots and the NH_3 concentration (Figure 32). The changing color, as a symptom, highlights the necessity of analyzing root health in the context of changing NH_3 and NH_4^+ concentrations.

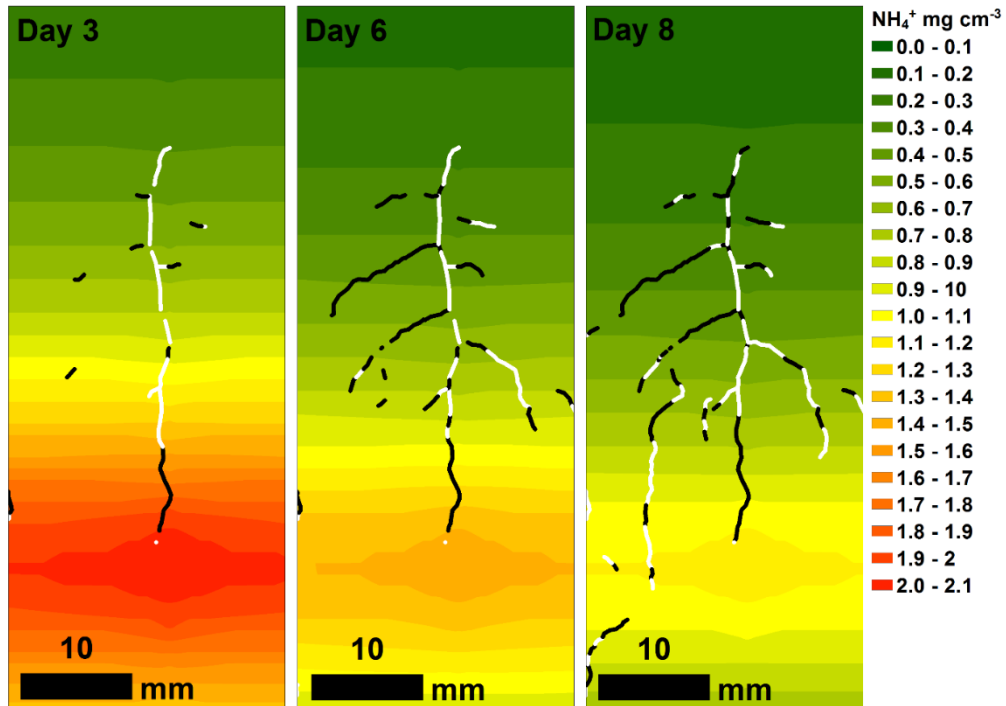


Figure 31: Root health as determined by color in relations to modeled NH_4^+ concentrations on 3,6, and DAP.

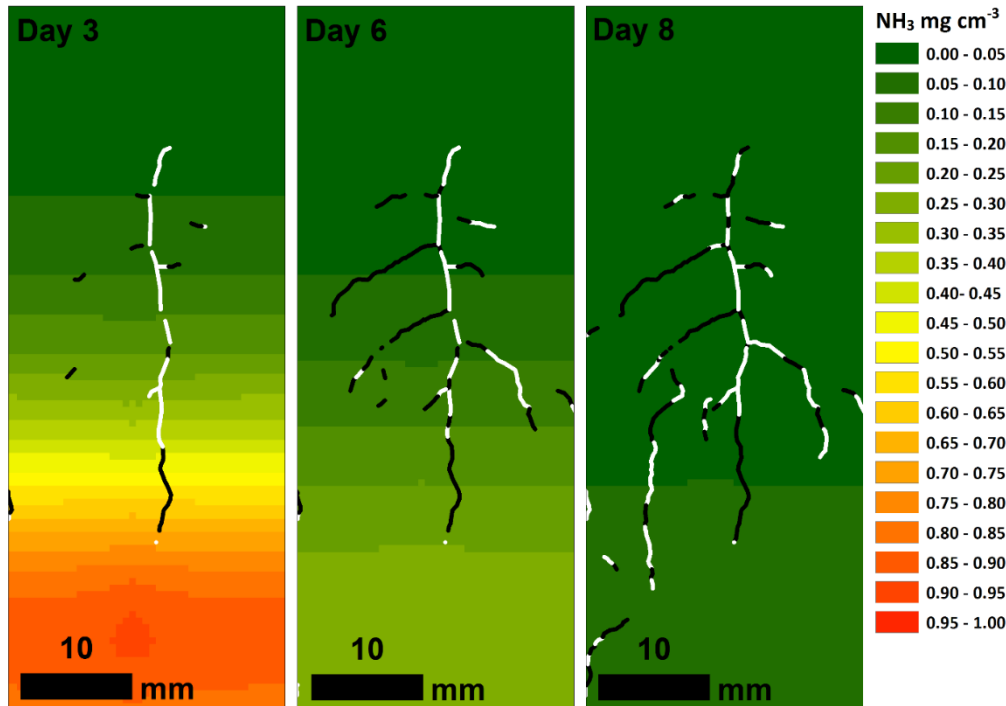


Figure 32: Root health as determined by color in relations to modeled NH_3 concentrations on 3, 6, and 8 DAP.

The correlation between the modeled NH_4^+ concentrations and the root color at 3, 6, and 8 DAP were plotted, but showed extremely weak to nonexistent correlations. In all cases there was a slight negative trend (Figure 33). These negative trends between NH_4^+ and color were as would be expected if background concentrations NH_4^+ were an important factor in the development of toxicity symptoms. The 3 DAP trend between modeled NH_4^+ and root color was the strongest correlation ($r^2 = 0.2$) (Figure 34). The weakness of the trends in general indicates that the background NH_4^+ concentrations does little to explain the occurrence of symptoms in the poisoned root. The most negatively sloping trend line was found to be on 6 DAP with a slope of -29.168 (Figure 35). By 8 DAP the modeled NH_4^+ showed an almost horizontal relationship with root color indicating that any negative relationship between the soil NH_4^+ concentrations and the root symptoms have disappeared (Figure 36). The decrease in the slope and correlation with the passage of time especially going from 6 DAP to 8 DAP, indicates the detectable

symptoms are losing their spatial association with the distribution of NH_4^+ as time goes on. The average color of all roots also decreases with time decreasing from a red value of 134.5 on 3 DAP to a red value of 118 on 8 DAP. This decrease in overall color value indicates, that although there is not a negative trend associated with increasing NH_4^+ concentrations in 8 DAP the root system as a whole may be exhibiting signs of stress.

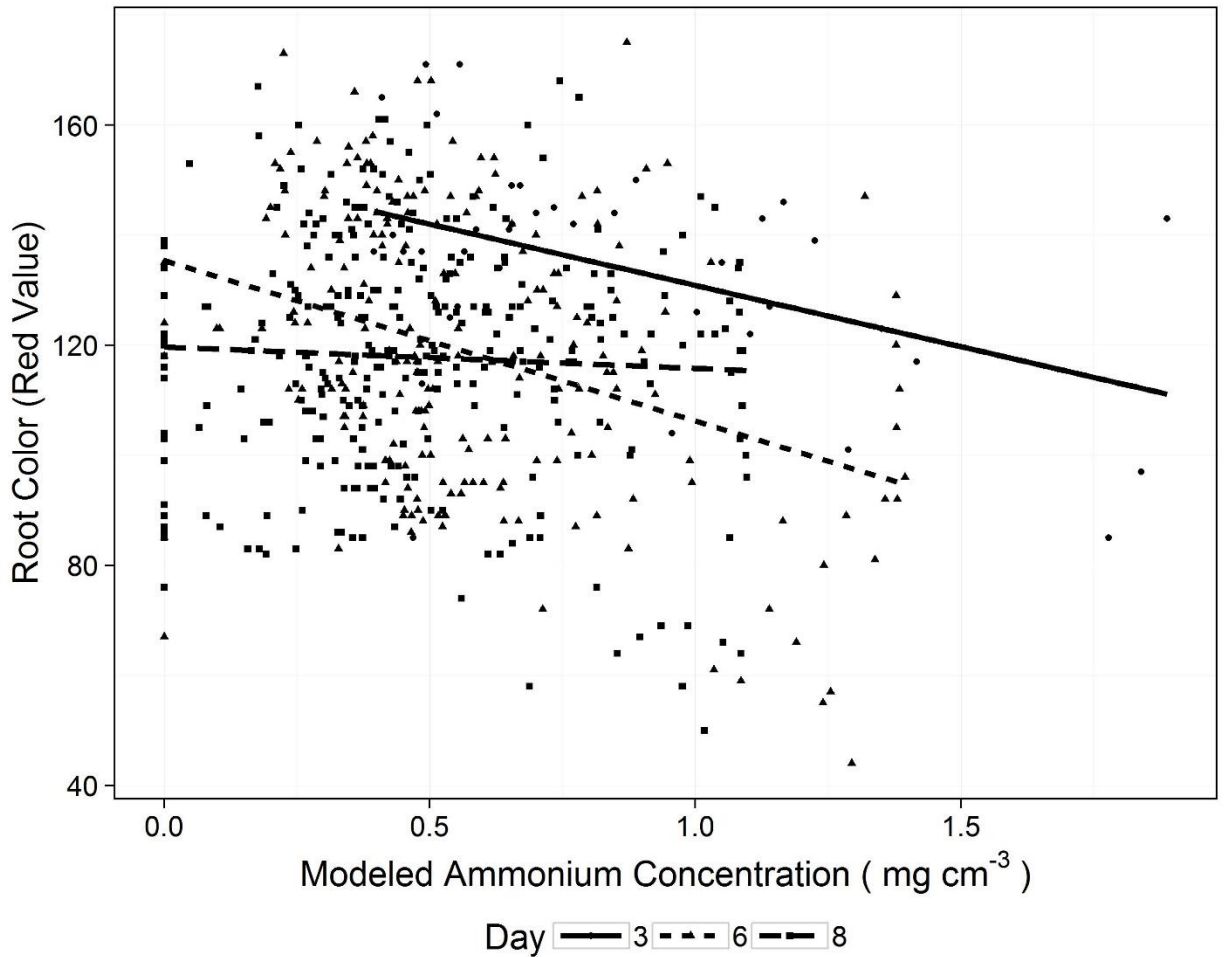


Figure 33: Correlations between root color and modeled NH_4^+ concentrations on 3, 6, and 8 DAP.

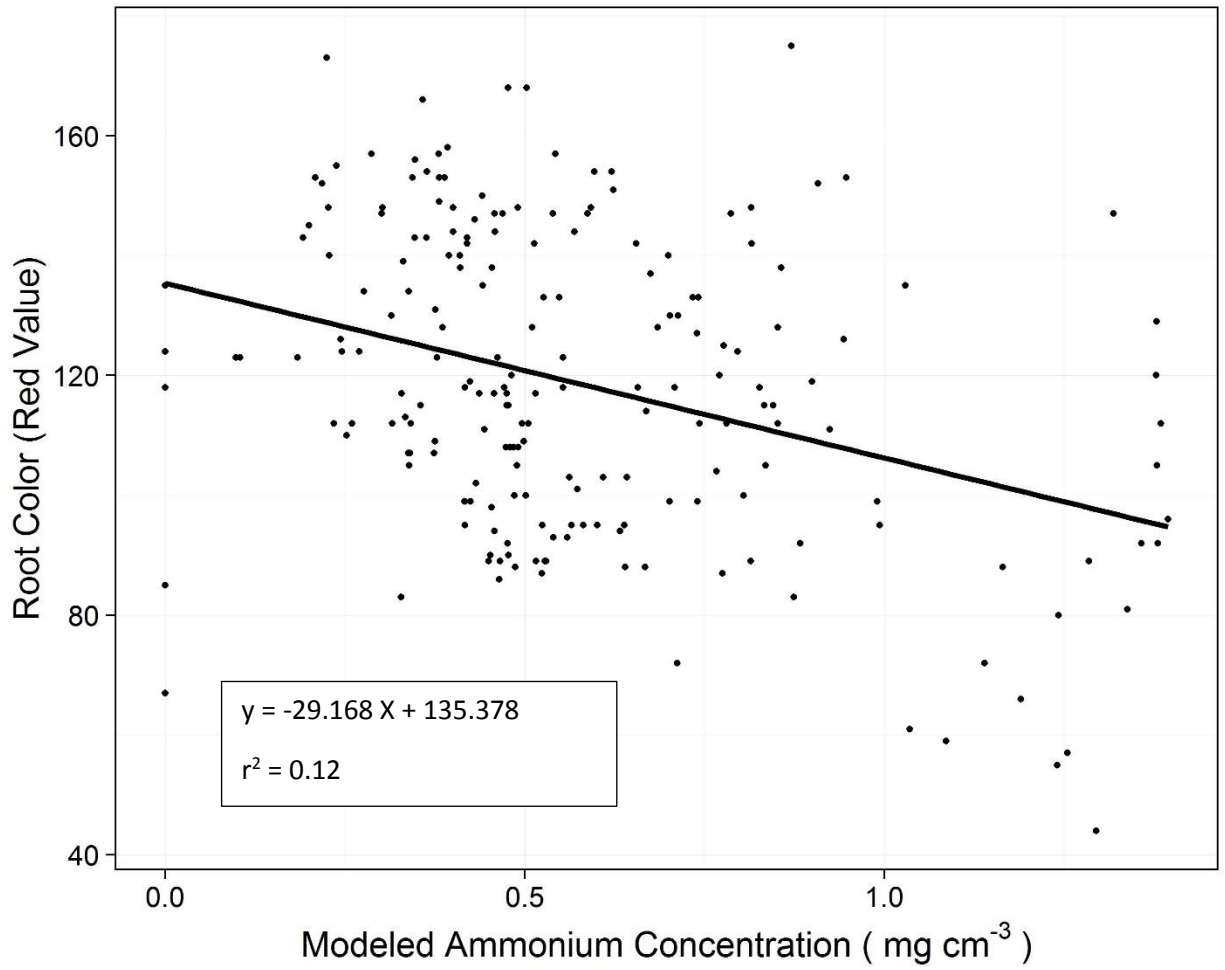


Figure 35: Correlation between root color and modeled NH_4^+ concentrations on 6 DAP.

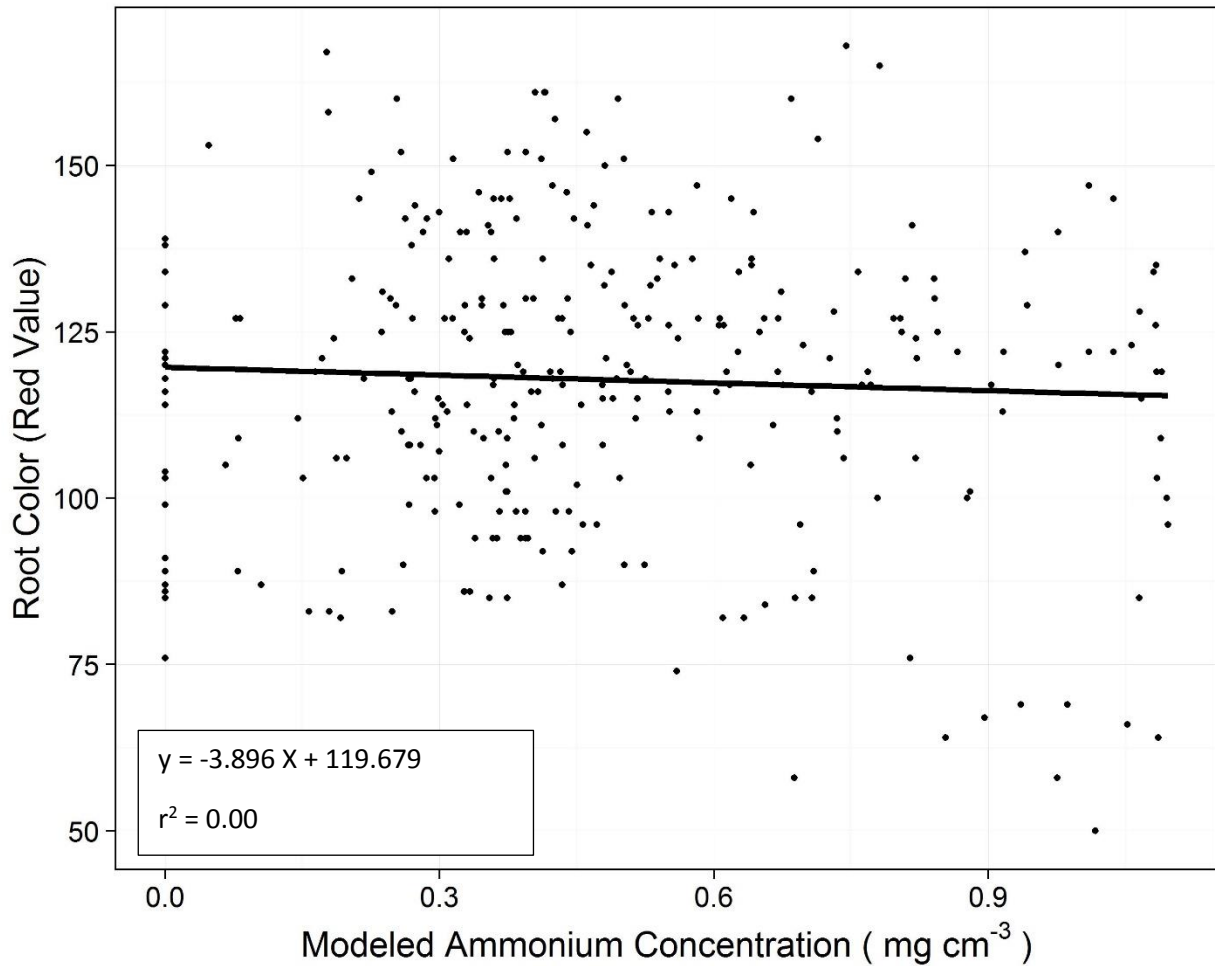


Figure 36: Correlation between root color and modeled NH_4^+ concentrations on 8 DAP.

Soil Moisture and Root Color

The modeled moisture showed decreases in moisture near the surface of the experiment with time (Figure 37). Unlike light transmission or x-ray experiments conducted on mature root systems, there was no drying front established in conjunction with root density (Doussan et al. 2006, Garrigues et al. 2006, Lobet and Draye 2013). Although no changes were observed in

moisture due to root uptake, the advancing drying front does allow for an analysis of changes in root color due to drying of the soil profile.

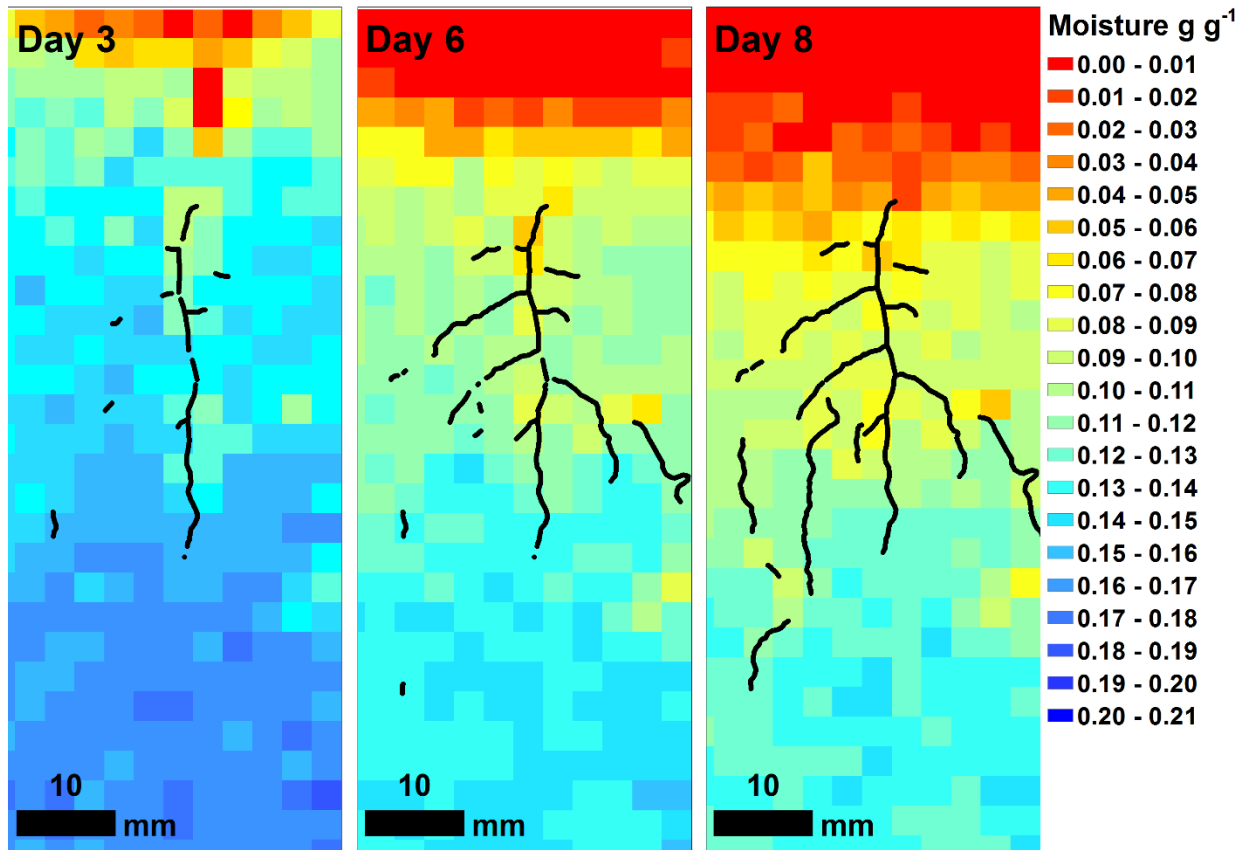


Figure 37: Gravimetric moisture and root skeleton overlay.

The relationships between root color showed similarly weak correlations with the highest r^2 of 0.15 occurring on 6 DAP (Figure 38 and 39). The relationships between moisture and color showed a negative relationship indicating that root color. The negative correlation between root color, as a proxy for root health, and moisture is surprising. An explanation can be found by comparing the progression of the relationship between root color and NH_4^+ as well as examining the mapped concentrations of NH_4^+

and moisture content (Figures 28, 29, & 30). The similar spatial gradients between moisture and NH_4^+ mean that both moisture and NH_4^+ correlations with root color will yield similar results. By reexamining the root images we can see that by 8 DAP all of the plants in the high treatment were showing browning all along the main tap root. The similarities between the trends in root brightness, whether looking at moisture or modeled NH_4^+ , could simply be an artifact of the general gradation of both the NH_4^+ and the moisture increasing with depth.

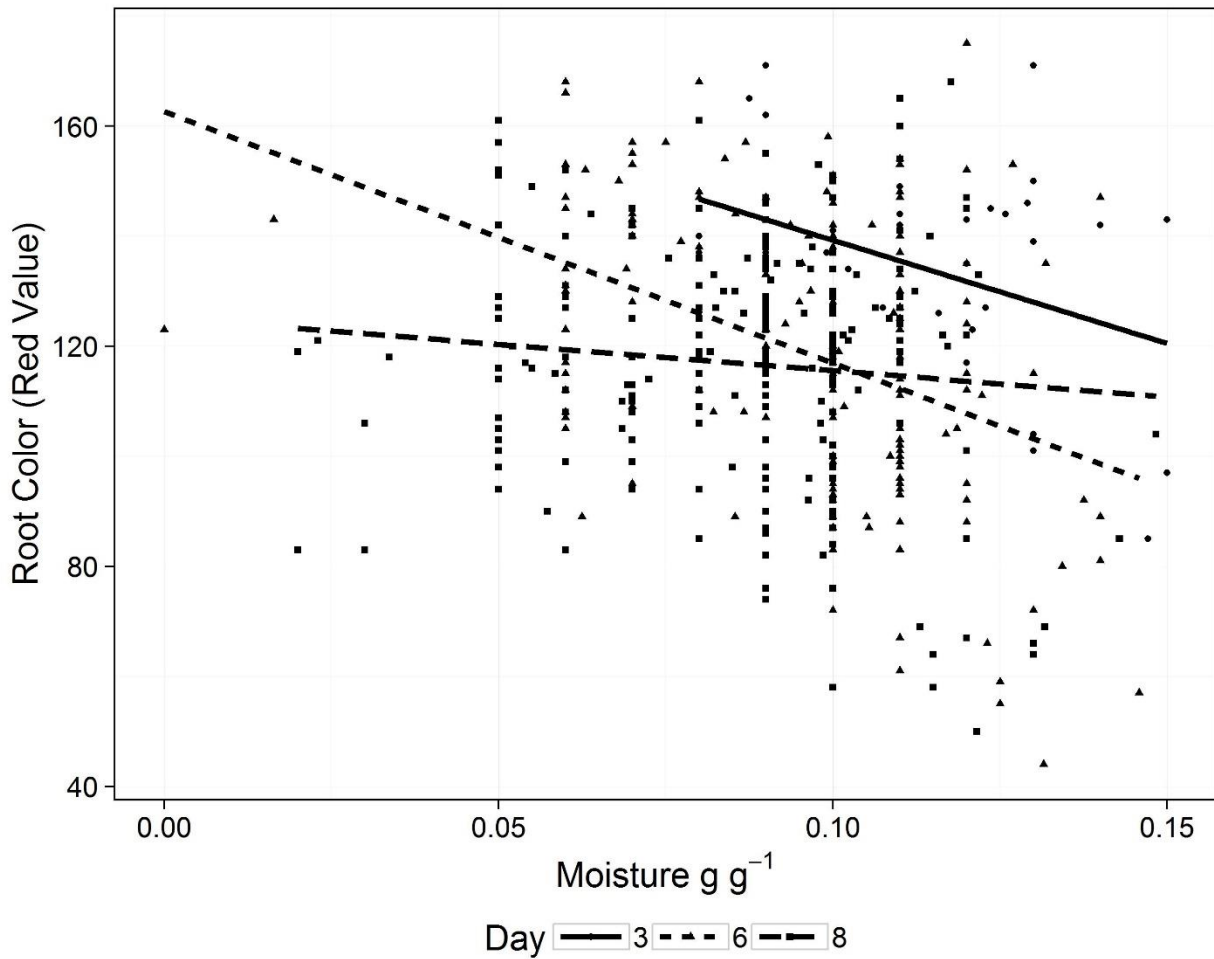


Figure 38: Correlations between moisture and root color on DAP 3, 6, and 8.

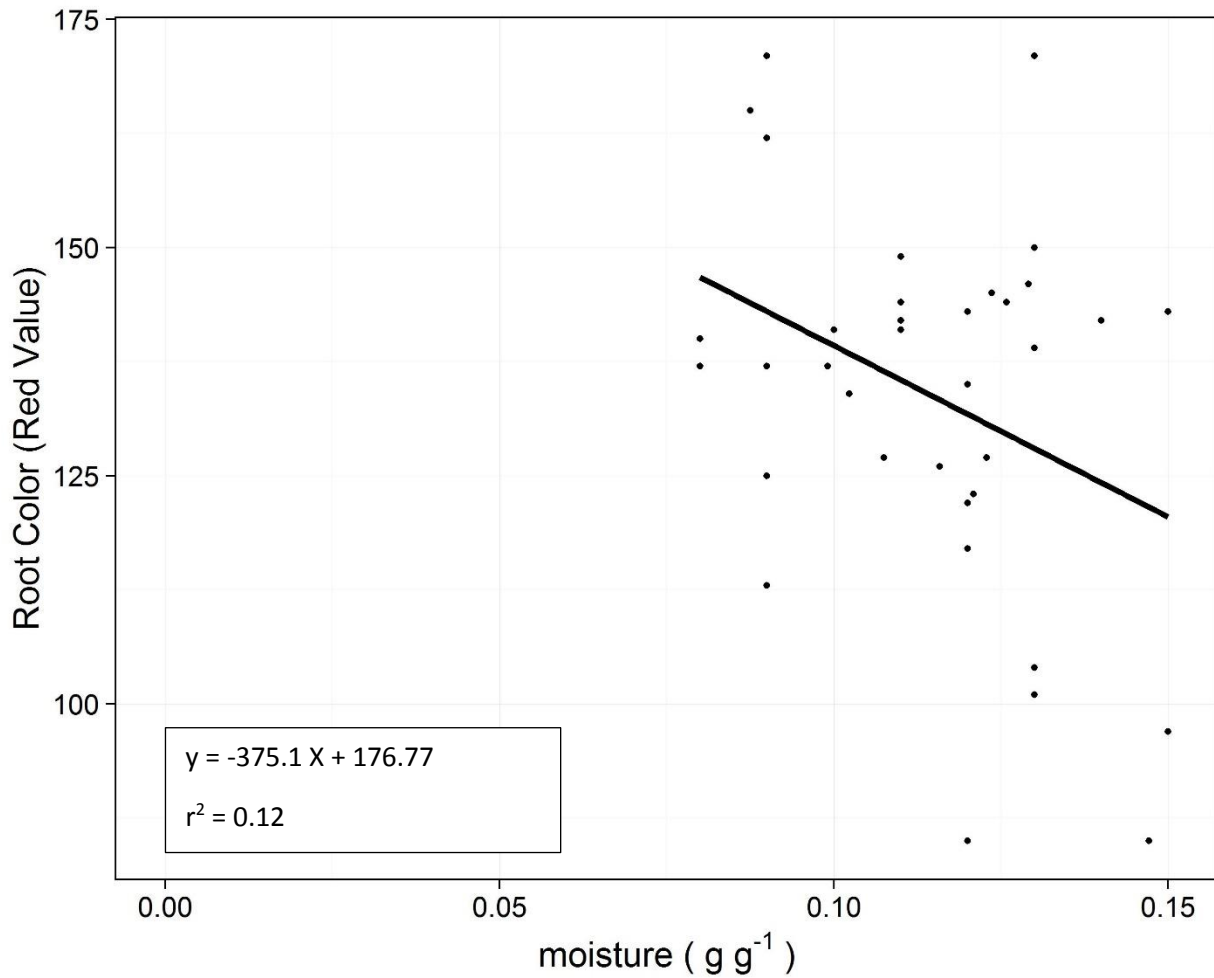


Figure 39: Correlations between moisture and root color on DAP 3.

Conclusion

- Root images confirmed symptoms of halted apical growth, premature lateral branching, root shrinkage, and discoloration of ammoniacal-N induced toxicity on the roots.
- Automated-pixel discrimination distinguished soil from roots with 98% agreement with visual identification.
- Models were successfully used to fill in time during which physical samples of $\text{NH}_3/\text{NH}_4^+$ could not be acquired.

- Image data can be augmented with chemiophysical data by leveraging portions of the image not used for direct analysis (color-moisture prediction) as well as implementing physical measurements and modeling efforts.
- While no strong correlations between root color and moisture or NH_4^+ emerged, the progression of the correlations from a steeper to a shallower slope indicated that as the NH_4^+ dissipates it had less of an effect on the root color.

CHAPTER 4: COVER CROPPING AND REDUCED TILLAGE EFFECTS ON SEQUENTIAL NITROGEN USE EFFICIENCY IN AN IRRIGATED POTATO-WINTER WHEAT-SWEET CORN CROPPING SEQUENCE IN THE PACIFIC NORTHWEST

Introduction

Nitrate Leaching the Columbia Basin

The Columbia Basin of central Washington is home to diverse irrigated cropping systems one of the key crops in the cropping sequence is potatoes (*Solanum tuberosum*). Potatoes are thought to be more susceptible to NO₃-N leaching than other crops due to their high N requirements and shallow root systems (Delgado et al. 2001). This loss of NO₃⁻-N into the ground water can prove to be a serious environmental and human health hazard (Smil 2011 and Galloway 2003). The Environmental Protection Agency has set a minimum safe drinking standard of 10.0 ppm of NO₃-N in ground water (EPA). Some wells in the Columbia basin have been found to have greater than 10.0 ppm NO₃-N (GWMA 2001). A ground water management area has been established in Franklin, Grant, Adams, and Lincoln counties. Together these four counties produced 14.1% of the U.S. potatoes in 2005 covering a total of 38,647 ha (NASS 2006). In addition to these four counties Benton County which is also in the Columbia basin produced 5.32% of the U.S. potatoes and the most of any county in the U.S. (NASS 2006).

Potatoes Susceptible to Leaching

In the Columbia basin a potato-winter wheat (*Triticum aestivum*) -sweet corn (*Zea mays*) cropping sequence is a dominant sequence. In cropping sequences in which potatoes are not followed by a winter crop the winter following the potatoes is commonly the most vulnerable to leaching (Delgado et al. 2001). However, in this sequence winter wheat is grown after potatoes,

and there are only two points in the sequence in which the soil is exposed during the winter the first is after the winter wheat is harvested and prior to the planting of sweet corn and the second is post sweet corn and prior to potatoes. Despite potatoes being immediately followed by winter wheat modeling studies have assessed the winter following the potatoes as the most vulnerable point in the rotation (Peralta and Stockle 2002). Potatoes are the most valuable and most leaching vulnerable crop in the region.

Cover Cropping Effects on Nitrogen Leaching and NUE

There are a plethora of strategies which have been developed for reducing NO_3^- leaching in irrigated cropping systems (Quemada et al. 2013, Meisinger and Delgado 2001). A common strategy for reducing leaching is over winter cover cropping (Tonitto et al. 2005, Dabney et al. 2001, Quemada et al. 2013, Meisinger et al. 1991, Meisinger and Delgado 2002). Non leguminous cover crops have been shown to reduce the NO_3^- being leached by up to 80% (Meisinger et al. 1991). Deep rooted cover crops have an advantage over shallow rooted cover crops in their ability to scavenge nitrogen from the profile and pull it once more to the surface (Delgado et. al 2001). While cover crops have been shown to reduce nitrogen loss they have also been shown to reduce nitrogen use efficiency (NUE) of the cropping system (Quemada et al. 2013).

Reduced Tillage Effects on Nitrogen Leaching and NUE

Reduced tillage has been shown to reduce N loss from leaching (Randall and Iragavarpu 1995, Hansen and Djurhuus 1997, Power and Schepers 1989, Dinnes et al., 2002). In addition to reducing leaching reduced tillage has also been shown to positively influence NUE (Devkota et al. 2013, Khaledian et al. 2011). While some tillage is always necessary when growing potatoes

minimizing tillage before and after potatoes while adhering to no-till in the non-potato years can offer additional benefits of reduced tillage (Alva et al. 2002, Mundy et al. 1999, Hoyt 1999). Reduced tillage and increased rotation in potatoes was found to reduce disease and rejuvenate beneficial properties in non-potato years (Peters et al. 2004, Carter et al. 2009).

Cover Crops in Cropping Sequence Including Potatoes

Several studies have evaluated the ability of cover crops to capture nitrogen and recycle it onto the next year (Collins et al. 2007, Weinert et al. 2002, Delgado et al. 2001, Bundy and Andraski 2005, Jahanzad 2014, Shrestha et al. 2010, Nyiraneza and Snapp 2007). The focus the past research had been on using cover crops to sequester N after potatoes (Bundy and Andraski 2005, Delgado et al. 2001). However, in a potato-winter wheat-sweet corn sequence the winter wheat can fill the role of scavenging N left behind by potatoes meaning that the primary role of the cover crop should be in retaining the N in the top 60 cm of the soil in order to maintain its availability for the potato. Rapeseed (*Brassica napus*), rye (*Secale cereale*), mustard (*Brassica hirta*), and winter wheat have all been used prior to planting potatoes (Weinert et al. 2002, Nyiraneza and Snapp 2007). Mustard is preferred as a cover crop prior to potatoes as it can be used as a bio fumigant (Collins et. al. 2006). The ability of pre-potato over wintering mustard to supply N from the previous year has been demonstrated using N¹⁵ (Collins et al. 2007).

NUE Assessments of Crop Sequences

While NUE has been demonstrated to decrease with the use of non-legume cover crops, NO₃⁻ loss through the soil profile has decreased indicating that the N recovered by the cover crop is being retained in the system (Quemada et al. 2013). Studies looking at N balances have shown that the surplus N, when cover crops are used, supports the theory of N being retained in the

system (Snapp et al. 2005). These studies have only looked at single year NUE. Due to the seasonal mechanisms of retention and recycling of N within these systems a multi season approach is needed to evaluate the impact effect of cover cropping and reduced tillage on NUE (Maaz 2014). For this study we will refer to the multiyear NUE as sequential NUE (sNUE) rather than rotational NUE.

Previous cover cropping studies used the changes in subsoil NO_3^- to indicate the effects of cover crops had on reducing leaching (Weinert et al. 2002). While NUE is useful for assessing the overall efficiency of the system it does not necessarily relate directly with NO_3^- leaching. Consequently it is important to track changes in NO_3^- in the soil profile as an indicator of leaching. NO_3^- which passes below the 60 cm range is considered to be below potato roots and unavailable for potatoes (Delgado et al. 2001).

In summary, NO_3^- leaching from potato systems is an important issue in the Columbia Basin. Cover cropping and reduced tillage have both been attempted as solutions to reduce NO_3^- leaching and erosion (Collins et al. 2007, Alva et al. 2002). While cover crops capture and recycling of N have been documented in this system (Collins et al. 2007), the effects of multi-year sequential NUE has not been examined in the Columbia basin. In this study we hypothesize that reduced tillage and cover cropping will reduce the over winter accumulation of NO_3^- in 90-120 cm depths of the soil, and increase the sNUE. Our objectives were 1.) to determine the effects of cover cropping and reduced tillage on the over winter NO_3^- in the rooting zone, and 2.) to determine the effects of cover cropping and reduced tillage on the N efficiency of the cropping sequence.

Materials and Methods

Experimental Site and Design

The field study was conducted in Prosser, WA on the Rosa unit Washington State University research farm. Irrigation was applied using a solid set system. The soil was a Warden Silt Loam a coarse-silty, mixed, superactive, mesic Xeric Haplocambids with 2.0% organic matter. Winter wheat, triticale (x *Triticolescale*), and mustard (*Brassica hirta*) cover crops were planted using a Fabro direct seed research drill at 19 cm row spacing. Corn rows were at 61 cm and potatoes at 75 cm. Three fields were established at different stages in the cropping sequence so that in any given year all three crops were grown. The sequence in field 1 was wheat-corn-potatoes, field 2 was corn-potatoes-wheat, and field 3 was potatoes-wheat-corn. Each field was separated into 4 replicated blocks and each replicate was separated into 4 plots. The four treatments were randomly assigned to the plots within each replicate. The initial soil samples and plots were established in the fall of 2011 the final samples were taken after harvesting the potatoes and corn in the fall of 2013.

The basic crop sequence was potato-winter wheat-fallow-sweet corn-fallow. In the triticale/mustard treatment the sequence was modified to be potato-winter wheat-triticale-sweet corn-mustard. The reduced tillage treatment used zero tillage during the corn and wheat seasons of the cropping sequence and only disked prior to potatoes. With the exception of 2013 when all plots following potatoes were ripped and disked due to unmanageably large soil clods. The conventional tilled treatments included ripping and disking prior to and following potatoes.

Plant and Soil Sampling and Analysis

Wheat grain yield data was collected using a Hege 140 plot combine (Hege Maschinen, Waldenburg, Germany). Wheat biomass was harvested from 2 m rows immediately adjacent to the path of the combine. Sweet corn was harvested in 6.10 m lengths from center two rows of each plot. Two whole plants were randomly selected for moisture and C and N analysis of both the corn ear and the stover, with the exception of 2012 when no C or N measurements were made on harvested sweet corn. Potato above ground biomass samples were made by cutting two 1 m rows from hills near the center of each plot prior to flail chopping of vines. Potato biomass samples were only collected in 2014. The potato rows were harvested with a single row mechanical digger and picked out by hand. Potatoes were picked from a 6.10 m length from two center rows. Subsets of tubers were randomly selected and bagged for C and N analysis which were run in 2013 and 2014.

Soil profiles samples were taken in the in the spring and fall of each year. Two soil cores were taken from near the center of each plot to 120 cm depth and segmented into 30 cm increments. The two depth samples were combined and homogenized. The spring samples were taken at the time of cover crop kill and before planting in late March or early April. Fall samples were taken post crop harvest and pre-fall planting in either the last half of August or the first half of September. All samples were analyzed for NO_3^- -N and NH_4^+ -N using a 1M KCl extraction and Lachat colorimetric measure using a Quickchem 8000 Series FIA+ system and AutoSampler (Lachat Instruments, Hach Company, Loveland, CO). Biomass C and N were analyzed using a Truspec Carbon and Nitrogen Analyzer (LECO corporation, St. Joseph, MI).

Statistical Analysis.

The calculations of fertilizer use efficiency (FEE), Nitrogen Export Efficiency (NEE), and sequential Nitrogen Export Efficiency (sNEE), and the partial Nitrogen balance all used a soil depth of 0-60 cm as this was the maximum depth for the potato roots.

$$\text{Eq 1. } FEE = N \text{ Harvested Portion} / \text{Fertilizer N}$$

$$\text{Eq 2. } NEE = N \text{ Harvested Portion (kg)} / (\text{Fertilizer N} + \text{Estimated Mineralization} + \text{Initial Inorganic N 0-60 cm})(\text{kg}) \text{ N export efficiency.}$$

$$\text{Eq 3. } sNEE = \Sigma N \text{ Harvested Portion} / (\Sigma \text{Fertilizer N} + \Sigma \text{Estimated Mineralization} + \text{Initial Inorganic N 0-60 cm})$$

$$\text{Eq 4. } sNUE = \Sigma \text{Harvested Portion} / (\Sigma \text{Fertilizer N} + \Sigma \text{Estimated Mineralization} + \text{Initial Inorganic N 0-60 cm})$$

$$\text{Eq 5. } N \text{ balance} = (\text{Initial Inorganic N 0-60 cm} - \text{Final Inorganic N 0-60 cm}) + \Sigma \text{Fertilizer N} - \Sigma N \text{ Harvested Portion}$$

The initial inorganic N term in the NEE calculation was the soil sample immediately preceding the planting of the crop being evaluated meaning that for wheat the preceding fall samples were used and for potatoes and corn the preceding spring samples were used. The calculation for sNEE were all conducted between the fall of 2012 and the fall of 2014, due to no nitrogen harvest data being collected for the corn and potatoes in 2012, meaning that sNEE was calculated for three cropping sequences potatoes-winter wheat (PW), winter wheat-sweet corn (WC), and sweet corn-potatoes (CP).

Efficiency calculations, ANOVA, and LSD were conducted using the ‘agricolae’ and ‘base’ packages of R statistical software and R studio (R Foundation for Statistical Computing, R, Vienna, Austria). Figure graphs were constructed in R using the ‘ggplot2’ package.

Results and Discussion:

Field and Year Effect

The study was designed so that each phase of the three year cropping sequence was represented every year, the effect of year was examined on crop performance (e.g. w-c-p, p-w-c, or c-p-w). Corn, potato, and wheat yields averaged 17,335, 43,547, and 7,332 kg ha⁻¹ respectively over all years and fields. Potato and corn yield differed significantly among years (Table 5). The plot yields for corn and potatoes were below the state averages of 21,072 and 67,200 kg ha⁻¹ (NASS 2016). The difference between the state average potato yield and the average yield in our results can be explained by the use of the Shepody variety which is an earlier season fresh market potato. Yukon Gold, another fresh market variety yielded an average of 47,703 kg ha⁻¹ during 2009 (Pavek and Knowles 2009). The lowest yielding potatoes were grown at field 3 in 2012 and yielded 34,290 kg ha⁻¹ as opposed to the greatest yield of 52,451 kg ha⁻¹ at site 1 in 2014. Potato yield decreased significantly from 2014 to 2013, but the difference (4,660 kg ha⁻¹) between these two years was less than half of the decrease from 2013 to 2012 (11,555 kg ha⁻¹). Additionally, the corn at site 3 in 2014 yielded 8,014 kg ha⁻¹, lower than the corn grown in site 2 in 2012. While not significantly different from 2012 or 2014 the 2013 wheat, also grown at site 3, was the lowest yielding wheat in all 3 years averaging 6,666 kg ha⁻¹. By normalizing all yields, the factors of field and year can be compared simultaneously across all fields suggesting field characteristics were responsible for the decreases in yield (Figure 40). Consequently it appears that the variation in yield is primarily driven by the field location rather

than the year in which it was grown. Additionally, N removal, cover crop biomass and C:N ratios in all cases also differed significantly ($p < 0.05$) among years, with the exception of the N removed by potatoes (Table 5 and Table 6). Furthermore, the soil available N and NEE of each crop were significantly ($p < 0.05$) changed depending on year (Table 6 and Table 7). Therefore, the dominant significance of year as a factor allowed for the analysis of each cropping sequence independently of each other, and the sequences of PW, WC, and CP were individually assessed for cover crop and tillage effects. Cover cropping did not affect individual crop yields. In contrast, reduced tillage affected the yields of corn and wheat across all years and fields. Corn fresh weight increased with reduced tillage from 16,062 kg ha⁻¹ to 18,977 kg ha⁻¹ (Table 5). In an irrigated cropping sequence with corn following wheat winter rye was shown to produce insignificant increases in corn yield (Vyn et al. 1999). Previous research following triticale with corn has shown significant increases of 1,500-1,600 kg ha⁻¹ (Andraski and Bundy 2005). However, our results show a non-significant decrease of 945 kg ha⁻¹ overall three years (Table 5). Wheat yield decreased with reduced tillage decreasing from 7,669 kg ha⁻¹ to 7,283 kg ha⁻¹, but was not significant (Table 5). Potatoes showed a non-significant increase of 1,881 kg ha⁻¹ due to reduced tillage of the previous crop. Previously reduced tillage has been shown to have negative impact on potatoes (Alva et al. 2002). Potato yield not significantly affected by cover cropping (Weinert et al. 2002).

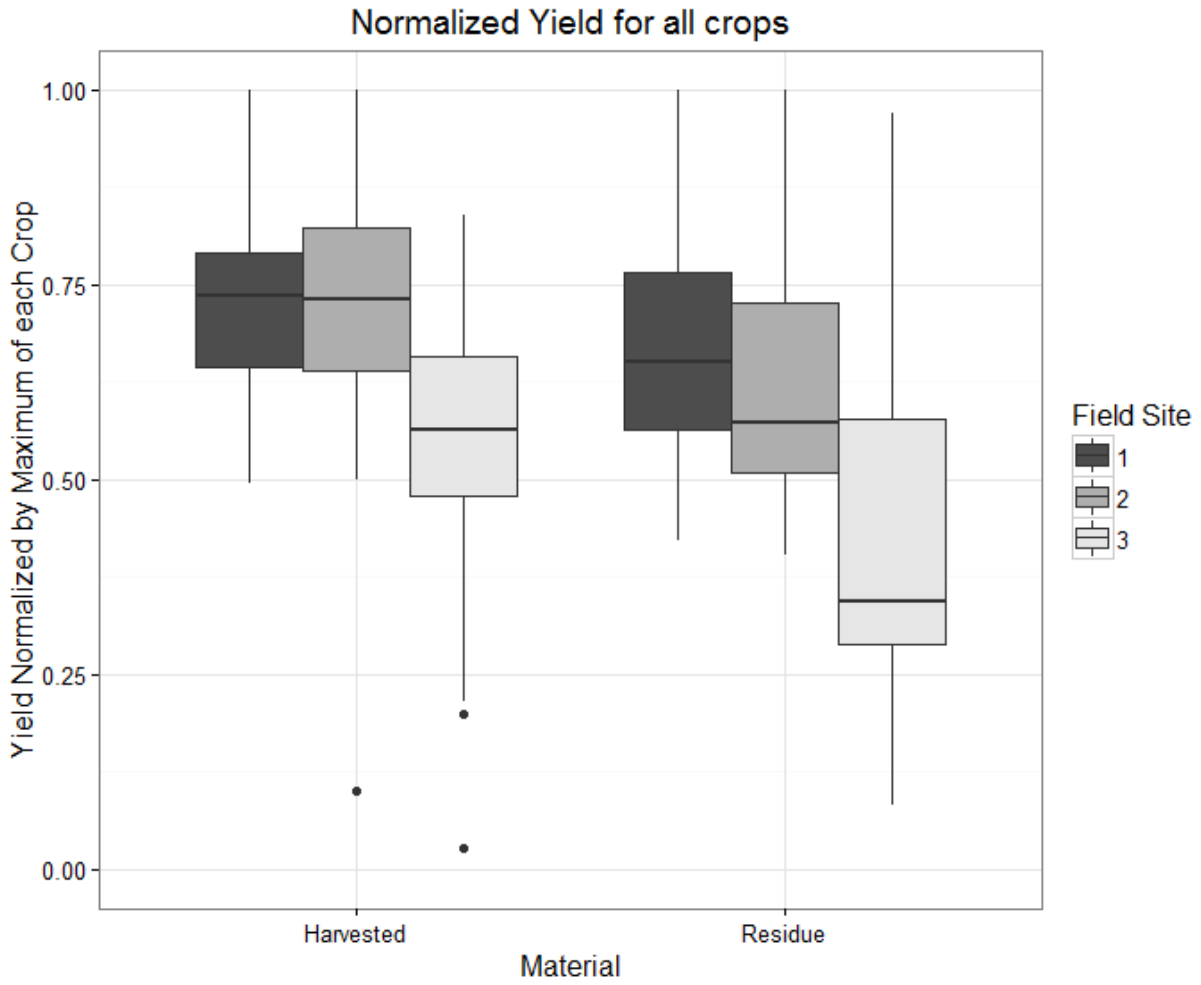


Figure 40: The normalized harvested and residue fractions of all crops overall

Table 5

		All Crops Yield by Year and Treatment					
		Harvested kg ha ⁻¹			N harvested kg N ha ⁻¹		
		Wheat	Corn	Potatoes	Wheat	Corn	Potatoes
2012	Cover Crop	7011	22046	35019	117.6	-	-
2012	Cover Crop	8050	17053	30976	133.8	-	-
2012	Fallow	7322	23842	37500	134.6	-	-
2012	Fallow	8382	19142	33664	145.7	-	-
2013	Cover Crop	7026	17537	47218	126.2	56.6	174.0756
2013	Cover Crop	6685	19550	41623	119.2	66.7	163.4874
2013	Fallow	6886	18622	46547	99.9	59.5	175.4227
2013	Fallow	7385	20197	47991	134.8	70.9	197.3123
2014	Cover Crop	8218	15181	51098	137.0	57.6	192.8895
2014	Cover Crop	7782	9807	48932	183.9	36.8	190.7837
2014	Fallow	7235	14417	49538	156.0	54.0	179.9958
2014	Fallow	7727	10622	52451	185.9	37.3	185.0726
Means							
	2012	7691	20521	34290	133	-	-
	2013	6666	18977	45845	120	63	178
	2014	7641	12507	50505	165	46	187
	Reduced Tillage	7283	18608	44487	129	57	183
	Conventional Tillage	7669	16062	42606	151	53	175
	Cover Crop	7462	16862	42478	136	54	178
	Fallow	7490	17807	44615	143	55	192
Statistics Table							
	Cover Crop	ns	ns	ns	ns	ns	ns
	Reduced Tillage	ns	ns	ns	*	ns	ns
	Year	**	***	***	*	**	ns
	Cover Crop X Reduced Tillage	ns	ns	ns	ns	ns	ns
2012	Cover Crop X Reduced Tillage	ns	ns	ns	ns	-	-
	Cover Crop	ns	ns	ns	ns	-	-
	Reduced Tillage	ns	ns	ns	ns	-	-
2013	Cover Crop X Reduced Tillage	ns	ns	ns	ns	ns	ns
	Cover Crop	ns	ns	ns	ns	ns	ns
	Reduced Tillage	ns	ns	ns	ns	*	ns
2014	Cover Crop X Reduced Tillage	ns	ns	ns	ns	ns	ns
	Cover Crop	ns	ns	ns	ns	ns	ns
	Reduced Tillage	ns	.	ns	.	.	ns

p < 0.001 = ***, 0.01 = **, 0.05 = *, 0.1 = .

Table 6

Cover Crop N Recovery					
			Biomass N (kg N ha ⁻¹)	C:N	Yield (kg ha ⁻¹)
2013	Mustard	Reduced Tillage	130.3	11.0	4002
2013	Mustard	Conventional Tillage	169.8	9.1	3807
2013	Triticale	Reduced Tillage	46.3	22.8	2442
2013	Triticale	Conventional Tillage	31.3	25.1	1781
2014	Triticale	Reduced Tillage	113.6	12.3	3125
2014	Triticale	Conventional Tillage	91.1	12.3	2727
Means					
	Mustard		150.0	10.0	3904.5
	Triticale		70.6	18.1	2518.6
	Reduced Tillage		96.7	15.4	3189.5
	Conventional Tillage		97.4	15.5	2771.7
	Species		***	***	***
	Tillage		ns	ns	ns
	Year		**	***	ns
	Species X Tillage		.	ns	ns

p < 0.001 = ***, 0.01 = **, 0.05 = *, 0.1 = .

Table 7

		Mineral N (NH ₄ ⁺ NO ₃ ⁻) in the Soil Profile					
		Mineral N 0-60 cm (kg N ha ⁻¹)			Mineral N 60-120 cm (kg N ha ⁻¹)		
		Wheat	Corn	Potatoes	Wheat	Corn	Potatoes
2012	Cover Crop	14.9	65.4	41.8	2.9	69.7	27.0
2012	Cover Crop	32.3	36.1	24.2	19.7	92.3	38.7
2012	Fallow	39.4	67.3	84.5	11.1	55.7	51.0
2012	Fallow	22.2	75.1	100.0	14.8	101.3	61.4
2013	Cover Crop	55.2	14.6	42.9	11.7	4.4	26.0
2013	Cover Crop	78.9	21.2	127.0	50.7	7.3	89.4
2013	Fallow	44.5	30.5	114.3	17.5	18.0	163.4
2013	Fallow	120.5	22.6	250.0	51.5	19.5	215.3
2014	Cover Crop	158.0	63.4	70.3	47.3	32.4	29.9
2014	Cover Crop	192.9	150.6	101.3	41.9	21.9	29.9
2014	Fallow	259.5	57.4	89.1	103.3	19.3	36.7
2014	Fallow	240.2	87.2	111.3	198.2	91.3	45.5
Means							
	Reduced Tillage	95.2	49.8	73.8	32.3	33.3	55.7
	Conventional Tillage	114.5	65.5	118.9	62.8	55.6	80.0
	Cover Crop	88.7	58.6	67.9	29.0	38.0	40.2
	Tillage	121.1	56.7	124.8	66.1	50.8	95.6
	Cover Crop	ns	ns	***	ns	ns	***
	Tillage	ns	ns	**	*	ns	.
	Year	***	***	**	***	*	***
	Cover Crop X Tillage	ns	ns	ns	ns	ns	ns
2012	Cover Crop X Tillage	ns	ns	**	ns	ns	ns
2013	Cover Crop X Tillage	ns	ns	ns	ns	ns	ns
2014	Cover Crop X Tillage	ns	ns	ns	ns	ns	ns

p < 0.001 = ***, 0.01 = **, 0.05 = *, 0.1 = .

Cover Cropping and Reduced Tillage Effects on Mineral N

Our first objective was to determine the effects of cover cropping and reduced tillage on over winter NO_3^- in the rooting zone. Spring mineral N in wheat, corn, and potatoes was significantly impacted by year. Cover cropping and reduced tillage did not change soil mineral N in the top 60 cm during years in which winter wheat was being grown (Table 7). During the spring of 2013, a significant decrease in mineral N in the top 60 cm was found prior to corn due to both over winter triticale and reduced tillage preceding potatoes. Over winter mustard plots preceding potatoes averaged $67.9 \text{ kg N ha}^{-1}$ as opposed to winter fallow plots which averaged $124.8 \text{ kg N ha}^{-1}$ overall site years. Similarly reduced tillage plots preceding potatoes had $73.8 \text{ kg N ha}^{-1}$ of mineral N while conventionally tilled plots had $124.8 \text{ kg N ha}^{-1}$ overall years. The decrease in mineral N due to cover cropping points to the success of over winter mustard in capturing excess N prior to potato planting. Therefore, we cannot reject our hypothesis that cover cropping and reduced tillage decreases the availability of mineral N in the spring.

The greatest changes of mineral N in the soil due to reduced tillage were found in the spring immediately preceding potato planting. Because, changes in soil properties due to reduced tillage frequently take more than one year to be detected, it was to be expected that the greatest changes in soil mineral N due to cover cropping would be after the wheat and corn years of the sequence. This interpretation of the tillage effect being most detectable prior to potatoes is corroborated by the fact that the tillage effect ($-1.0 \text{ kg N ha}^{-1}$) in 2012, in the first year that reduced tillage was initiated, was insignificant and decreased with tillage in comparison to the tillage effect ($26.5 \text{ kg N ha}^{-1}$) in 2014 after two years of zero tillage. Unlike cover cropping, reduced tillage did not have significant reductions in mineral N in the top 60 cm in 2012, 2013, and 2014 preceding potatoes. This observation indicates that the effects of reduced tillage require time to become apparent, whereas the effects of cover cropping on reducing mineral N are noticeable within a season.

Cover cropping and reduced tillage decreased the mineral N ($\text{NH}_4^+ + \text{NO}_3^-$) in the 60-120 cm depths in the spring samples of all crops (Table 7). This effect was significant in the reduced tillage plots in the wheat, cover crops, and the potatoes following the no-till wheat and corn. The spring soil samples were taken when the wheat was already established, and decreased significantly with reduced tillage in both 2013 and 2014. In potatoes, both cover cropping and reduced tillage of previous crop significantly decreased the amount of mineral N in the 60-120 cm depths of the soil. Cover cropping significantly reduced the mineral N in the 60-120 cm zone due to cover cropping in both 2013 and 2014. If we consider the 60-120 cm zone as being below the root zone of most irrigated plants we can consider both reduced tillage and cover cropping as reducing the amount of mineral N which proceeds to deep in the profile. Therefore, these findings support our hypothesis that cover cropping and reduced tillage decrease the amount of mineral N below 60 cm in the soil profile.

Cover Cropping Effects on NO_3^- Leaching

The initial NO_3^- showed high levels of variation in the 90-120 cm zone in fields 2 and 3 (Figure 41). The over winter change in NO_3^- was used to estimate leaching (Figure 42-44). Cover cropping reduced over winter increases of NO_3^- in the 30-90 cm depths of the soil. The greatest differences in over winter NO_3^- change were found at field 2 during the winter of 2013 (Figure 42). These reductions corresponded to a healthy over wintering mustard which successfully took up $150.5 \text{ kg N ha}^{-1}$ into biomass (Table 6). The difference in the over winter changes in NO_3^- at field 1 during 2013 corresponded to triticale taking up $38.8 \text{ kg N ha}^{-1}$ (Table 6). However, at field 3, during the winter of 2013 there was no significant change in the over winter NO_3^- change due to cover cropping effect even when triticale took up $102.4 \text{ kg N ha}^{-1}$. The reductions in the over winter change of NO_3^- in the 30-90 cm depths of the soil profile in two out of the three instances implies cover cropping treatments successfully established indicates reductions in NO_3^- leaching is attainable with winter cover cropping establishment.

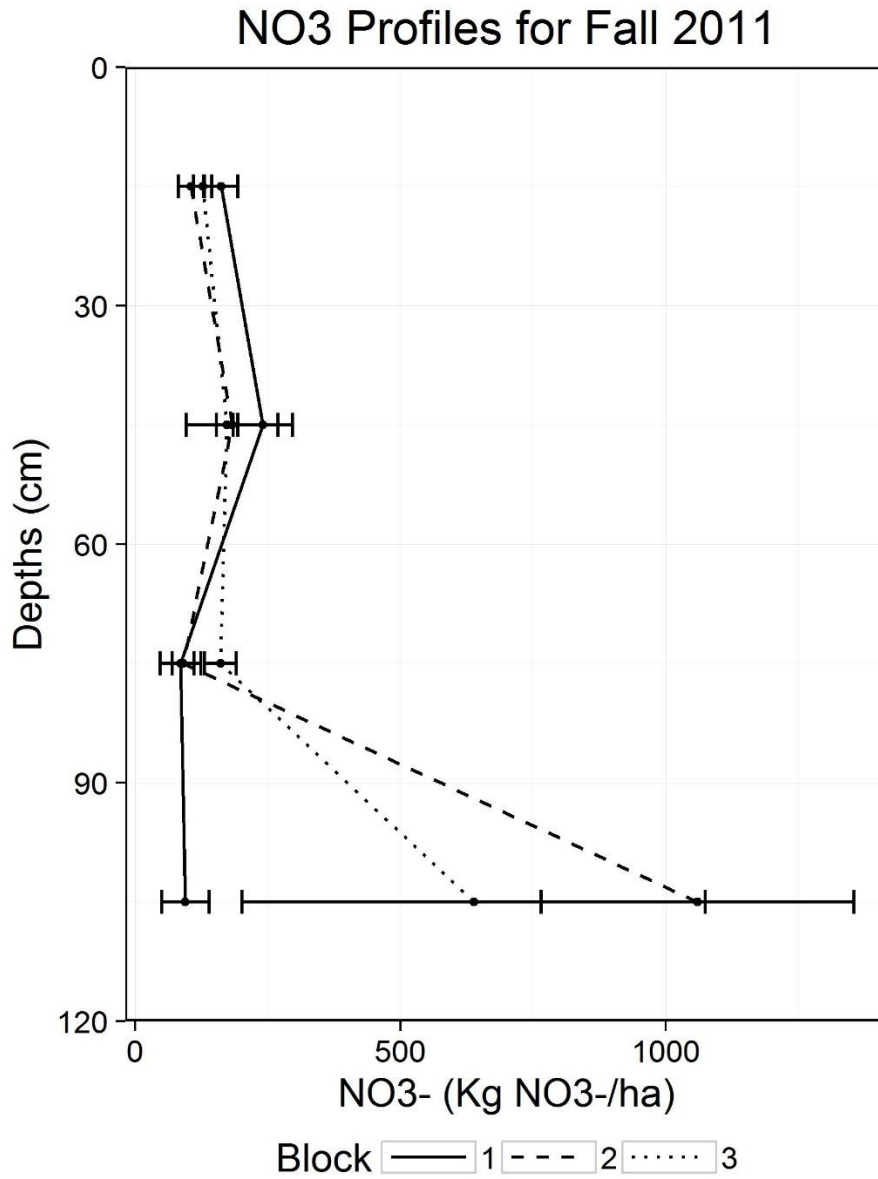


Figure 41: Initial soil NO₃⁻ in the fall of 2011.

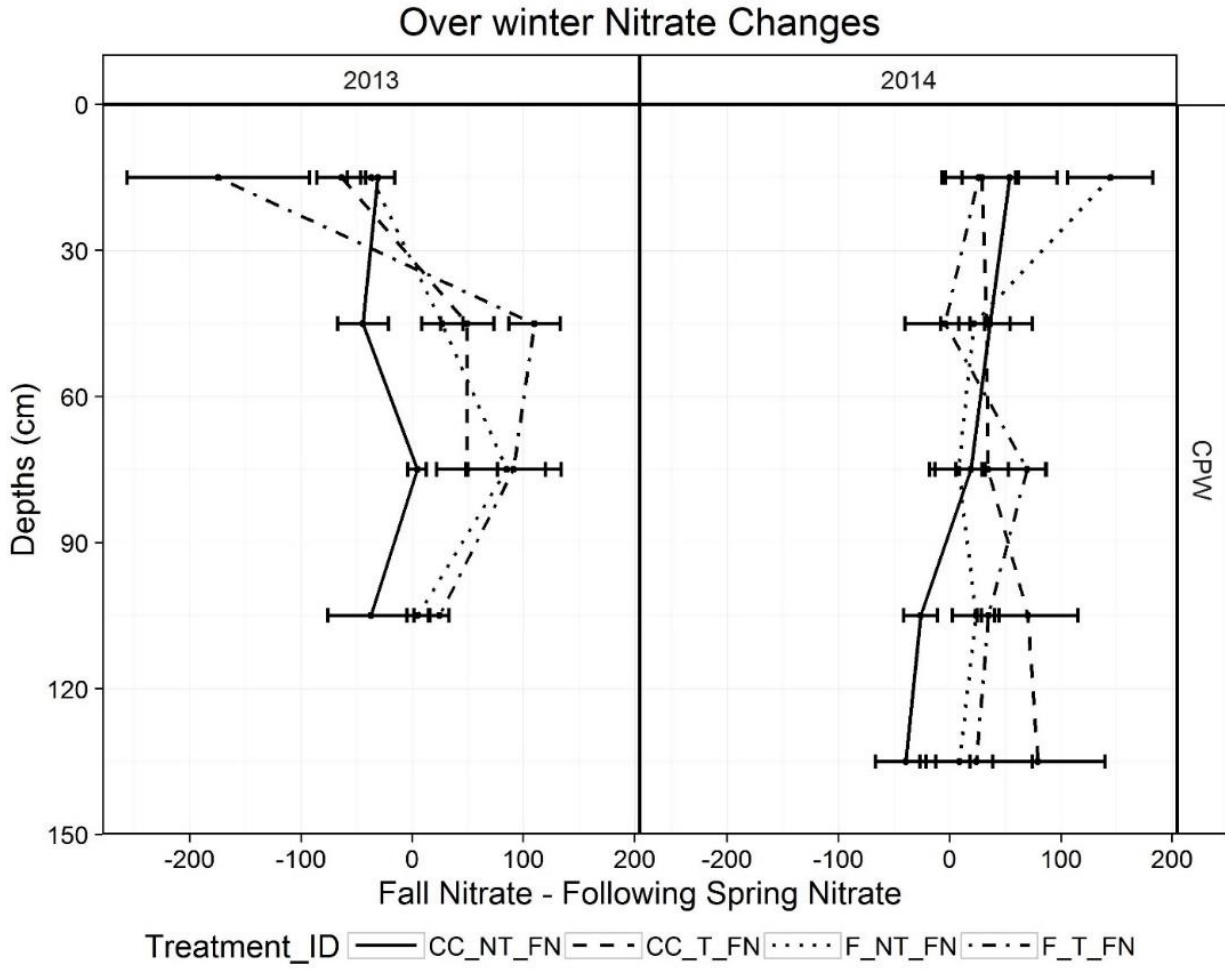


Figure 42: Over winter NO_3^- changes in the CPW sequence in the winters of 2012-2013 and 2013-2014.

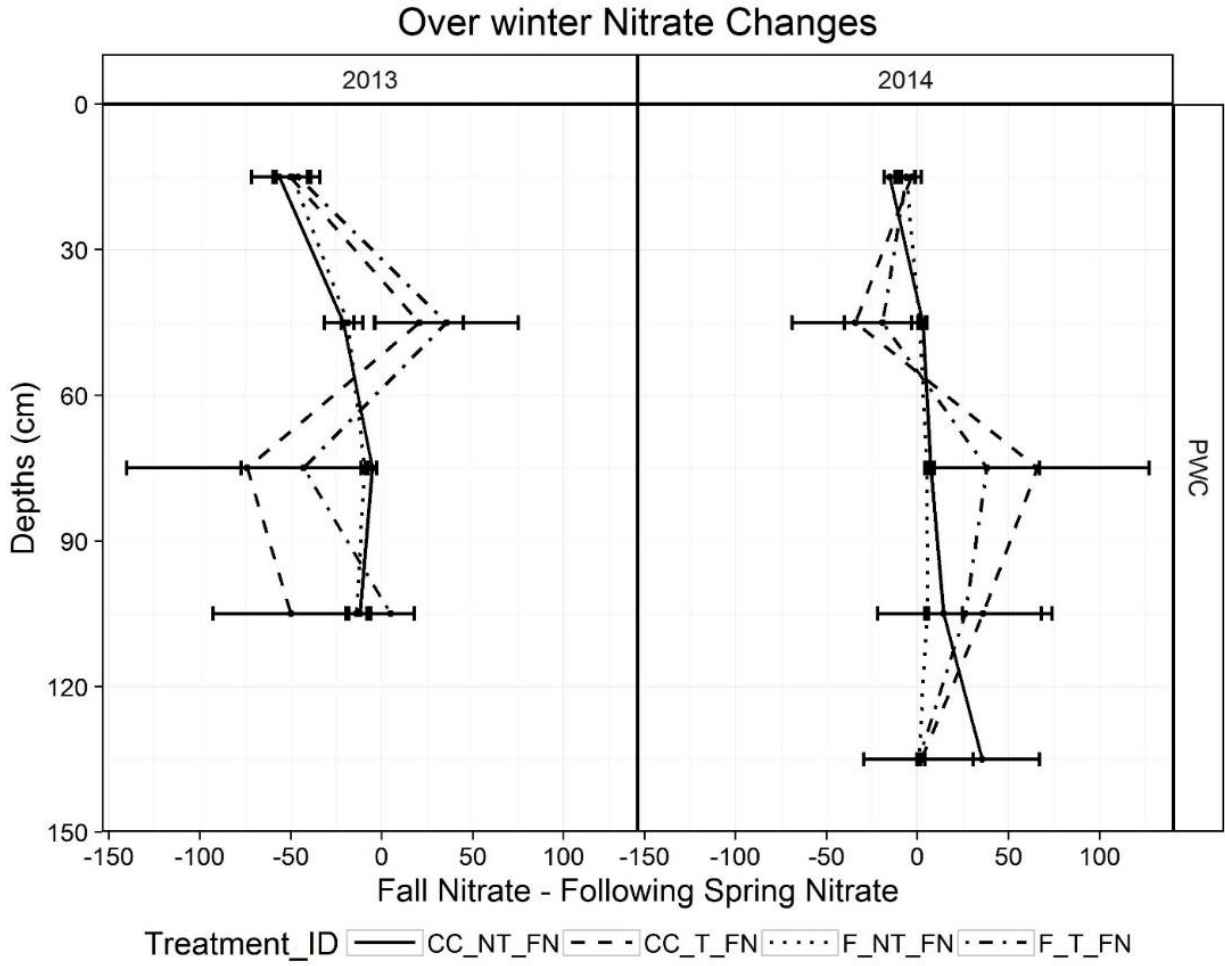


Figure 43: Over winter NO_3^- changes in the PWC sequence in the winters of 2012-2013 and 2013-2014.

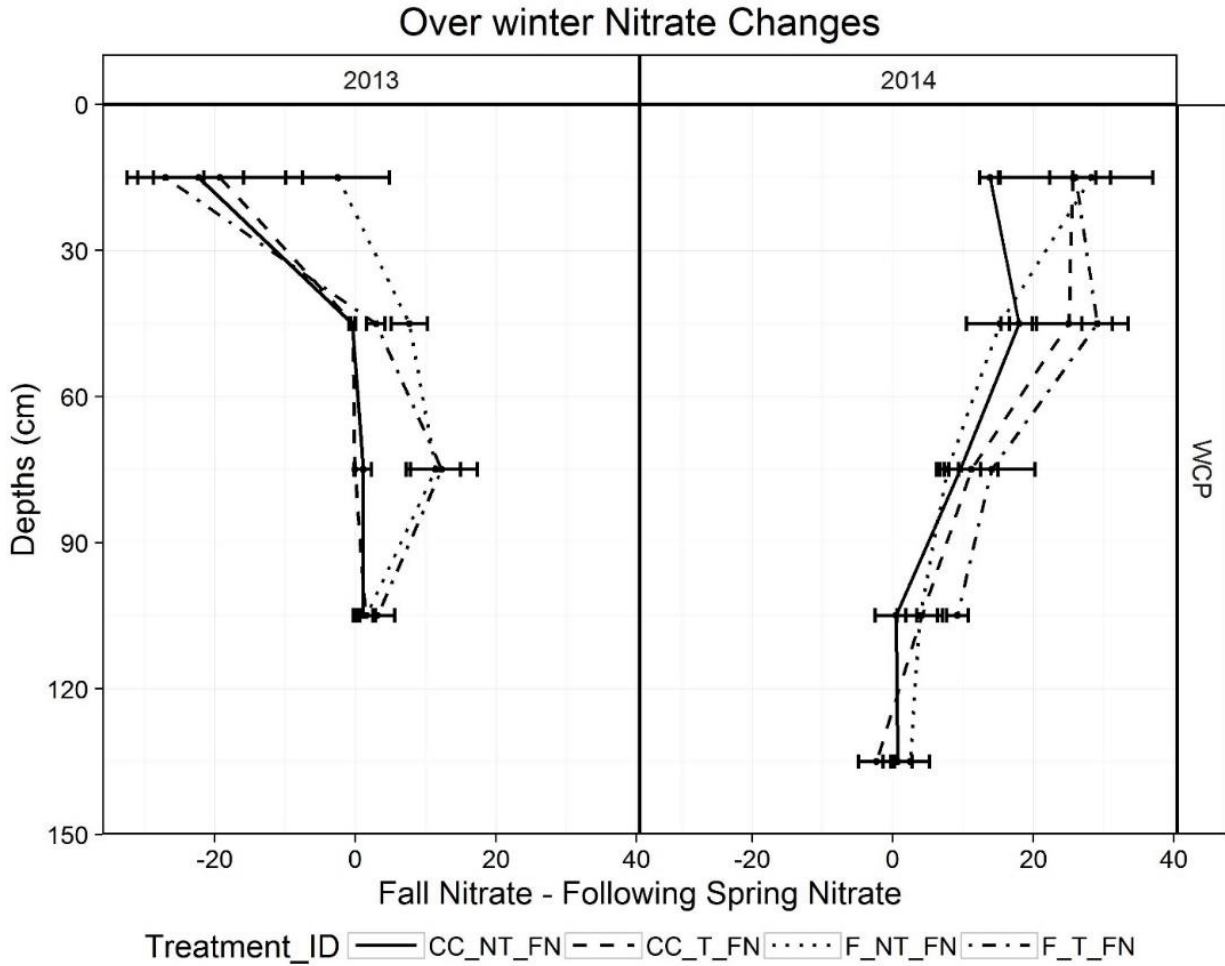


Figure 44: Over winter NO_3^- changes in the PWC sequence in the winters of 2012-2013 and 2013-2014.

Cover Cropping and Reduced Tillage Effects on Single Year NEE

Our third objective was to determine the effect of cover cropping and reduced tillage on single season NEE. As expected, NEE varied greatly among the crop species with wheat, corn, and potatoes averaging 0.89, 0.31, and 0.89 respectively. Potato NEE increased significantly due to both cover cropping and reduced tillage across all years, from 0.78 to 1.01 with the implementation of cover cropping and from 0.80 to 0.99 with reduced tillage. Wheat also had significant increases in NEE due to reduced tillage in 2014. The effects of reduced tillage on corn NEE was not consistent across years, and

corn had a significant increase in NEE in 2014 but significant decrease in 2013. Cover cropping did not affect NEE of wheat and corn. The lack of change in NEE due to cover cropping aligns well with previous studies showing a decrease or no change in NUE due to cover cropping in irrigated systems (Quemada et al. 2013). The increase of NEE in the potato seasons indicates that mustard prior to potatoes successfully recycles N from the previous corn year and into the current potatoes (Collins et al. 2007).

Table 8

			Annual NEE calculated by crop		
			Wheat	Corn	Potatoes
2013	Cover Crop	Reduced Tillage	0.64	0.40	1.15
2013	Cover Crop	Conventional Tillage	0.68	0.45	0.81
2013	Fallow	Reduced Tillage	0.60	0.38	0.73
2013	Fallow	Conventional Tillage	0.71	0.47	0.57
2014	Cover Crop	Reduced Tillage	1.28	0.27	1.12
2014	Cover Crop	Conventional Tillage	1.08	0.13	0.96
2014	Fallow	Reduced Tillage	1.27	0.26	0.94
2014	Fallow	Conventional Tillage	0.84	0.16	0.87
			Means		
			0.95	0.33	0.99
			0.83	0.30	0.80
			0.92	0.31	1.01
			0.85	0.32	0.78
			0.89	0.31	0.89
Stats Table					
			<i>ns</i>	<i>ns</i>	*
			<i>ns</i>	<i>ns</i>	**
Year			***	***	*
All Years	Cover Crop X Reduced Tillage		<i>ns</i>	<i>ns</i>	<i>ns</i>
2013	Cover Crop		<i>ns</i>	<i>ns</i>	.
2013	Reduced Tillage		<i>ns</i>	*	*
2013	Cover Crop X Reduced Tillage		<i>ns</i>	<i>ns</i>	<i>ns</i>
2014	Cover Crop		<i>ns</i>	<i>ns</i>	*
2014	Reduced Tillage		.	*	<i>ns</i>
2014	Cover Crop X Reduced Tillage		<i>ns</i>	<i>ns</i>	<i>ns</i>

p < 0.001 = ***, 0.01 = **, 0.05 = *, 0.1 = .

Cover Crop and Reduced Tillage Effects on sNEE in the CP Sequence

The final objective was to determine the effects of cover cropping and reduced tillage on cropping sequence NEE. The CP sequence was expected to respond to cover cropping since with the absence of winter wheat, the cover crop would have two winters in which recapture NO_3^- that would otherwise be leached in the fallow period of both winters. However, sNEE showed no significant changes due to cover cropping or reduced tillage treatment in the CP sequence, with the maximum average being 0.94 sNEE in the cover crop tilled treatment and the minimum being 0.92 in the in the cover crop reduced tillage treatment. The potatoes showed a significant ($p < 0.01$) positive increase in NEE due to cover cropping during the 2014 season (Table 8). The lack of significant increases in sNEE due to cover cropping in the CP rotation can be traced to a diminished uptake of N by the cover crop biomass in both 2013 and 2014 (Table 6).

During the winter of 2013, the triticale cover crop prior corn took up $38.8 \text{ kg N ha}^{-1}$ compared to the triticale grown in the WC sequence which took up $102.4 \text{ kg N ha}^{-1}$ during the winter of 2014. The uptake in N in the 2013 growing season is reflected by a profile wide reduction in available N from $23.8 \text{ kg N ha}^{-1}$ in the cover crop plots to $45.3 \text{ kg N ha}^{-1}$ in the fallow plots (Table 7). While the triticale successfully reduced the available N in the soil profile, cover cropping did not improve the NEE of the corn in the following year (Table 8).

Furthermore, the mustard grown in the CP sequence winter killed completely during the winter of 2014 resulting in no collectable biomass by the spring. Although the mustard did not survive winter, there was a significant increase in the NEE of potatoes in 2014 due to cover cropping, suggesting that the fall growth of the mustard had captured some of the escaping NO_3^- prior to winter death. The total available N in the soil profile decreased significantly from $94.2 \text{ kg N ha}^{-1}$ in the fallow plots to $57.9 \text{ kg N ha}^{-1}$ in the mustard cover cropped plots. While over wintering cover crops have been shown to cause greater reductions in NO_3^- leaching, winter killed cover crops have also been shown to reduce NO_3^- leaching loss (Weinert et al. 2002). A closer look at the over winter change in soil NO_3^- profiles in the winter of 2014

shows that comparatively smaller increase in the mustard cover crop in the top 30 cm, but no significant differences in the other depth increments.

Cover Crop and Reduced Tillage Effects on sNEE in the PW Sequence

The PW sequence, with a high sNEE and low N balance, also showed a change in sNEE due to cover cropping. The average sNEE was 0.76 in the cover cropped plots and 0.67 in the winter fallow plots (Table 9). While not significant, the trend is towards higher sNEE in the cover cropped plots. Similarly, there was a trend towards reduced tillage plots having an increased sNEE (Table 9). However, when looking at the combined cover crop and reduced tillage plots you can see that, while the cover cropped plots had greater sNEE than fallow in the tilled plots, the difference was only 0.01 between the reduced tillage fallow and the reduced tillage cover cropped.

The increased efficiency of the cover crop tilled versus the fallow tilled can also be seen by looking at the single year NEE of potatoes in 2013 and wheat in 2014, both the cover crop and reduced tillage plots have the highest single year NEE for potatoes and wheat among all years (Table 7). An important driver for the changes in NEE can be the substantial reductions in soil available N due to cover cropping in both the spring of 2013 and the spring of 2014. However, the reductions of N in the spring of 2014 were not significant, which is understandable considering that any cover crop effect during the spring of 2014 would be negligible as the winter wheat was planted in all plots. The NEE differences in the wheat correspond with large, but insignificant differences which were found in the available N in the upper 60 cm during the spring of 2013. In the lower 60 cm of the soil profile there was also reductions in spring available N due to the over winter mustard in both tilled and reduced till plots indicating that the mustard prevented the vertical movement of NO_3^- down the profile.

While the single season yield and N removal did not vary significantly due to the treatments of cover cropping or reduced tillage, cover cropping did lead to an insignificant decrease in yield from 47,269 kg ha⁻¹ to 44,420 kg ha⁻¹ in potatoes during the 2013 growing season. However, the yield

difference between the conventional till and the reduced tillage were negligible (Table 5). The N harvested as tubers in the 2013 reflects the decreases in yield. As the reductions in exported N would lead to a lower NEE given the same N supply, it is evident that the increased NEE due to cover cropping is dependent on major reductions in the available N in the soil. The following wheat yields showed the opposite trend with the wheat yield increasing with cover crop from 7,481 kg ha⁻¹ in the fallow plots and 8,000 kg ha⁻¹ in the

Cover cropping showed a large (66 kg N ha⁻¹) but non-significant reduction in harvested N when compared with the corresponding tilled treatment (Table 5). This decrease in N harvested corresponded to significant decreases in soil N in both the top 60 cm and the bottom 60 cm of the soil profile. This indicates that, while there is not a significant decrease in yield, the decrease in N in the soil profile due to cover cropping may be contributing to a reduction in the amount of N being harvested which in turn is leading to a lower NEE.

Cover Crop and Reduced Tillage Effects on sNEE in the WC Sequence

The WC sequence, at field 3, had significant yield depressions, discussed above was the location of the wheat corn sequence (Figure 40). There were no significant changes in sNEE due to cover cropping or reduced tillage. The difference between the average reduced tillage sNEE and conventional tillage sNEE in the WC sequence was only 0.1, which was identical to the change in sNEE from cover crop to fallow in the WC sequence (Table 9). However, cover crop inactivity cannot explain the lack of significance between cover crop treatments in the WC sequence, as it did in the CP sequence. In the winter of 2013-2014 triticale biomass recovered 102.4 kg N ha⁻¹, but no-significant differences in soil mineral N were observed in the soil profile.

While cover cropping did not have a significant effect on the 2014 corn NEE, reduced tillage did have a significant effect on the NEE with the average tilled plot having an NEE of 0.15 and the average reduced till plot having an NEE of 0.26. The reduced tillage plots showed lower levels of available N in the top 60 cm of the soil. In addition to this the yield was lower in the conventionally tilled plots in the

2014 corn plots. The combination of high yields and reduced N supply due to cover cropping led to significant increases in NEE due to reduced tillage. The trend of single year NEE of wheat in 2013 was the opposite of the trend of the following corn in 2014, which decreased with reduced tillage averaging 0.62 in the reduced tillage plots and 0.70 in the tilled plots. The NEE reduction of wheat in 2013 due to reduced tillage was explained by the reduction in available N in reduced tillage plots in the spring of 2013. Considering the over winter changes in NO_3^- during the winter of 2013 in the WC sequence, we can see that the patterns differed by tillage rather than by cover crop (Figure 43). The reduced tillage plots showed over winter decreases in NO_3^- at all depths between 0-120 cm as opposed to the tilled plots which showed increases in the 30-60 cm and decreases in the 60-90 cm zone. The increase in NO_3^- in the 30-60 cm could be due to inactivity of roots in the fall, or the increased mineralization due to tillage. During the winter of 2014, the trend in the conventionally tilled plot reverses and the NO_3^- in the 30-60 cm range decreases while the 60-90 cm range increases. This mirroring of NO_3^- changes in the profile from the winter of 2013 to the winter of 2014 maybe a contributing factor in the reversing effects of reduced tillage between 2013 and 2014. The negative and positive changes of NEE in the 2013 wheat and 2014 corn of the WC sequence appear to cancel each other out with respect to sNEE leaving tillage and cover cropping with no effect on sNEE in the WC sequence.

Table 9

	sNUE, sNEE, and N Balance Analyzed by Treatment									
	sNUE			sNEE			N balance (kg N ha ⁻¹)			
	CP	PW	WC	CP	PW	WC	CP	PW	WC	
Cover Crops	Reduced Tillage	46.5	74.8	27.0	0.92	1.11	0.52	70.1	-49.5	77.9
Cover Crops	Tilled	46.0	67.9	25.8	0.94	1.10	0.47	65.6	-89.7	178.1
Fallow	Reduced Tillage	45.3	59.3	24.8	0.93	1.09	0.48	22.6	-91.4	112.5
Fallow	Tilled	44.7	51.5	24.6	0.93	0.87	0.50	22.5	-96.5	183.6
Means										
	Reduced Tillage	45.90	67.04	25.90	0.93	1.10	0.50	46.35	-70.45	95.19
	Tilled	45.34	59.70	25.24	0.94	0.98	0.49	44.05	-93.10	180.84
	Cover Crop	46.25	71.33	26.43	0.93	1.10	0.50	67.85	-69.60	128.01
	Fallow	44.99	55.40	24.71	0.93	0.98	0.49	22.55	-93.95	148.02
Statistics Table										
	Reduced Tillage	ns	.	ns	ns	ns	ns	ns	ns	ns
	Cover Crop	ns	ns	ns	ns	ns	ns	ns	ns	ns

p < 0.001 = ***, 0.01 = **, 0.05 = *, 0.1 = .

Summary:

NO_3^- leaching is a serious concern in the Columbia Basin (GWMA 2001). One potential source of NO_3^- is agricultural systems with potatoes as a dominant crop. Studies have been done showing that cover cropping and reduced tillage in irrigated systems can reduce NO_3^- leaching (Weinert et al. 2002). Our study aimed to address whether sNEE could be increased by the use of cover cropping and reduced tillage. While there were no significant changes in sNEE there were some significant improvements in single year NEE, specifically in potatoes. Even without increases in NEE non-legume cover crops and reduced tillage were shown to decrease NO_3^- movement down through the soil indicating that leaching would be reduced if cover crops were more widely adopted in the Columbia Basin.

Conclusion:

- Cover cropping and reduced tillage had no significant impacts on sNEE.
- The greatest increases in NEE in potatoes were instances where both cover cropping and reduced tillage were used as management practices.
- Cover cropping and reduced tillage appear to have decreased the movement of NO_3^- down through the soil profile.

CHAPTER 5: THE UTILITY OF A FEDERAL RESEARCH DATABASE IN DETERMINING FUTURE RESEARCH NEEDS RELATED TO BEST MANAGEMENT PRACTICES FOR CONTROLLING THE LOSS OF REACTIVE NITROGEN FROM AGRICULTURE TO THE ENVIRONMENT

Introduction

Nr Loss from Agricultural Systems

Reactive Nitrogen (Nr) is essential for all life, and yet can be toxic and environmentally damaging if high concentrations accumulate in the wrong place (Galloway et al. 2003, Smil 1999, Smil 2002). A large amount of the Nr that escapes in the environment is lost from agriculture and is leached to ground water, run off to surface water, and be emitted into the atmosphere as a greenhouse gas (Smil 1999). The negative impacts of Nr loss to the environment have been detailed elsewhere, but there has been a lack of solution.

Nr Loss to the Environment is as a “Wicked Problem”

The biogeochemical, economical, and environmental complexities of Nr loss to the environment has been described as a ‘wicked problem’ (Thornton et al. 2013, Shortle and Horan 2016). A ‘wicked problem’ first described Rittel and Webber (1973) with ten key characteristics which can be summarized in two main points 1) there is no common consensus about what the problem is, and 2) multiple parties and agendas with conflicting interests are involved. The list of all ten requirements is far more rigorous and Thornton et al. 2013 goes into depth showing how eutrophication of freshwater is a wicked problem. As eutrophication is partially a sub problem of the Nr loss to the environment problem, Nr loss can be treated as a

‘wicked problem’. This is important because by definition wicked problems have not been solved before so there is no framework for solving them. In addition to this the lack of consensus among stakeholders is aspect of the wicked problem. An example of an individual taking part in such a problem without fully understanding the externalities of their decisions is that of “the good farmer” (Macgregor et al. 2006, Silvasti 2002). The view from downstream is more prone to vilify the upstream farmer as the hurt is coming downstream. This highlights that not only may stakeholders perspectives of what the problem is may vary, but the motives of other stakeholders themselves may be warped. Opposing views as to what the problem is and even perceptions on the stakeholders may even be found at the agency level. Indeed conflicting perspectives on the problem may be intrinsic to the mandates of individual agencies. Take for instance the United States Department of Agriculture (USDA) whose primary purpose is the support of U.S. agriculture and ensuring a secure supply of food to the people of the U.S. At the nexus of soil and water this purpose may come into direct conflict with that of the Environmental Protection Agency’s (EPA) purpose to maintain clean water for the people of the U.S.

Potential Role of Scientific Knowledge in Reducing Nr Loss

Scientific research and knowledge can be used to improve stakeholder’s understandings of Nr loss sources and pathways. This often takes the form of monitoring networks, meta-analysis, and largescale modeling approaches (SAB 2011). Another role of scientific research and knowledge is to pursue potential technological solutions. Research can be used to both develop new solutions which and verify existing technological solutions (SAB 2011). In order to assure that scientific research and knowledge are achieving their maximum potential contribution to reducing Nr loss to the environment there must be a sound research policy in

place, and in order to assure a sound research policy some understanding of the research policy subsystem must be achieved.

The Policy Subsystem With in Which the Research of Nr Loss Exists

The research of Nr loss from agriculture to the environment takes place in a policy subsystem involving agricultural and environmental policy makers and the USDA Research, Education, and Economics Mission Area (REE) (Figure 45). Normatively this research-policy subsystem follows the ‘Interactive Model’ of research-policy interactions described Weis (1976). A key point of the interactive model is that researchers and policymakers are working towards a common goal. However, an ‘Interactive Model’ may have a propensity to break down when faced with a ‘wicked problem’ such as Nr loss to the environment. In this case the subsystem may move into a ‘Political Model’ or a ‘Tactical Model’. In the ‘Political’ and ‘Tactical’ models policy is being used to inform research rather than research to inform policy (Stehr 2012). In order to retain Nr loss subsystem within the ‘Interactive Model’ it is critical that the connections between agricultural and environmental research and both agricultural and environmental policy makers and agricultural research funding agencies is maintained (Figure 45 E & F).

In this subsystem policy makers are presented with the problem of reducing Nr loss to the environment while not reducing agricultural production. The apparent lack of solutions leads agricultural and environmental policy makers to fund research looking for technological solutions which will reduce Nr while maintaining food production. Once voted on by the legislature the executive signs it into law and passes it down to the USDA research agencies (e.g. Agricultural Act of 2014). The most prominent USDA research agencies are the Agricultural Research Service (ARS), the National Institute of Food and Agriculture (NIFA), the Economic

Research Service (ERS), and the National Agricultural Statistical Service (NASS). The ARS, ERS, and NASS all conduct intramural research, meaning that the research done at these agencies is done by federally employed researchers, but NIFA directs extramural research through granting, primarily to land grant institutions (U.S. 301-308).

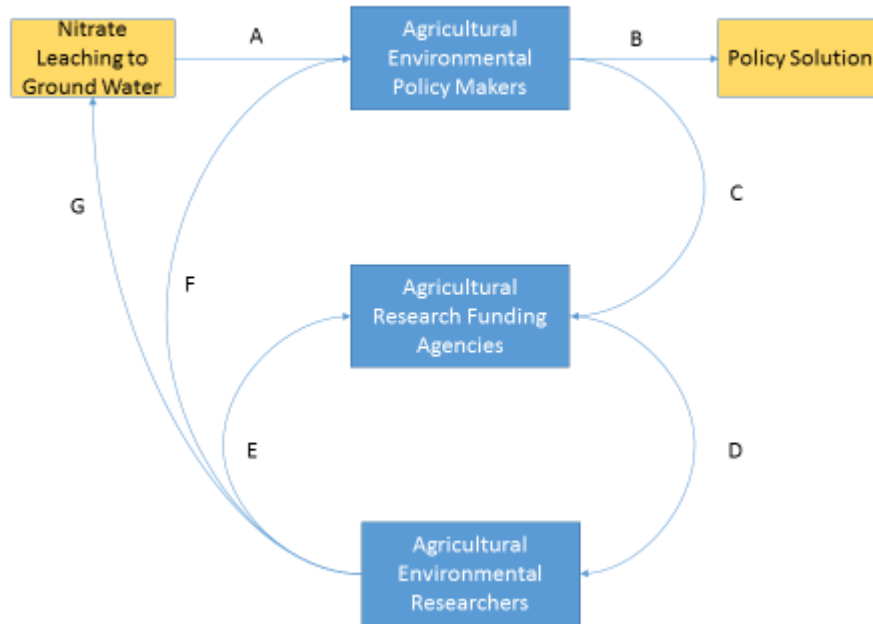


Figure 45: Model of the policy subsystem in which NO_3^- loss to the environment research is directed and funded. (A) NO_3^- leaching to ground water is a problem which requires policy attention in the agricultural and environmental policy subsystems. (B) Ideally policy agricultural and environmental policy makers will base policy in sound scientific knowledge. (C) In order to make sure that the policy is grounded in research the agricultural and environmental policy makers will pass over arching research goals on to agricultural research agencies. (D) The agency personal in charge of funding research then fund the research. (E & F) Next the newly acquired information is used to inform the policy makers of potential policy solutions. In

addition to informing the agricultural and environmental policy makers the state of the scientific knowledge should be used to inform leaders at the agricultural research funding agencies.

The model of the policy subsystem presented here is in no way exhaustive. On the contrary, for the sake of simplicity and readability, it ignores important public policy and private players. Both the Environmental Protection Agency and the United States Geological Survey (USGS) have vested interest in the transport Nr from agriculture and into the environment. The EPA's responsible for the enforcement of both the Clean Water and Clean Air Acts each of which have direct implications on Nr loss from agriculture. The USGS is charges with the monitoring of streams and rivers in the U.S. many of which have become loaded with Nr. In addition to the pantheon of government agencies there is plethora of other interested parties including private individuals, fertilizer industry groups, environmental groups and farmers. All of whom have interests to protect.

The REEIS Database.

The USDA-REE mandate area has developed a database called The Research, Education, and Economics Information System (REEIS) for the precise purpose providing feedback from researchers to the REE staff (reeis.gov 2016). The REEIS database houses a complete record of the NIFA funded projects from 2002 onward. In addition to the NIFA funded projects there are projects conducted by the ARS, ERS, Forest Service (FS) and the State Agriculture and Extension Services (SAES). While the REEIS houses a vast number of project reports, summaries, and bibliographies addressing all facets of agricultural research, it is unclear how the database might be used as a source of meaningful information specifically for informing policy and research enacting agencies. The goal of this work is to strengthen the connection between

agricultural and environmental research and USDA-REE mandate area. Specifically to aid NIFA in a more cohesive understanding of the state research as regards Nr loss to the environment, with the intention of aiding in the development of future RFPs.

REEIS Question.

In order to apply the REEIS database in such a way that it serves to inform NIFA in the development of future RFPs a specific question is required. Extremely broad questions such as, “How can we solve the problem of Nr loss to the environment” is essentially an unsearchable questions. However, what we can do is try to find what specialists perceive as a gap or a need for greater research. The EPA Science Advisory Board published a report on Nr loss to the environment in August 2011 (SAB 2011). The purpose of this report was to, “provide advice to EPA on integrated nitrogen research and control strategies.” (SAB 2011). One of the many recommendations made by the SAB advisory board was increased research comparing the effectiveness, efficiency, and cost of BMPs in reducing Nr loss to the environment. From this statement we formulated the null hypothesis that NIFA has conducted extensive “Research regarding the effectiveness efficient and cost of BMPs in reducing Nr loss to the environment.”

Methods

Query Development

In order to effectively search for evaluative research of BMPs in the query of the REEIS database was designed find all projects having to do with the analysis of the effectiveness of BMPs in reducing Nr loss. The query was designed using standard Boolean search terms and consisted of four parts joined by “AND”. The terms were BMP, Evaluation, Nr forms, and Loss Pathway, meaning that every project returned must have to do with a BMP related to Nr forms

and loss pathways and has some sort of evaluation of efficacy (Table 10). As such a query has the potential for returning improper results all returned project entries were checked for relevance.

Table 10: Query search terms

Term	Synonyms Used In Query
BMP	("nutrient management" OR "manure management" OR "wetland restoration" OR "wetland creation" OR "riparian buffers" or "conservation tillage" OR "erosion control" OR "cover crops" OR "grazing management" OR "ecological production systems" OR "organic production systems" OR BMP OR "best management practice")
Evaluation	(effectiveness OR efficiency OR cost)
Nr Forms	(nutrient OR nitrogen OR nitrate OR nitrite OR "nitrous oxide" OR ammonium OR ammonia OR "Dissolved organic nitrogen" OR "Dissolved inorganic nitrogen" OR "DON" OR "DIN" OR "NO _x " OR "N ₂ O" OR "NH ₃ " OR "NH ₄ " OR "NO ₃ " OR "NO ₂ ")
Loss Pathways	(loss OR pollution OR emission OR leach* OR runoff OR loading)

Each project was classified based on its relevance to evaluating the use of BMPs in reducing Nr loss to the environment. In order for a project to be classified as ‘highly relevant’ it was required that the project meet all the key terms in the query terms. For instance “Surface Water Pollution and Harmful Algal Bloom Production in Estuarine Waters: An Evaluation of Potential BMPs” was coded as highly relevant as it directly addressed the comparison of BMPs. For a project to be coded as ‘highly relevant’ it was required that the project include specific BMPs designed for Nr loss to the environment and an evaluation component comparing the cost, effectiveness, or efficacy of the BMP. On the other hand projects which did not have these three components were classified as “weakly relevant”. For instance a project titled “Understanding Livestock Manure Use Impacts on Crop Production Systems and Environment in the Northern

Great Plains” was classified as weakly relevant as it did not involve a specific comparison of the effectiveness, efficiency, or cost of differing BMPs. Projects which were difficult to classify as either fitting the criteria or not were classified into the third category of ‘somewhat relevant’.

The resulting ‘highly relevant’ results were then visualized using Microsoft excel to look at the break down of research projects by agency and over time (Microsoft). The location of the research projects was mapped by state using ArcMap (ESRI).

Results and Discussion:

Query Results:

The query returned 1,073 projects from the REEIS data base of these 253 projects were classified as ‘highly relevant’, 167 as ‘moderately relevant’, and 616 as ‘weakly relevant’. After conducting the quality control there were 253 projects found to have been funded between 2002 and 2013 (Figure 45). Notice that around 2007 the number of projects is cur roughly in half, and remains low from 2007-2012. This phenomena roughly corresponds with the implementation of larger CAP grants as a result of AFRI legislation in 2008 (NIFA 2008). Hence although the overall number of projects declined the funding or actual amount of research being done probably did not decline. This highlights as weakness of the REEIS database which is that the funding for each project is not rigorously recorded so coming up with an estimate of the investment would be difficult given only the REEIS database. Looking at the projects broken down by agency we can see that 54% were NIFA funded projects 40% were ARS funded projects 15% were funded by state agriculture experiment stations, and <1% by the Forest Service (Figure 46).

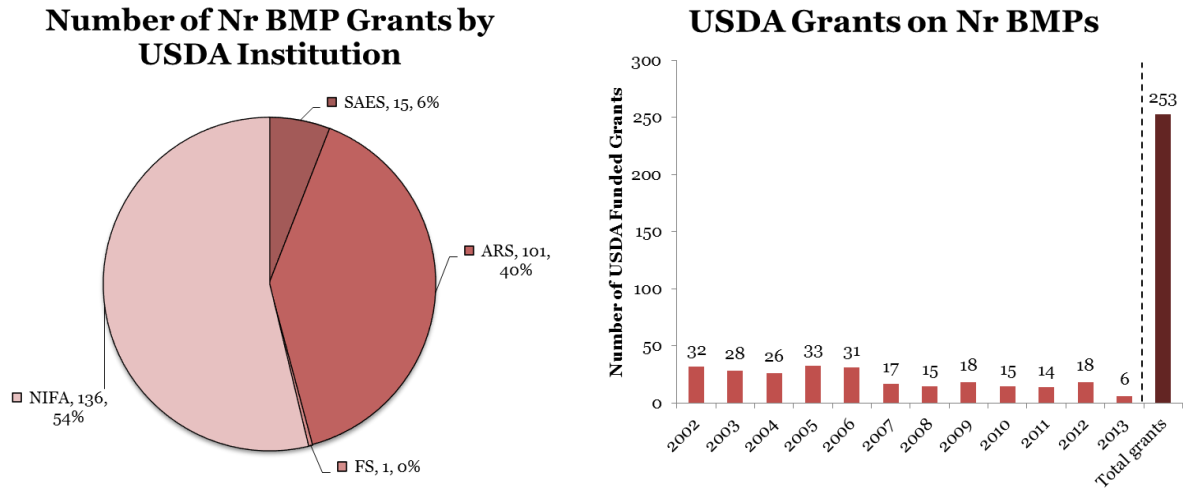


Figure 46: (Left) Break down of BMP assessment research by agency. (Right) Number of BMP assessment projects over time.

BMP Evaluation Projects on a State By State Basis

Much work has been done looking at importance of geographic location on the potential effectiveness of agricultural and environmental policy for reducing Nr loss to the environment. At the farm scale measures of intra-farm variation in residual N than inter-farm variation indicating that farm gate efficiency policies may not be an appropriate means of regulating N loss (Beek et al. 2003). At the watershed scale variation in land use becomes a driver Nr loss to the environment (Babiker et al. 2004). The watershed scale is the most natural division by which to approach reductions in Nr loss, but faces the problem of defining the boundaries of the full watershed (Johnson et al. 1996, Lockwood 2000, Osmond 2012). Variation from catchment to catchment makes accurate predictions as to the efficacy of BMPs difficult (Lord et al. 1999). In addition to agricultural, physical geography, and climactic heterogeneity, socioeconomic heterogeneity may impact the demand for fertilizers (Hansen 2004). Even so it is paramount that any federal regulatory policies be applied across watersheds evenly as reductions in Nr through

regulation in one watershed may lead to increased Nr loss from unregulated watersheds (Doering 1999). Spatial heterogeneity at multiple scales and on multiple factors makes the formulation of national policies difficult.

The inherent physical, social, and economic heterogeneity requires that any policy addressing Nr loss to the environment take a spatially explicit approach in policy solutions. Consequently research policy must also be spatially aware. Iowa followed by Pennsylvania had the greatest number of BMP evaluation projects done (Figure 47). BMP evaluation projects mapped by state shows Iowa and Pennsylvania as ranked in the greatest category of 15-18 grants. This is as would be expected as both of these states are important agricultural producers in two of the nation's susceptible watersheds, the Mississippi river and the Chesapeake Bay. From this map we can see that the majority of research assessing BMPs has been done in the Mississippi river basin. The data exported from REEIS allows us to assess the number of BMP research projects conducted by state, but does not allow us to look at any finer scale. This is a great disadvantage when assessing where research has focused as it does not allow us to consider regions which may fall within state boundaries (e.g. the Columbia Basin of E. Washington offers unique challenges in reducing Nr loss than the agricultural systems less than 50 miles away in the Palouse region of E. Washington).

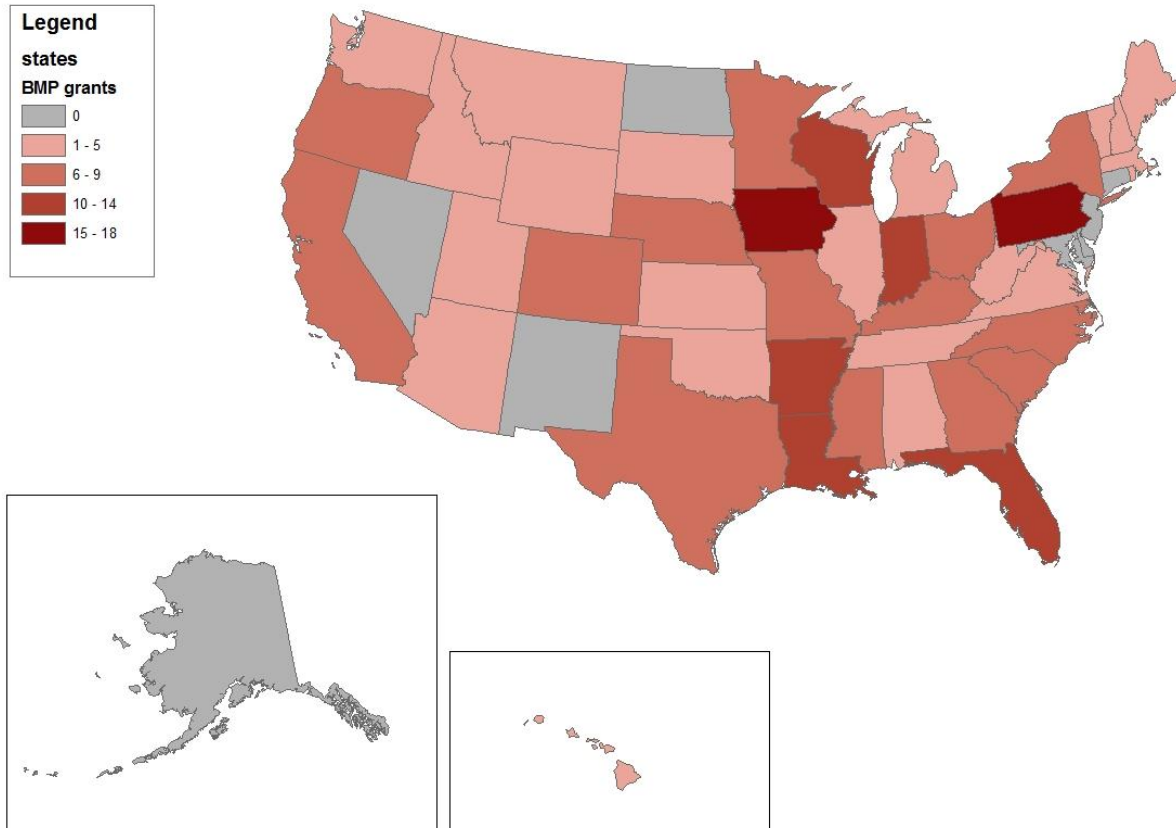


Figure 47: Number BMP evaluation projects by state.

Meta-Analysis and Literature Reviews of BMPs

Based on the results from the query of the REEIS database it was surmised that the evaluation of BMPs is a very mature field of research. The Conservation Effects Assessment Project (CEAP), which was headed up by the Natural Resource Conservation Service (NRCS), developed lists of BMPs and indicated whether these BMPs had been shown to decrease Nr loss (Sharpley et al. 2007). Meta-analysis and reviews considering the impacts of cover cropping, riparian buffers, and fertilizer management. Cover cropping has consistently shown reductions in Nr loss (Valkama et al. 2015, Tonitto et al. 2006, Gabriel et al. 2013). The range with in which Nr loss is reduced varies within BMPs and between BMPs depending the factors varying above.

However, it is certain that if these BMPs were widely adopted and properly implemented there would be reductions in overall Nr loss to the environment.

BMPs in Policy Solutions.

The fact that these BMPs are not being widely adopted indicates there is some barrier to adoption. Multiple studies looking at a variety of BMPs have noted that while the BMPs are effective at reducing the flow of Nr into the environment they are often not economically viable for the grower. An evaluation of over-winter green cover crops, spreading of manure over greater areas, restrictions in the timing of manure application, and the restrictions of fertilizer inputs to not exceed recommendations showed decreasing Nr loss across ten different watersheds (Lord et al. 1999). However, in order to implement such a plan farmers were subsidized to spread the manure over greater distances. The need to subsidize BMPs is a common theme in the literature (Gabriel et al. 2013, Huang et al. 1994, Haslar 1998, Powell et al. 2010, Lee 1998). From this it appears that BMP research as a general rule has gone beyond the point of needing to assess the efficacy and costs of BMPs and to the point of implementation.

Recommendations to NIFA Regarding BMP Evaluation Research

1. NIFA has funded at least 253 projects assessing the efficacy of BMPs and these projects are spread relatively evenly across U.S. agriculture.
2. Continued research on BMPs should be in the form of filling in geographic and systems gaps. (e.g. making sure the BMP is applicable to all systems).
3. Increase the functionality of the REEIS database. There is great opportunity to increase the functionality of the REEis database. The first step would be to simply

4. Looking for the next win-win scenario. Funding should go towards innovative BMPs which have not been tested yet.

Bibliography

1.

Abbès, C., Parent, L. E., Karam, A. & Isfan, D. Onion response to ammoniated peat and ammonium sulfate in relation to ammonium toxicity. *Can. J. Soil. Sci.* **75**, 261–272 (1995).

2.

Aloni, R., Aloni, E., Langhans, M. & Ullrich, C. I. Role of Cytokinin and Auxin in Shaping Root Architecture: Regulating Vascular Differentiation, Lateral Root Initiation, Root Apical Dominance and Root Gravitropism. *Ann Bot* **97**, 883–893 (2006).

3.

Alva, A. K., Collins, H. P. & Boydston, R. A. Corn, Wheat, and Potato Crop Residue Decomposition and Nitrogen Mineralization in Sandy Soils Under an Irrigated Potato Rotation. *Communications in Soil Science and Plant Analysis* **33**, 2643–2651 (2002).

4.

Alva, A. K., Hodges, T., Boydston, R. A. & Collins, H. P. Effects of irrigation and tillage practices on yield of potato under high production conditions in the Pacific Northwest. *Communications in Soil Science and Plant Analysis* **33**, 1451–1460 (2002).

5.

Andraski, T. W. & Bundy, L. G. Cover Crop Effects on Corn Yield Response to Nitrogen on an Irrigated Sandy Soil. *Agronomy Journal* **97**, 1239 (2005).

6.

Angus, J. F., Gupta, V. V. S. R., Pitson, G. D. & Good, A. J. Effects of banded ammonia and urea fertiliser on soil properties and the growth and yield of wheat. *Crop. Pasture Sci.* **65**, 337–352 (2014).

7.

Babiker, I. S., Mohamed, M. A. A., Terao, H., Kato, K. & Ohta, K. Assessment of groundwater contamination by nitrate leaching from intensive vegetable cultivation using geographical information system. *Environment International* **29**, 1009–1017 (2004).

8.

Beek, C. L. van, Brouwer, L. & Oenema, O. The use of farmgate balances and soil surface balances as estimator for nitrogen leaching to surface water. *Nutrient Cycling in Agroecosystems* **67**, 233–244 (2003).

9.

Bell, C. Ammonia: A Review of Mechanistic Models of Ammonia Volatilization and Theoretical Studies of the Catalytic Reduction of Dinitrogen to Ammonia by A Boron Cation, A Boron Dihydride Cation, And Beryllium Dihydride. (Texas Tech University, 2006).

10.

Bennett, A. C. & Adams, F. Concentration of $\text{NH}_3(\text{aq})$ Required for Incipient NH_3 Toxicity to Seedlings. *Soil Science Society of America Journal* **34**, 259–263 (1970).

11.

Blanchar, R. Determination of the partial pressure of ammonia in soil air. *Soil Science Society of America Proceedings* 791–794 (1967).

12.

Blossfeld, S., Gansert, D. & Wade, B. Planar optodes: promising tools for non-invasive 2D imaging of rhizospheric dynamics of pH, O_2 and CO_2 . *The Proceedings of the International Plant Nutrition Colloquium XVI* (2009).

13.

Bouma, T. J., Nielsen, K. L. & Koutstaal, B. Sample preparation and scanning protocol for computerised analysis of root length and diameter. *Plant and Soil* **218**, 185–196 (2000).

14.

Britto, D. T. & Kronzucker, H. J. NH₄⁺ toxicity in higher plants: a critical review. *Journal of Plant Physiology* **159**, 567–584 (2002).

15.

Bundy, L. G. & Andraski, T. W. Recovery of Fertilizer Nitrogen in Crop Residues and Cover Crops on an Irrigated Sandy Soil. *Soil Science Society of America Journal* **69**, 640 (2005).

16.

Canon. Color Image Scanner CanoScan Lide 700F.

17.

Carminati, A. *et al.* Dynamics of soil water content in the rhizosphere. *Plant Soil* **332**, 163–176 (2010).

18.

Carter, M. R., Noronha, C., Peters, R. D. & Kimpinski, J. Influence of conservation tillage and crop rotation on the resilience of an intensive long-term potato cropping system: Restoration of soil biological properties after the potato phase. *Agriculture, Ecosystems & Environment* **133**, 32–39 (2009).

19.

Collins, H. P. *et al.* Soil microbial, fungal, and nematode responses to soil fumigation and cover crops under potato production. *Biol Fertil Soils* **42**, 247–257 (2006).

20.

Collins, H. P., Delgado, J. A., Alva, A. K. & Follett, R. F. Use of Nitrogen-15 Isotopic Techniques to Estimate Nitrogen Cycling from a Mustard Cover Crop to Potatoes. *Agronomy Journal* **99**, 27 (2007).

21.

Comas, L. H., Eissenstat, D. M. & Lakso, A. N. Assessing root death and root system dynamics in a study of grape canopy pruning. *New Phytologist* **147**, 171–178 (2000).

22.

Coskun, D., Britto, D. T., Li, M., Becker, A. & Kronzucker, H. J. Rapid Ammonia Gas Transport Accounts for Futile Transmembrane Cycling under $\text{NH}_3/\text{NH}_4^+$ Toxicity in Plant Roots. *Plant Physiol.* **163**, 1859–1867 (2013).

23.

Creamer, F. L. & Fox, R. H. The Toxicity of Banded Urea or Diammonium Phosphate to Corn as Influenced by Soil Temperature, Moisture, and pH. *Soil Science Society of America Journal* **44**, 296 (1980).

24.

Dabney, S. M., Delgado, J. A. & Reeves, D. W. Using Winter Cover Crops to Improve Soil and Water Quality. *Communications in Soil Science and Plant Analysis* **32**, 1221–1250 (2001).

25.

Dardanelli, J. L., Ritchie, J. T., Calmon, M., Andriani, J. M. & Collino, D. J. An empirical model for root water uptake. *Field Crops Research* **87**, 59–71 (2004).

26.

Delgado, J. A. Quantifying the loss mechanisms of nitrogen. *Journal of Soil and Water Conservation* **57**, 389–398 (2002).

27.

Delgado, J. A. *et al.* Evaluation of Nitrate-Nitrogen Transport in a Potato–Barley Rotation. *Soil Science Society of America Journal* **65**, 878 (2001).

28.

Devkota, M. *et al.* Tillage and nitrogen fertilization effects on yield and nitrogen use efficiency of irrigated cotton. *Soil and Tillage Research* **134**, 72–82 (2013).

29.

Dinnes, D. L. *et al.* Nitrogen Management Strategies to Reduce Nitrate Leaching in Tile-Drained Midwestern Soils. *Agronomy Journal* **94**, 153–171 (2002).

30.

Doering, O. C. Economic linkages driving the potential response to nitrogen over-enrichment. *Estuaries* **25**, 809–818 (2002).

31.

Doussan, C., Pierret, A., Garrigues, E. & Pagès, L. Water Uptake by Plant Roots: II – Modelling of Water Transfer in the Soil Root-system with Explicit Account of Flow within the Root System – Comparison with Experiments. *Plant and Soil* **283**, 99–117 (2006).

32.

Dowling, C. W. SEED AND SEEDLING TOLERANCE OF CEREAL, OILSEED, FIBRE AND LEGUME CROPS TO INJURY FROM BANDED AMMONIUM FERTILIZERS. (University of New England, 1998).

33.

Esser, H. G., Carminati, A., Vontobel, P., Lehmann, E. H. & Oswald, S. E. Neutron radiography and tomography of water distribution in the root zone. *Z. Pflanzenernähr. Bodenk.* **173**, 757–764 (2010).

34.

Fenn, L. & Kissel, D. The Influence of Cation Exchange Capacity and Depth of Incorporation on Ammonia Volatilization from Ammonium Compounds Applied to Calcareous Soils. **40**, 394–398 (1976).

35.

Gabriel, J. L., Garrido, A. & Quemada, M. Cover crops effect on farm benefits and nitrate leaching: Linking economic and environmental analysis. *Agricultural Systems* **121**, 23–32 (2013).

36.

Gahoonia, T. S., Care, D. & Nielsen, N. E. Root hairs and phosphorus acquisition of wheat and barley cultivars. *Plant and Soil* **191**, 181–188 (1997).

37.

Galloway, J. N. *et al.* The Nitrogen Cascade. *BioScience* **53**, 341–356 (2003).

38.

Garrigues, E., Doussan, C. & Pierret, A. Water Uptake by Plant Roots: I – Formation and Propagation of a Water Extraction Front in Mature Root Systems as Evidenced by 2D Light Transmission Imaging. *Plant and Soil* **283**, 83–98 (2006).

39.

Gasch, C. K., Collier, T. R., Enloe, S. F. & Prager, S. D. A GIS-based method for the analysis of digital rhizotron images. *Plant Root* **5**, 69–78 (2011).

40.

Giles, M., Morley, N., Baggs, E. M. & Daniell, T. J. Soil nitrate reducing processes - drivers, mechanisms for spatial variation, and significance for nitrous oxide production. *Front Microbiol* **3**, (2012).

41.

Grant, C. A., Derksen, D. A., McLaren, D. & Irvine, R. B. Nitrogen Fertilizer and Urease Inhibitor Effects on Canola Emergence and Yield in a One-Pass Seeding and Fertilizing System. *Agronomy Journal* **102**, 875 (2010).

42.

Gregory, P. J. *Plant Roots: Growth, Activity and Interactions with the Soil*. (Wiley, 2006).

43.

Grose, M. J., Gilligan, C. A., Spencer, D. & Goddard, B. V. D. Spatial heterogeneity of soil water around single roots: use of CT-scanning to predict fungal growth in the rhizosphere. *New Phytologist* **133**, 261–272 (1996).

44.

Hammac, W. A., Pan, W. L., Bolton, R. P. & Koenig, R. T. High resolution imaging to assess oilseed species' root hair responses to soil water stress. **339**, 125–135 (2012).

45.

Hansen, E. & Djurhous, J. Nitrate leaching as affected by soil tillage and catch crop. **41**, 203–219 (1997).

46.

Hansen, L. G. A deposit-refund system applied to non-point nitrogen emissions from agriculture. *Environ Econ Policy Stud* **2**, 231–247 (2014).

47.

Hanson, B. R., Šimůnek, J. & Hopmans, J. W. Evaluation of urea–ammonium–nitrate fertigation with drip irrigation using numerical modeling. *Agricultural Water Management* **86**, 102–113 (2006).

48.

Heaney, J. Products of Urea Hydrolysis in Soil Alter the Solubility, Plant Uptake, and Transport of Elements. (University of Alberta, 2001).

49.

Hoyt, G. D. Tillage and Cover Residue Affects on Vegetable Yields. *HortTechnology* **9**, 351–358 (1999).

50.

Ingram, K. T. & Leers, G. A. Software for Measuring Root Characters from Digital Images. *Agronomy Journal* **93**, 918 (2001).

51.

Izaurrealde, R. C., Kissel, D. E. & Cabrera, M. L. Simulation Model of Banded Ammonia in Soils. *Soil Science Society of America Journal* **54**, 917 (1990).

52.

Jahanzad, E. COVER CROP AND NITROGEN FERTILIZER MANAGEMENT FOR POTATO PRODUCTION IN THE NORTHEAST. *Doctoral Dissertations May 2014 - current* (2015).

53.

Johnson, A., Shrubsole, D. & Merrin, M. Integrated Catchment Management in northern Australia: From concept to implementation. *Land Use Policy* **13**, 303–316 (1996).

54.

Jury, W. & Horton, R. *Soil Physics*.

55.

Kaspar, T. C. & Ewing, R. P. ROOTEDGE: Software for Measuring Root Length from Desktop Scanner Images. *Agronomy Journal* **89**, 932 (1997).

56.

Keyes, S. D. *et al.* High resolution synchrotron imaging of wheat root hairs growing in soil and image based modelling of phosphate uptake. *New Phytol* **198**, 1023–1029 (2013).

57.

Kissel, D. E., Cabrera, M. L. & Paramasivam, S. in *Nitrogen in Agricultural Systems* 101–155 (2008).

58.

Kosegarten, H., Grolig, F., Wieneke, J., Wilson, G. & Hoffmann, B. Differential Ammonia-Elicited Changes of Cytosolic pH in Root Hair Cells of Rice and Maize as Monitored by 2[prime],7[prime]-bis-(2-Carboxyethyl)-5 (and -6)-Carboxyfluorescein-Fluorescence Ratio. *Plant Physiol.* **113**, 451–461 (1997).

59.

Kostenko, I. V. Scanning study of the optical parameters of sandy soddy-steppe soil samples from the southern Ukraine. *Eurasian Soil Science* **42**, 1012–1020 (2009).

60.

Le Bot, J. *et al.* DART: a software to analyse root system architecture and development from captured images. *Plant Soil* **326**, 261–273 (2010).

61.

Lee, L. K. Groundwater Quality and Farm Income: What Have We Learned? *Appl. Econ. Perspect. Pol.* **20**, 168–185 (1998).

62.

Levin, N., Ben-Dor, E. & Singer, A. A digital camera as a tool to measure colour indices and related properties of sandy soils in semi-arid environments. *International Journal of Remote Sensing* **26**, 5475–5492 (2005).

63.

Ling, G. & El-Kadi, A. A lumped parameter model for nitrogen transformation in the unsaturated zone. *Water Resources Journal* **34**, 203–212

64.

Lobet, G. & Draye, X. Novel scanning procedure enabling the vectorization of entire rhizotron-grown root systems. *Plant Methods* **9**, 1 (2013).

65.

Lobet, G., Pagès, L. & Draye, X. A Novel Image-Analysis Toolbox Enabling Quantitative Analysis of Root System Architecture. *Plant Physiol.* **157**, 29–39 (2011).

66.

Lockwood, Allan Curtis, M. Landcare and Catchment Management in Australia: Lessons for State-Sponsored Community Participation. *Society & Natural Resources* **13**, 61–73 (2000).

67.

Logsdon, S. D., Timlin, D. & Ahuja, L. R. in *Advances in Agricultural Systems Modeling* (American Society of Agronomy, Crop Science Society of America, Soil Science Society of America., 2013).

68.

Lord, E. i., Johnson, P. a. & Archer, J. r. Nitrate Sensitive Areas: a study of large scale control of nitrate loss in England. *Soil Use and Management* **15**, 201–207 (1999).

69.

Ma, Q., Tang, H., Rengel, Z. & Shen, J. Banding phosphorus and ammonium enhances nutrient uptake by maize via modifying root spatial distribution. *Crop. Pasture Sci.* **64**, 965–975 (2013).

70.

Maaz, T. M. Nitrogen uptake and cycling by canola, pea, and wheat: implications for rotational nitrogen use efficiency. (WASHINGTON STATE UNIVERSITY, 2014).

71.

Macfall, J. S., Johnson, G. A. & Kramer, P. J. Comparative water uptake by roots of different ages in seedlings of loblolly pine (*Pinus taeda* L.). *New Phytologist* **119**, 551–560 (1991).

72.

Mason, M. Effects of urea, ammonium nitrate and superphosphate on establishment of cereals, linseed and rape. *Aust. J. Exp. Agric.* **11**, 662–669 (1971).

73.

Meisinger, J. J. & Delgado, J. A. Principles for managing nitrogen leaching. *Journal of Soil and Water Conservation* **57**, 485–498 (2002).

74.

Meisinger, J. J., Hargrove, W. L., Mikkelsen, R. L., Williams, J. R. & Benson, V. W. Effects of cover crops on groundwater quality. in *Cover crops for clean water* 57–68 (Soil and Water Conservation Society, 1991).

75.

Meurant, G. & Ponnampereuma. *Flooding and Plant Growth*. (Academic Press, 2012).

76.

Moldrup, P. *et al.* Predicting the Gas Diffusion Coefficient in Repacked Soil Water-Induced Linear Reduction Model. *Soil Science Society of America Journal* **64**, 1588–1594 (2000).

77.

Mundy, C., Creamer, N. G., Wilson, L. G., Crozier, C. R. & Morse, R. D. Soil Physical Properties and Potato Yield in No-till, Subsurface-till, and Conventional-till Systems. *HortTechnology* **9**, 240–247 (1999).

78.

Neumann, G., George, T. & Plassard, C. Strategies and methods for studying the rhizosphere—the plant science toolbox. *Plant and Soil* **321**, 431–456 (2009).

79.

Nyiraneza, J. & Snapp, S. Integrated Management of Inorganic and Organic Nitrogen and Efficiency in Potato Systems. *Soil Science Society of America Journal* **71**, 1508–1515 (2007).

80.

Osmond, D., Meals, D., Hoag, D. & Arabi, M. Improving conservation practices programming to protect water quality in agricultural watersheds: Lessons learned from the National Institute of Food and Agriculture–Conservation Effects Assessment Project. *Journal of Water and Soil Conservation*

81.

Pan, W. L., Madsen, I. J., Bolton, R. P., Graves, L. & Sistrunk, T. Ammonia/Ammonium Toxicity Root Symptoms Induced by Inorganic and Organic Fertilizers and Placement. *Agronomy Journal* **108**, 2485–2492 (2016).

82.

Pan, W. L., Bolton, R. P., Lundquist, E. J. & Hiller, L. K. Portable rhizotron and color scanner system for monitoring root development. *Plant and Soil* **200**, 107–112 (1998).

83.

Pan, W. L. & Bolton, R. P. Root Quantification by Edge Discrimination Using a Desktop Scanner. *Agronomy Journal* **83**, 1047 (1991).

84.

Pang, P. C., Hedlin, R. A. & Cho, C. M. Transformation and movement of band-applied urea, ammonium sulfate, and ammonium hydroxide during incubation in several manitoba soils. *Can. J. Soil. Sci.* **53**, 331–341 (1973).

85.

Passioura, J. B. & Wetselaar, R. Consequences of Banding Nitrogen Fertilizers in Soil: II Effects on the Growth of Wheat Roots. *Plant and Soil* **36**, 461–473 (1972).

86.

Passioura, J. B. Water Transport in and to Roots. *Annual Review of Plant Physiology and Plant Molecular Biology* **39**, 245–265 (1988).

87.

Patrick, W. H. & Reddy, K. R. Nitrification-Denitrification Reactions in Flooded Soils and Water Bottoms: Dependence on Oxygen Supply and Ammonium Diffusion. *Journal of Environmental Quality* **5**, 469–472 (1976).

88.

Pavek, M. & Knowles, R. 2009 Potato Cultivars Field and Postharvest Quality Evaluations. (2009).

89.

Persson, M. Estimating Surface Soil Moisture from Soil Color Using Image Analysis. *Vadose Zone Journal* **4**, 1119–1122 (2005).

90.

Peters, R. D., Sturz, A. V., Carter, M. R. & Sanderson, J. B. Influence of crop rotation and conservation tillage practices on the severity of soil-borne potato diseases in temperate humid agriculture. *Can. J. Soil. Sci.* **84**, 397–402 (2004).

91.

Pierret, A., Doussan, C., Garrigues, E. & Mc Kirby, J. Observing plant roots in their environment: current imaging options and specific contribution of two-dimensional approaches. *Agronomie* **23**, 471–479 (2003).

92.

Pohlmeier, A. *et al.* Changes in Soil Water Content Resulting from Ricinus Root Uptake Monitored by Magnetic Resonance Imaging. *Vadose Zone Journal* **7**, 1010–1017 (2008).

93.

Powell, J. M., Gourley, C. J. P., Rotz, C. A. & Weaver, D. M. Nitrogen use efficiency: A potential performance indicator and policy tool for dairy farms. *Environmental Science & Policy* **13**, 217–228 (2010).

94.

Power, J. F. & Schepers, J. S. Nitrate contamination of groundwater in North America. *Agriculture, Ecosystems & Environment* **26**, 165–187 (1989).

95.

Quemada, M., Baranski, M., Nobel-de Lange, M. N. J., Vallejo, A. & Cooper, J. M. Meta-analysis of strategies to control nitrate leaching in irrigated agricultural systems and their effects on crop yield. *Agriculture, Ecosystems & Environment* **174**, 1–10 (2013).

96.

Randall, G. W. & Irgavarapu, T. K. Impact of long-term tillage systems for continuous corn on nitrate leaching to tile drainage. *Journal of Environment Quality* 360–366 (1991).

97.

Reid, J. B., Sorensen, I. & Petrie, R. A. Root demography in kiwifruit (*Actinidia deliciosa*). *Plant, Cell & Environment* **16**, 949–957 (1993).

98.

Sánchez-Marañón, M., Ortega, R., Miralles, I. & Soriano, M. Estimating the mass wetness of Spanish arid soils from lightness measurements. *Geoderma* **141**, 397–406 (2007).

99.

Shah, S. B., Wolfe, M. L. & Borggaard, J. T. Simulating the fate of subsurface-banded urea. *Nutrient Cycling in Agroecosystems* **70**, 47–66 (2004).

100.

Shortle, J. & Horan, R. D. Nutrient Pollution: A Wicked Challenge for Economic Instruments. *Water Econs. Policy* 1650033 (2016). doi:10.1142/S2382624X16500338

101.

Shrestha, R. K., Cooperband, L. R. & MacGuidwin, A. E. Strategies to Reduce Nitrate Leaching into Groundwater in Potato Grown in Sandy Soils: Case Study from North Central USA. *Am. J. Pot Res* **87**, 229–244 (2010).

102.

Silva, J. Beyond Roots Alone: Novel Methodologies For Analyzing Complex Soil And Minirhizotron Imagery Using Image Processing And GIS Tools. *Dissertations, Master's Theses and Master's Reports - Open* (2014).

103.

Smil, V. Nitrogen and Food Production: Proteins for Human Diets. *AMBIO: A Journal of the Human Environment* **31**, 126–131 (2002).

104.

Snapp, S. S. *et al.* Evaluating Cover Crops for Benefits, Costs and Performance within Cropping System Niches. *Agronomy Journal* **97**, 322–332 (2005).

105.

Sperling, O. & Lazarovitch, N. Characterization of Water Infiltration and Redistribution for Two-Dimensional Soil Profiles by Moment Analyses. *Vadose Zone Journal* **9**, 438–444 (2010).

106.

Su, W. *et al.* Effect of depth of fertilizer banded-placement on growth, nutrient uptake and yield of oilseed rape (*Brassica napus* L.). *European Journal of Agronomy* **62**, 38–45 (2015).

107.

Thornton, J. A. *et al.* Eutrophication as a ‘wicked’ problem. *Lakes Reserv Res Manage* **18**, 298–316 (2013).

108.

Tonitto, C., David, M. B. & Drinkwater, L. E. Replacing bare fallows with cover crops in fertilizer-intensive cropping systems: A meta-analysis of crop yield and N dynamics. *Agriculture, Ecosystems & Environment* **112**, 58–72 (2006).

109.

Valkama, E., Lemola, R., Känkänen, H. & Turtola, E. Meta-analysis of the effects of undersown catch crops on nitrogen leaching loss and grain yields in the Nordic countries. *Agriculture, Ecosystems & Environment* **203**, 93–101 (2015).

110.

Vollsnes, A. V., Futsaether, C. M. & Bengough, A. G. Quantifying rhizosphere particle movement around mutant maize roots using time-lapse imaging and particle image velocimetry. *European Journal of Soil Science* **61**, 926–939 (2010).

111.

Vyn, T. J., Faber, J. G., Janovicek, K. J. & Beauchamp, E. G. Cover Crop Effects on Nitrogen Availability to Corn following Wheat. *Agronomy Journal* **92**, 915 (2000).

112.

Wang, Bear & Shaviv. Modelling simultaneous release, diffusion and nitrification of ammonium in the soil surrounding a granule or nest containing ammonium fertilizer. *European Journal of Soil Science* **49**, 351–364 (1998).

113.

Weinert, T. L., Pan, W. L., Moneymaker, M. R., Santo, G. S. & Stevens, R. G. Nitrogen Recycling by Nonleguminous Winter Cover Crops to Reduce Leaching in Potato Rotations. *Agronomy Journal* **94**, 365–372 (2002).

114.

Werner, T. & Schmülling, T. Cytokinin action in plant development. *Current Opinion in Plant Biology* **12**, 527–538 (2009).

115.

Yadvinder-Singh & Beauchamp, E. G. Nitrogen transformations near urea in soil: Effects of nitrification inhibition, nitrifier activity and liming. *Fertilizer Research* **18**, 201–212 (1988).

116.

Zhang, X. K. & Rengel, Z. Temporal dynamics of gradients of phosphorus, ammonium, pH, and electrical conductivity between a di-ammonium phosphate band and wheat roots. *Aust. J. Agric. Res.* **53**, 985–992 (2002).

APPENDIX A: ABBREVIATIONS

Chapter 2 & 3

UAN = urea ammonium nitrate

DAP = di-ammonium phosphate

MAP = mono-ammonium phosphate

AS = ammonium sulfate

FRZ = fertilizer reaction zone

RSA = root system architecture

DAP = days after planting

ML = maximum likelihood

Chapter 4:

FEE = fertilizer export efficiency

NEE = nitrogen export efficiency

sNEE = sequential nitrogen export efficiency

NUE = nitrogen use efficiency

sNUE = sequential nitrogen use efficiency

FUE = fertilizer use efficiency

PW = Potato – Winter Wheat

WC = winter wheat – sweet corn

CP = sweet corn – potatoes

Chapter 5:

Nr = reactive nitrogen

USDA = United States Department of Agriculture

EPA = Environmental Protection Agency

REE = Research, Education, and Economics

ARS = Agricultural Research Service

NIFA = National Institute of Food and Agriculture

ERS = Economic Research Service

NASS = National Agricultural Statistical Service

USGS = United States Geological Survey

REEIS = Research, Education, and Economics Information System

FS = Forest Service

SAES = State Agriculture Extension Services

RFP = request for proposals

BMP = best management practices

CAP = coordinated agricultural projects

AFRI = Agriculture and Food Research Initiative

CEAP = Conservation Effects Assessment Project

NRCS = Natural Resource Conservation Service

APPENDIX B: SOIL COLOR-MOISTURE CALIBRATION AND APPLICATION USING FLATBED SCANNERS

Introduction:

Flatbed scanners have become a popular method for measuring the length and branch initiation of clean root samples extracted from soils or from plants grown in solution culture (Pan and Bolton, 1991; Kaspar and Ewing 1997; Bouma et al. 2000). Scanners that can be operated at any orientation are now being used as image capture elements for tracking in-situ root growth and development. Improvement of image resolution has also allowed examination of root hair development and comparison between species of crop plants (Hammac et al. 2011; Pan et al. 1998).

Over the last several decades there have been various attempts to characterize the water uptake of roots on an ecosystem, field, plant, and single root scale (Passioura 1988; Dardanelli et al. 2004). Because soil water- root relationships present a much larger challenge to study than above-ground plant development, models have been developed to portray these relationships. Current imaging technologies provide opportunities for model testing and verification. .

Several root imaging methods have emerged from the medical field for examining in-situ root characterization, including CT-scans, MRIs, and X-rays (Doussan et al. 2006; Grose et al. 1996; Macfall et al. 1991; Pohlmeier et al. 2008). MRIs can have high resolution and have been shown to have the ability to image root hairs growing in 3D (Keyes et al. 2013). Nevertheless, root imaging in the visible spectrum has the distinct advantage of being cost effective digital cameras and scanners being widely available.

There are two major design options when using the visible light spectrum: the light transmission method (LTM) and light reflection method (LRM). In LTM experiments the light sensor and light source are on the opposite sides of the flow tank or rhizotron being imaged; consequently the medium being imaged using LTM must be translucent. LTM has been successfully used to visualize a drying front around root systems (Garrigues et al. 2004). In LRM experiments the light sensor and the light source are on same side of the object being imaged allowing for the outside surface of opaque substances such as soils to be imaged. Scanners use LRM and offer the high resolution required for root hair studies (Hammac et al. 2011).

Soil color-moisture calibrations using LRM have been established and parameterized by the characteristics of soil types (Persson 2005; Sanchez-Maranon et al. 2007). Persson (2005) used a digital camera with a standard CCD and collected reflectance in HSV and RGB color space, and found organic matter to be the most important factor in curve variation. Sanchez-Maranon (2007) used a spectrophotometer and converted it into a CIELab color space, and found the initial ‘greyness’ of the dry soil to be the most important factor in the variation in the calibration curves. Both studies concluded strong calibrations of a single soil type can be developed, but a general model describing multiple soil series was not achievable.

Successfully applying a color-moisture calibration to a rhizotron or flow tank experiment depends on the visual heterogeneity of the image to which the calibration is being applied. Visible heterogeneity depends on the structure of the growth medium and the resolution of the image capturing device. Previous studies applying calibration curves to in-situ studies used sandy soils (Garrigues et al. 2006; Sperling and Lazarovitch 2010). Sandy soils tend to have less aggregation than silty and clayey soils resulting in a maximum structural unit the size of the sand particle. The

resolutions used in these studies were 1.3mm/pixel (using a digital camera) and 300 ppi (~0.084 mm/pixel) (using a flatbed scanner) respectively (Garrigues et al. 2006; Sperling and Lavarovitch 2010). The combination of an unstructured soil and low resolution leads to the production of a homogenous image facilitating the application of soil moisture calibrations.

Table 11

Rhizosphere Features and the corresponding resolution at which each feature will become a pixel.	
Rhizosphere features scale	mm
Texture	
Clay	<0.002
Silt †	0.002-0.05
Sand ††	0.05-2.0
Pores	
Macropores ††	0.08-5+
Mesopores ††	0.03-0.08
Micropores†	0.005-0.03
Roots	
Root diameters††	<4.0
Root hair diameters (wheat) ††	0.012
†† Visible as one or more pixel at 2400 ppi	
† Visible as one or more pixel at 9600 ppi	

Low resolution images work well for describing overall root architecture and soil dry down in the root zone (Garrigues et al. 2006). However, looking at features such as wheat root hairs 0.012mm higher resolution imaging is required (Gahoonia et al. 1997). The CanoScan LiDE 700F has an optical resolution of 9600X9600 dpi (0.00256 mm/pixel) and a reflective resolution of 4800X4800 dpi (0.00529 mm/pixel) with an interpolated resolution of 19,200x19,200 dpi (0.00132 um)(Canon 2009). By increasing the image resolution, the image heterogeneity of soil pores, particles and aggregates are captured. Soil particles such as sand (2.0mm-0.5mm) and silt (0.002-0.5mm), and soil pores ranging from micropores (0.005-0.08mm) to mesopores (0.03-0.08mm) and macropores

(0.08-5mm) become increasingly visible (USDA)(Table 11). Due to the observation of the additional physical data at high resolutions; the additional step of discriminating between the physical features of the growth medium is required before accurate applications of color moisture calibrations can be made.

Effectively utilizing spatially rich heterogenous data sets collected at hi resolution requires the use of spatially sensitive software capable of manipulating large data sets. A wide range of software available for making root measurements based on rhizotron images (Le Bot et al. 2010). ArcGIS is among the types of software previously used in root studies (Gasch et al. 2011). Software designed specifically for root measurement has also followed along the lines of GIS software which stores data layers linked by location (Lobet et al. 2011). In this study ArcMap was used for coupling spatial color change with moisture movement. ArcMap was primarily chosen for its intuitive interface and capabilities to classify spatial heterogeneity.

The relationship between color and moisture has a high potential for determining the water content of soil microsites. The relationship between color and moisture is highly dependent on soil characteristics. The first objective of this study was to develop color-moisture calibrations for various soils and to assess the impacts of certain soil properties on the calibration models. Physical heterogeneity in the soil matrix can lead to inconsistencies in applying the calibrations. The second objective of the study was to apply color moisture calibrations in a spatially heterogeneous microenvironment.

Methods:

Calibration:

Thirteen soils from across the state of Washington with varying textural properties were collected (Table 12). 60 grams of each soil were placed in the bottom of a (5 cm x 5 cm) square petri dish so that the bottom was evenly covered. The dry weight of the soils was recorded and wetted to saturate. The soil-paste mixtures were allowed to equilibrate for over 12 hours. The soil samples were then heated for 1 min using a hair dryer and the lid was replaced on the soil. The sample was then weighed and scanned. The drying and scanning cycle was repeated 10-13 times until the moisture was 1% above field capacity at which point the drying increments were reduced to 5 seconds.

In-situ application methods:

An image collected during a fertilizer banding rhizotron experiment was used to demonstrate the application of the calibrations. The image was cropped (2.54 cm X 2.54 cm) with the location of urea placement near the center of the cropped image. The selection was made based on a visible



Figure 48: In-situ image of color change (A) surrounding the site of urea dissolution (B).

color change between the soil immediately surrounding the fertilizer band and the bulk soil (Figure 48). The assumption was made that the color change is due to a moisture change, and the moisture change was due to the increase in solute potential caused by fertilizer band dissolved.

The cropped image was loaded into ArcMap GIS software without assigning a spatial reference system. Two circle shape files were drawn in the 'dark' and 'light' zones of the image, and RGB color values were extracted using ArcMaps extract tool. In order to analyze the impacts of structural heterogeneity detectable image on color change detection the 'light' circle was visually discriminated into five different classes of dark pore spaces, light pore spaces intermediate zones, large aggregates, and small aggregates (Figures 49 & 50). The light and the dark pore spaces were selected from zones in the image which were darker due to the shadows created from the surrounding aggregates. The intermediate zone was classified as zones between aggregates and pores and usually a transition between a pore space and an aggregate. Large aggregates were defined as regions which shifted between the intermediate zone classification and the aggregate classification without having pore space classification. Aggregates were classified as the regions of the image where the aggregates were most clearly visible. The RGB values were then extracted from the visually classified areas. The visually defined physical classifications were converted to ArcMap training samples and used in a maximum likelihood classification of the entire image to create a re-classified image. The re-classified image was then compared to the initial image and the physical classifications were assessed for similarities to the moisture based color change in the initial image.

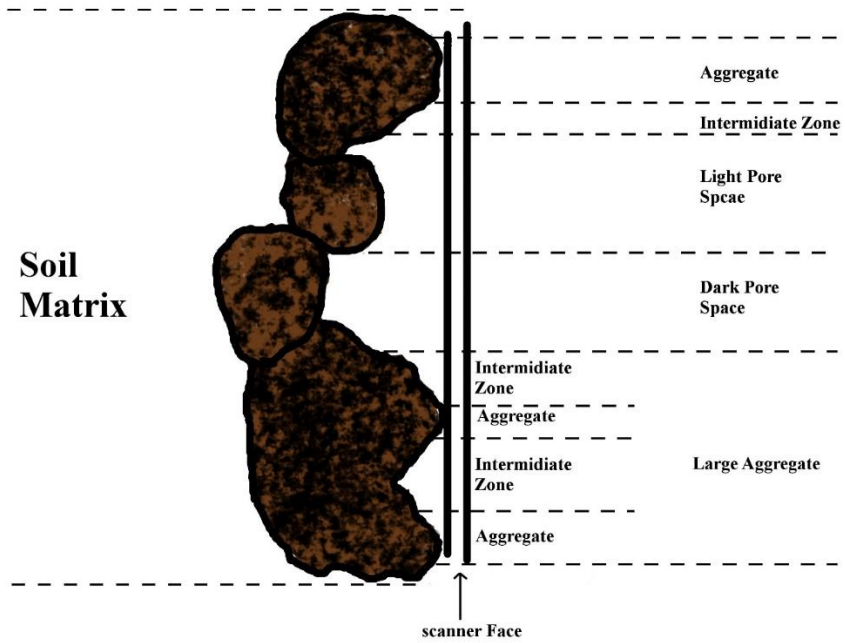


Figure 49: Illustration of a cross section of the scanner face-soil matrix continuum demonstrating the different micro-topographical features of the soil.

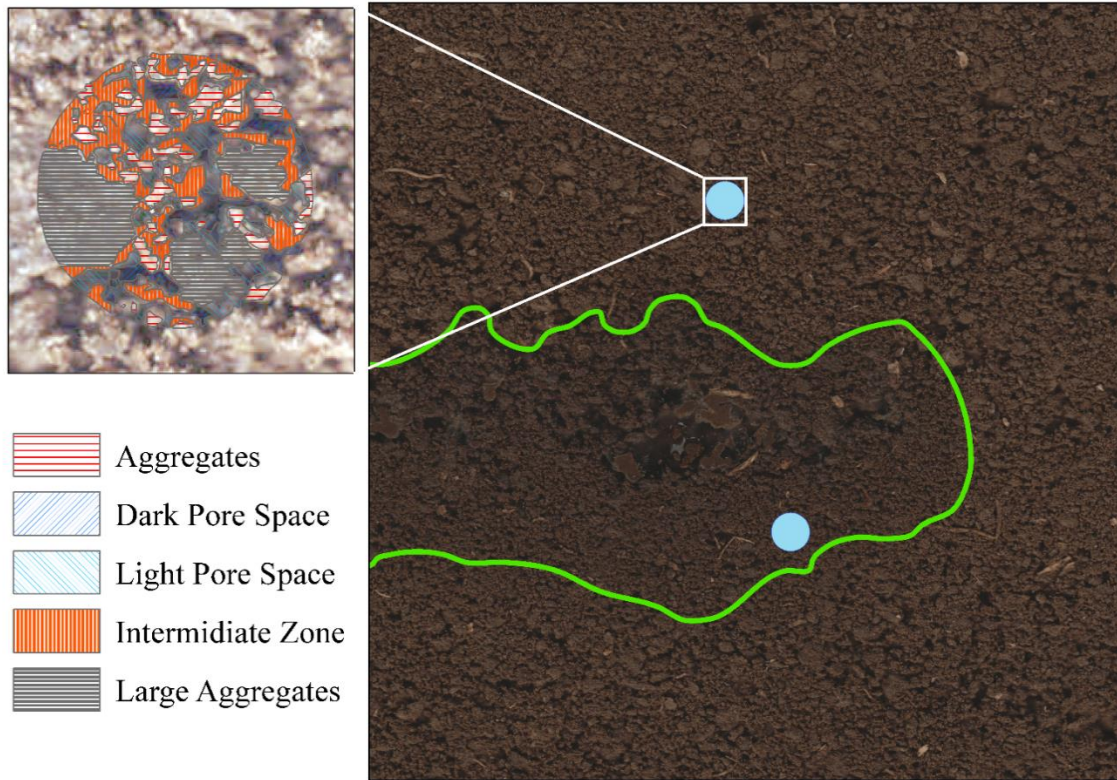


Figure 50: Demonstrates the manual classification of soil micro-topography using GIS.

Software used for Calibration Analysis:

The color analysis for both soils was conducted using ROOTLAW (Washington State University Research Foundation, Pullman, WA) was used to give the average color in RGB and HSV color spaces of the sampled soils. ArcMap was used to look at spatial variation with in the images and plot the red value distributions. R and Sigma Plot were used for statistical analysis and graph production.

Results

Calibration:

Using the average red value (ARV) of the calibration images had on average higher r^2 values than using the average Blue, Green, R-G, R-B, or G-B. The single highest calibration was found using

R-G and R-B with the Springdale soil and had an r^2 of 0.97 (Table 12). When using ARV the strength of the calibration ranged from r^2 values 0.74-0.95 (Table 12). With intercepts ranging from 16.8 ARV to 86.25 ARV and slopes from -0.27 to -1.98. The moisture levels in these calibrations range from field capacity to 7% above 0% gravimetric moisture allowing for a simple linear regression by removing the directional changes in the calibration curves near field capacity and permanent wilting point.

In-situ Application:

The extraction of colors from the 'dark' and 'light' regions had an ARV of 63.9 and 71.4 respectively and bimodal histograms (Figure 51). The ARV values extracted from the visually classified areas were 94.4, 84.2, 76.9, 53.3, and 39.7 for aggregates, large aggregates, transition zones, light pore spaces, and dark pore spaces. The histograms for each of the five extracted values was normal in comparison with the bimodal histograms of the larger 'light' sample from which they were classified (figure 52). The reclassification of source image with the five different physical features of aggregates, large aggregates, transition zones, light pore spaces and dark pore spaces was used to produce 5 different maps each displaying the area classified as a different physical feature (figure 53).

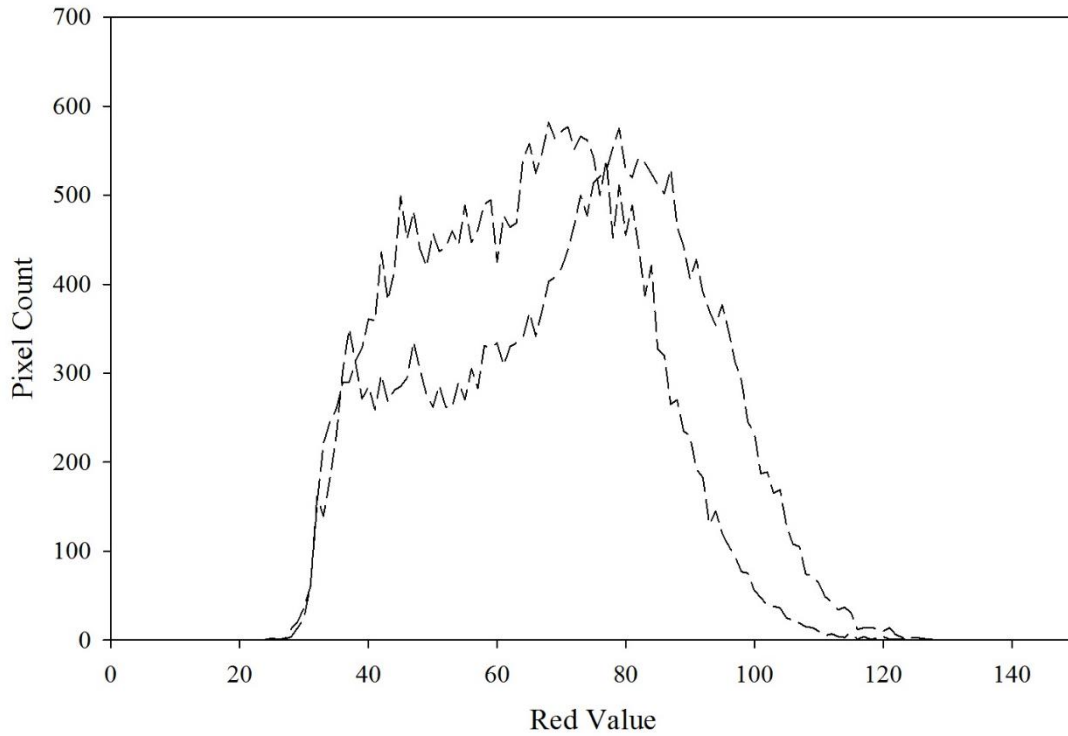


Figure 51: Histograms of the 'light' and 'dark' areas surrounding the site of urea dissolution.

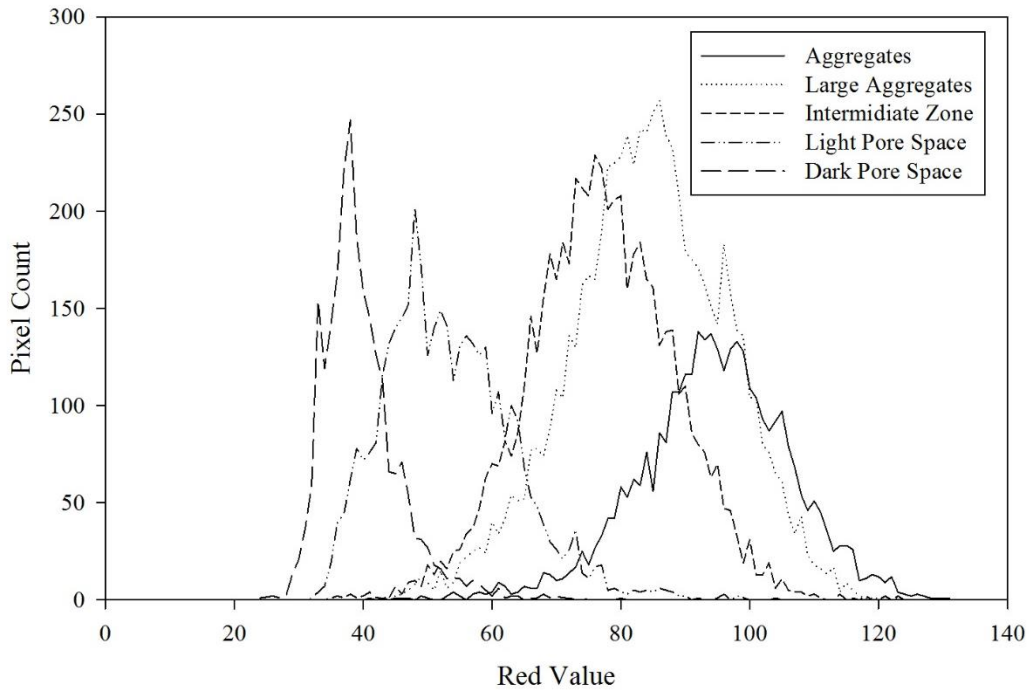


Figure 52: Histogram of the red value of the 'light' zone near the site of urea dissolution.

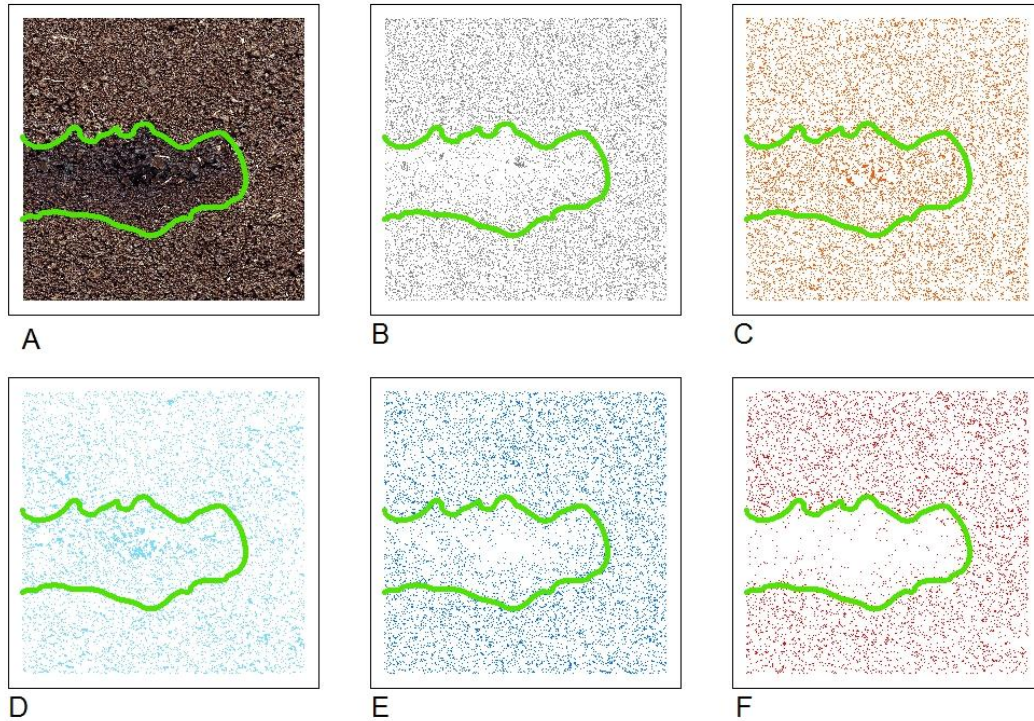


Figure 53: Reclassification of original image (A), using the five categories of 'large aggregates' (B), 'intermediate space' (C), 'light pore space' (D), 'dark pore space' (E), and 'aggregates' (F).

Discussion:

Color Calibration and Texture

The development of moisture calibration curves was successful between FC and PWP. The red value of the soil proved to be the most relevant metric collected out of the RGB and HSV color spaces. The coefficient of determination for the calibrations varied between and r^2 0.74-0.95 for soil types. The strong intra-soil type color-moisture correlation and weak inter-soil series correlations agrees with previous calibration studies using LRM data collected in HSV, CIELab, and GS color spaces (Persson 2005; Sanchez-Maranon et al. 2007; Sperling and Lazarovitch 2009). In the HSV, CIELab, and GS color spaces the value (v), and lightnes (L), and brightness were found to have the best calibrations with moisture of the soil. The intensities of the RGB colors

correspond loosely to v, L, and brightness of the other color spaces respectively (Persson 2005; Sanchez-Maranon et al. 2007; Sperling and Lazarovitch 2009).

Data points in excess of FC and below the lower limit did not fit well into a linear model and were excluded for the sake of maintaining a simple linear model. The strength of the linear relationship between PWP and FC was also observed by Sanchez-Maranon (2007). Sanchez-Maranon (2007) cited the size of the pore spaces being filled as the probable reason for these changes in the color-moisture calibration slopes (Sanchez-Maranon 2007).

The texture, structure, organic matter and mineralogy impact the colorimetric and hydraulic properties of soil. Color-moisture calibrations conducted on soils with high organic matter varying from 2.0-5.8% found soils with lower organic matter and lighter starting colors had higher correlations than darker soils with higher soil organic matter (Persson 2005). Calibrations using reagasols showed the starting color to be the most important factor in model formation (Sanchez Marnon 2007). The data presented here showed that the field capacity of the soil was the most determinate factor in the formation of the soil moisture calibration curve and that there is a weak linear relationship between the slope of the calibration and the FC of the soil (Figure 54 and Table 12). Because field capacity is strongly impacted by texture and structure, it is expected that texture and structure impact the soil moisture curves. A statistical test of covariance was also run in which texture was the covariate, color the independent variable, and moisture was the dependent variable. The results showed a significant interaction ($p < 0.001$) between the texture groupings. The grouping of soils based on textural class shows that clay loams and silty clay loams have steeper calibration curves than loams, silt loams, loamy sand, and sandy loams corroborating the impact

of field capacity (Figure 54). In effect this means that the starting point on the X axis (Dry Soil brightness or ARV) and the ending point on the Y axis (FC) are the most impactful factors on the models for the soil calibration.

Table 12

Soils Used for the Analysis of texture effects on the Heterogeneity of Slopes

Soil Name	Textural Analysis							Regression	
	Texture Class	%Clay	%Silt	%Sand	Field Capacity	Slope	Intercept		
Bong	Sandy Loam	9	30	61	0.09	-0.25	15.95		
Kennewick	Silt Loam	10	52	38	0.127	-0.37	26.32		
Marble	Loamy Sand	8	15	77	0.079	-0.27	14.5		
Ottmar	Clay Loam	32	35	33	0.269	-1.44	65.2		
	Silty Clay								
Palouse Eroded Hilltop	Loam	34	53	13	0.248	-1.31	59.1		
Palouse Footslope	Silt Loam	26	58	16	0.227	-1.03	43.6		
Phoebe	Sandy Loam	7	31	62	0.131	-0.4	23.1		
Puget	Silt Loam	13	75	12	0.24	-0.68	50.94		
Shano	Silt Loam	9	63	28	0.196	-0.51	32.98		
Springdale	Loam	10	41	49	0.165	-0.59	31.64		
Umapine	Loam	19	49	32	0.237	-0.44	33.12		
Warden	Loam	9	41	50	0.124	-0.33	22.31		
Wishkah	Clay Loam	27	49	24	0.358	-1.14	72.68		

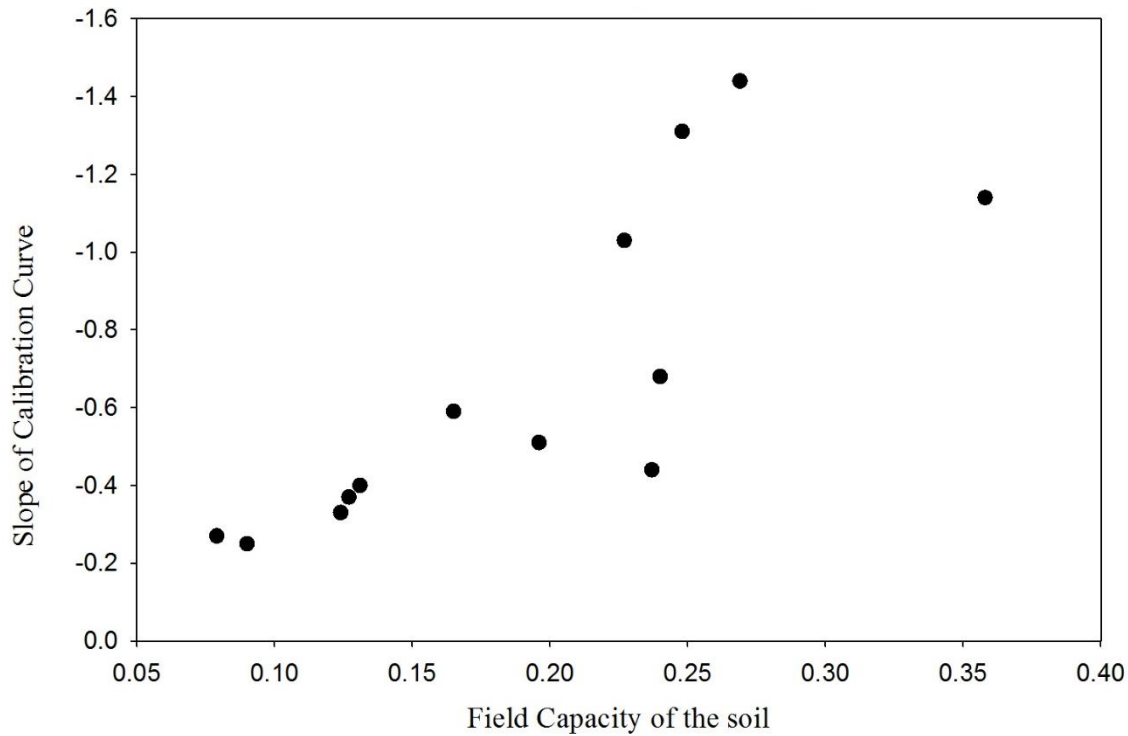


Figure 54: The relationship between the field capacity and the slope of the color-moisture calibration curve.

In-situ use of color change (issues of heterogeneity)

To apply the color-moisture calibrations to an in-situ rhizotron image taken of a fertilizer microsite, and showing a high degree of color contrast was selected (Figure 1). It was assumed that the dark zone immediately surrounding the original position of the fertilizer was caused by increased moisture content due to an increase in solute potential as the fertilizer dissolved. Two circles selected from the bulk soil (71.4) and fertilizer microsite (63.9) showed a small shift in ARV, but also showed a bimodal distribution of red color values in comparison with color distributions taken from calibration images (Figure 4 and 5). The discrepancy between in-situ images and calibration images suggests greater heterogeneity in the in-situ studies.

It has been suggested the soil micro-topography may be responsible for a high level of visible heterogeneity at the soil surface making color moisture-calibrations difficult to acquire and implement (Persson 2005). An assessment of the contributions soil micro-topography to image heterogeneity was conducted by splitting into five visible physical classifications of aggregate, intermediate zone, light pore space, dark pore space, and large aggregates (Figure 2). The five classes showed normal distributions when compared to the original light and dark samples (Figure 7). The five classifications were then used to classify the whole image and it was seen that the 'aggregate' classification aligned best with the visually perceived color difference and consequently moisture change surrounding the fertilizer microsite.

The aggregates classification was best aligned with the observed color change. Aggregates were expected to be the most accurate representation of moisture as the macro pores visible, as dark patches in the image would not be filling until the soil nears saturation (Jury and Horton 2004). However, the mesopores and micropores which would be filling between permanent wilting point and field capacity would be integrated with in the aggregate classification of the image. The in-situ images taken at 2400 dpi which translates to a single pixel being 0.01 mm. At this resolution mesopores would be 3-8 pixels. However, with the minimum classification size set to 10 pixels all image locations classified as a pore must be a macropore. Changes in moisture content below field capacity would be occurring through filling pores which are not detectable in the image, but would rather appear as a change in aggregate color giving a physical basis for the color change being most closely connected to the aggregate classification in the images.

Root-soil interactions are spatially and temporally dynamic and take place in the opaque substance of soil. These challenges have led to a plethora of ingenious methods for visualizing and modeling

roots and the surrounding soil. Each technique has advantages and disadvantages mini-rhizotrons and full scale rhizotrons can be used to study root length density and root system architecture. Models have been used to upscale from single plant to field scale. The methods set forward in this paper are purposed for describing changes in the soil and root microenvironment. Measuring the spatiotemporal relationships of soil factors in relationship to roots and root hair growth may prove useful in future rhizosphere work and should be called ‘2D Rhizocartography’. This basic idea was suggested by Lussenhop (1991), with increased resolution and software designed for handling multiple layers of spatial data this approach can be reopened.

Conclusions:

- There is a strong correlation between the % moisture of an individual soil and the color of that soil.
- Texture and field important factors in modelling color-moisture calibrations.
- In spatially heterogeneous rhizotron images the aggregates in direct contact with the scanner face were shown to have the greatest moisture driven color change.